R. & M. No. 2821
(13,541)
(A.R.C. Technical Report)

MINISTRY OF SUPPLY

AERONAUTICAL RESEARCH COUNCIL
REPORTS AND MEMORANDA



# Critical Mach Numbers for Thin Untapered Swept Wings at Zero Incidence

*By*
S. NEUMARK, Techn.Sc.D., A.F.R.Ae.S.



LONDON: HER MAJESTY'S STATIONERY OFFICE
1954
PRICE £1 0*s* 0*d* NET

# Critical Mach Numbers for Thin Untapered Swept Wings at Zero Incidence

*By*
S. NEUMARK, Techn.Sc.D., A.F.R.Ae.S.

COMMUNICATED BY THE PRINCIPAL DIRECTOR OF SCIENTIFIC RESEARCH (AIR),
MINISTRY OF SUPPLY



*Reports and Memoranda, No. 2821**
*November*, 1949

*Summary.*—In this paper, which is a continuation of two earlier ones (R. & M.'s 2713[34] & 2717[48]), the subsonic flow past untapered swept wings, at zero incidence, is further investigated using linear theory. Methods for calculating 'lower' and 'upper' critical Mach numbers are given, the solution of the main problem being preceded by a short analysis of critical Mach numbers for the simpler cases of infinite wings (straight, sheared and yawed).

The determination of critical Mach numbers depends on the knowledge of velocity distribution over the wing surface, the problem dealt with in the previous reports mostly for the case of the simple biconvex parabolic profile. These earlier results have been extended here to cover a wide class of profiles. Hence it has been possible to determine critical Mach numbers for wings with four different profiles, showing the effect of thickness ratio and of angle of sweep-back (or sweep-forward) in each case. The method applies strictly to wings of large aspect ratio, but no significant corrections are necessary except for very low aspect ratios.

The results and examples, illustrated by a number of tables and graphs, provide a basis for more general discussion. Several conclusions concerning the practical use of swept-wing design are presented.

1. *Introduction.*—The delay in the onset of shock-waves, *i.e.*, the raising of the critical Mach numbers, due to the use of swept wings, was apparently first mentioned by Busemann[3] in 1935. During the years 1939–1945, the idea was further developed in Germany, notably by Göthert[6,7] and Ludwieg[8,23], and led not only to further experimental research, but also to practical attempts at producing fast flying aircraft with highly swept-back wings. After the war, the conception spread far and wide, considerable research work has been done and, at present, the swept-back wing is almost a commonplace in high-speed design. And yet, the fundamental problem of actually calculating critical Mach numbers has not hitherto been solved, and so the true advantage to be gained through sweep-back in various conditions has been only vaguely known. The inadequacy of our knowledge in this respect was strongly emphasized at the Anglo-American Aeronautical Conference of 1947[40]. It appeared that, while the designer had to pay heavy penalties in several aspects of his work for sweeping the wings back, he could not estimate precisely what he was getting in return.

The present report is a continuation of two previous papers (R. & M. 2713[34] and 2717[48]) and aims at solving this problem theoretically in the case of untapered swept wings of large and medium aspect ratios with arbitrary profiles. There are usually a number of additional factors to increase the complexity of the problem, such as: more elaborate wing geometry (taper, twist, spanwise profile changes, very small aspect ratio, etc.), varying incidence, and fuselage or nacelles. All these have been ignored here, and even so the problem is much more complicated than it seemed to be in the initial stage.

* R.A.E. Report Aero. 2355, received 24th November, 1950.

The original approach consisted in considering the simplest case of an infinite straight wing, *yawed* through an angle $\varphi$ from its initial position at right-angles to the wind (Fig. 3, upper part). Resolving the flow into components parallel and perpendicular to the wing edges, one sees that the first component is without significance (apart from the effects of viscosity) and all that matters is the wind component normal to the edges. The flow to be considered is two-dimensional, and this problem may well be termed 'quasi two-dimensional'. The normal component flow has the undisturbed velocity $U \cos \varphi$, and the 'effective' Mach number can be taken as $M_0 \cos \varphi$, where $M_0$ is the Mach number of the undisturbed flow $U$. Therefore, if a certain value $M_c$ of $M_0$ has been found 'critical' for the given wing at $\varphi = 0$, then, for a yawed wing, critical conditions will only occur when $M_0 \cos \varphi = M_c$, or $M_{cy} = M_c \sec \varphi$. This simple 'secant law' applies rigorously only to an infinite yawed wing. It shows, *e.g.*, that if $\varphi = 60$ deg, then the critical Mach number is doubled.

Unfortunately, an infinite yawed wing is not a proper basis for aircraft design; the latter requires a wing formed by joining two symmetrical finite semi-wings, with a kink in the middle. Such a wing does not achieve the whole gain in critical Mach number predicted by the above oversimplified 'theory'. However, it achieves some part of the expected gain, and it is clearly important to know what that part is.

The main reasons of the large discrepancies between the ideal sec $\varphi$ law and the true gain are as follows. First of all, a simple yawing of the wing, although so easily performed in tunnel experiments, is not usually the designer's procedure. The latter will rather consider as fundamental the profile of a section parallel to the main symmetry plane of the aircraft, *i.e.*, parallel to the usual flight direction. Both parts of the swept wing are not yawed but '*sheared*', its consecutive sections having been shifted backwards or forwards from their positions in an unswept wing, the profile shape remaining unchanged. The profile in the section normal to the wing edges has thus its thickness ratio increased in the ratio sec $\varphi$ : 1 compared with that of the fundamental section (*see* Fig. 3, lower part, or Fig. 29). The critical Mach number for a profile in two dimensions depends effectively on thickness ratio, decreasing when the latter increases. Therefore, the gain in $M_c$ for a sheared wing must be lower than for a yawed one, although still quite considerable*. A still more important reduction of the gains in critical $M$ is due to the sharp *kink*, or geometrically more complicated *junction*, with which the two halves of the swept wing are joined. There is a region round the junction, where the flow is far from 'quasi two-dimensional' but essentially three-dimensional, and here serious changes in the flow take place, causing a significant reduction of $M_c$, and requiring a more elaborate treatment. Similar, though usually less important, complications occur near the *wing tips*.

It is now recognised that the problem of critical Mach numbers for swept wings is a serious scientific problem which cannot be solved by an empirical 'guess' (such as, for instance, the notorious but shortlived $\sqrt{(\sec \varphi)}$ law). A rational solution reduces to the following four stages:—

(a) Rigorous definition of the critical conditions of the flow, *i.e.*, of those conditions which being reached and overpassed make supersonic phenomena (shock-waves) possible, at least locally.

(b) Determination of the velocity distribution over the surface of the wing, especially maximum incremental velocities (supervelocities) and their location, first at low Mach numbers, *i.e.*, in incompressible flow.

(c) Determination of modifications in the velocity distribution with increasing Mach numbers (in high subsonic flow), especially the maximum supervelocities at high Mach numbers.

(d) Combination of the results of the three above investigations for calculating critical Mach numbers for particular wings.

* It is important to differentiate between the two methods of producing oblique wings and in appreciating their performance, and especially to guard against applying the experimental results obtained with a straight model at several angles of yaw—to swept wings with similar angles of sweep but with a constant profile parallel to the direction of wind.

There was, at first, some confusion with respect to the stage (a). It was known that critical conditions occurred when the local velocity of the flow reached the local sonic value, but it was not quite clear whether this applied to the total velocity or to some component of it. Treating an infinite yawed or sheared wing on the lines of Busemann's initial suggestion, it was natural to conclude that only the velocity component normal to the wing edges had to reach the sonic value, and this point of view was advocated by Betz and Ludwieg[8]. Surprisingly enough, Göthert[7] insisted on the total velocity being taken into account, and thus obtained much more pessimistic results even for infinite sheared or yawed wings. The question was studied, from a more general point of view, by Ringleb[5], Scherberg[15] and Bickley[12, 16], and gradually the way has been paved for the *general criterion of critical conditions* which is: that the velocity component in the direction of the pressure gradient (or normal to the isobars) becomes equal to the local sonic value. The criterion was finally substantiated by Bickley (R. & M. 2330[24]) on strictly mathematical grounds. It is clear that, for thin sheared or yawed wings, ' normal to the isobars ' means simply ' normal to wing edges ', and hence Busemann's original idea is a particular case of a more general one. A yawed or sheared wing may be viewed as a device for making isobars run at a required angle relative to the wind, so as to create in some cases the possibility of ' flying at supersonic speed, while pretending to fly subsonic ', *i.e.*, being subject to subsonic aerodynamics. The general criterion also solves the problem for the troublesome regions near the kinks or tips. It becomes clear that not only the maximum velocities but the entire velocity field over the wings must be determined, and that only the velocity components normal to the isobars play the decisive part in defining critical conditions. Since the isobars cross the central kink section at right-angles, the full velocities in this section must be taken into account, and hence the ' local critical Mach number ' will always be less than 1. It is seen that critical conditions are not reached simultaneously on the entire wing surface, and therefore the present report suggests introducing the notions of ' lower ' and ' upper ' critical Mach numbers. The former refers to critical conditions being reached at a single point of the ' first danger section ' (often, but not always, the central kink), the latter to the entire wing being embraced by critical or supercritical conditions. Thus, we have to deal with a *critical range of Mach numbers*, instead of a single critical value*.

The importance of stage (b) can now be seen. The first (unsuccessful) attempt to determine the velocity distribution over swept wings with a kink was made by Ludwieg[23] and, after several more efforts by different authors[34, 36, 38, 43, 48] the problem may be considered as theoretically solved at least for untapered wings, of small thickness (linear approximation), whether of infinite or finite aspect ratio. Owing to mathematical difficulties, all previous papers dealt mostly with the simplest profile (biconvex parabolic—*see* Fig. 5, profile B), and this was a serious handicap from the practical point of view, especially as no experimental data for wings with such a profile have been available. It has therefore been decided to try to generalize the earlier method so as to obtain effective solutions for a wider class of profiles. These solutions, for all symmetrical profiles expressible by polynomial equations of a degree not exceeding 5, are given in Appendix III. Several examples have been worked out, namely for the profiles C and Q (Fig. 5), and illustrated by graphs of velocities and pictures of isobars (*see* Figs. 6 to 19). These examples make it clear, when and why the maximum velocity may occur not in the kink section but in the regular region of the wing, and sometimes even at the tips. The analysis of the examples finally leads to the conclusion that, for actually calculating critical Mach numbers, it suffices to work out the maximum supervelocities in the kink section and in the regular region, and this can be done for every profile. Tables 5 to 8 contain these maxima for 4 profiles B, C, Q, R, the latter having a rounded nose. Figs. 20 to 28 illustrate the results for a wide range of angle of sweep.

---

* It should be mentioned that Griffith[21] and McKinnon Wood[22] have interpreted Bickley's criterion in such a way that, on the wing surface the normal acceleration due to curvature must also be included. This interpretation would lead to surprising and paradoxical results, entirely different from those generally accepted, even in two-dimensional problems. The question is a very difficult one. In this paper, the normal acceleration has been left out, in accordance with the common practice (*see* further remarks in the footnote under section 5).

The stage (c) had its ground well prepared by the Glauert-Prandtl law[1, 2, 4] which, however, was initially known in its two-dimensional form only, and was sometimes applied wrongly to three-dimensional problems. The law is based on the linear perturbation theory for thin wings, and is therefore only approximate. There were several attempts at improving the accuracy of this law by introducing higher order corrections[9, 13, 17, 44]. None of these corrections has been used in this report, as the velocity field in incompressible flow past swept wings can only be predicted to the first order accuracy, and hence higher accuracy in a later stage would be illusory. The correct generalization of the law for three dimensions was first produced by Göthert[6]. There were some misinterpretations and controversies, especially as regards bodies of revolution[41, 47], but the method does not now present any difficulties, at least within the first order accuracy. A clear and rigorous exposition of the method, in the form particularly suitable for swept wings, was given by Dickson[26].

By combining the above results, it is possible to work out simple methods for calculating the critical Mach numbers, and this has been done in this report, first for infinite straight wings (section 2), then for infinite yawed or sheared wings (section 3), and finally for finite swept-back and swept-forward wings (section 4). Several examples have been worked out numerically, involving four different profiles, as shown in Fig. 5. Final results are given in Tables 9 to 12 and illustrated by Figs. 30 to 33.

Section 5 contains a discussion of advantages to be gained by sweeping the wings, and several general conclusions for the designer's use.

Acknowledgements are due to Mrs. J. Collingbourne for her help in working out numerical examples of velocity distribution, to R. P. Purkiss who has done most of the computational work, and to A. R. Beauchamp who has prepared the illustrations.

2. *Critical Mach Numbers for Infinite Straight Wings (two-dimensional)*.—Before dealing with more complex cases, it will be useful to summarize the results for the simple case of two-dimensional flow past an arbitrary profile (Fig. 1), using the linear theory. Suppose that, in incompressible flow, the maximum velocity occurs at a point $A_m$ of the profile, and is equal to $U(1 + \delta_i)$. Then, in compressible sub-critical flow, at Mach number $M_0$, the maximum velocity, according to Glauert-Prandtl law[1, 2], should occur at the same point $A_m$ and be equal to:

$$V_m = U\left(1 + \frac{\delta_i}{(1 - M_0^2)^{1/2}}\right). \quad \ldots \quad (2.1)$$

Critical conditions will be reached when $V_m$ is equal to the local speed of sound which differs from that ($a_0$) corresponding to conditions of undisturbed flow, and may be found from the Bernoulli equation for compressible flow:

$$\frac{\gamma - 1}{2} U^2 + a_0^2 = \frac{\gamma - 1}{2} V^2 + a^2 , \quad \ldots \quad (2.2)$$

where $V$ and $a$ are local flow velocity, and local speed of sound. In this equation, we may put $U = M_0 a_0$, where $M_0$ is the Mach number of undisturbed flow; also, if conditions are to be critical, $V$ and $a$ must be equal and may be denoted either by $V_c$ or $a_c$. The equation (2.2) then yields:

$$a_c = a_0 \left(1 - \frac{\gamma - 1}{\gamma + 1} (1 - M_0^2)\right)^{1/2} , \quad \ldots \quad (2.3)$$

which may also be written:

$$V_c = U\left(1 + \frac{2}{\gamma + 1} \frac{1 - M_0^2}{M_0^2}\right)^{1/2} , \quad \ldots \quad (2.4)$$

and it is seen that the critical value $a_c = V_c$ is greater than $U$, and less than $a_0$.

The critical conditions occur when $V_m$ becomes equal to $V_c$ and, equating (2.1) and (2.4), and denoting by $M_c$ the critical value of $M_0$ we obtain the *fundamental equation* :

$$\delta_i = (1 - M_c^2)^{1/2} \left[ \left( 1 + \frac{2}{\gamma + 1} \frac{1 - M_c^2}{M_c^2} \right)^{1/2} - 1 \right] . \qquad .. \qquad .. \qquad (2.5)$$

This equation was first given, in almost identical form, by B. Göthert[6]. The equation is not simply solved for $M_c$, with given $\delta_i$. However, it is easy to tabulate $\delta_i$ against $M_c$, and interpolate to find $M_c$ corresponding to any given $\delta_i$, with any required accuracy. Tables 1 and 1a* give the values of $\delta_i$ versus $M_c$, or $M_c$ versus $\delta_i$, respectively, the range being $1 > M_c > 0{\cdot}54$, or $0 < \delta_i < 0{\cdot}60$. The relationship is also represented graphically in Fig. 2 (full line).

It should be noticed that equation (2.5) is a first order approximation, since the incompressible profile characteristic $\delta_i$ and the compressibility correction used in deriving the corresponding critical Mach number are each calculated by linearized theory. This is the justification for using the Glauert-Prandtl law or its three-dimensional equivalent throughout this report. To use one of the several more refined formulae, proposed as alternatives to this law[9, 13, 17, 44], would only produce an illusion of greater accuracy so long as $\delta_i$ remains a first order approximation. The first order method is the only one at present available for the theoretical determination of the supervelocities for swept wings, and therefore it would not be reasonable to introduce any refinements to Glauert-Prandtl law. The matter is not so simple when we have to deal with experimental results, or with highly accurate theories of two-dimensional flow, and some relevant remarks are given in Appendix I. In Fig. 2, an additional thin curve shows the correction which would be introduced if von Kármán's correction to the Glauert-Prandtl rule were used.

The formula (2.5) may be criticized from the opposite point of view, as being too complicated (especially insoluble for $M_c$). This question is also discussed in Appendix I, and it is found that a simpler formula can hardly be derived to replace (2.5) without the risk of too great errors. Very crude approximate formulae (I.36, 37), corresponding to a similar formula of Liepmann and Puckett[32], may only be recommended for rough estimates. A better approximation may be obtained by using series (I.33, 35), but those are almost more complicated than (2.5).

Fig. 2 also contains a graph of the first derivative ($-\, dM_c/d\delta_i$), obtained by differentiating (2.5):

$$-\frac{d\delta_i}{dM_c} = \frac{M_c}{(1 - M_c^2)^{1/2}} \left[ \frac{1 + \dfrac{2}{\gamma + 1} \dfrac{1 - M_c^4}{M_c^4}}{\left( 1 + \dfrac{2}{\gamma + 1} \dfrac{1 - M_c^2}{M_c^2} \right)^{1/2}} - 1 \right] , \qquad .. \qquad .. \qquad (2.6)$$

and it is seen that its value, while varying from $\infty$ to 0, does not differ much from 1 in the interval about $0{\cdot}04 < \delta_i < 0{\cdot}19$, or $0{\cdot}9 > M_c > 0{\cdot}75$. Most interesting practical cases lie within this interval, and hence we may risk a very crude mnemotechnic rule: a reduction of $0{\cdot}01U$ in the maximum supervelocity gives a gain of about $0{\cdot}01$ in the critical Mach number. The latter gain, which is equivalent to about 7 miles per hour, is certainly not negligible. This shows that errors in $\delta_i$ should not exceed $0{\cdot}01$, or if possible should be kept below this value. The linear perturbation method can generally ensure this for thin profiles; for thicker ones, the errors in $\delta_i$ may become greater, but the values of the derivative ($-\, dM_c/d\delta_i$) decrease rapidly, so that the accuracy of $M_c$ should be little affected. It is seen that the first-order theory may be considered as sufficient for practical needs, but one must not expect greater accuracy than within $0{\cdot}01$ error in the critical Mach number.

* When calculating the tables, $\gamma$ was assumed to be $1{\cdot}403$, following R. & M. 1891[10]. This applies to all following tables and numerical data, unless stated otherwise. The value $1{\cdot}4$ is often used now. The difference is irrelevant for our purposes, the order of accuracy of the theory being low.

The formula (2.5), Tables 1 and 1a, and diagram in Fig. 2, apply to *all profiles*. One must bear in mind, however, that while the parameter $\delta_i$ (maximum supervelocity ratio in incompressible flow) is proportional to thickness ratio $\vartheta = t/c$ for every thin profile, the proportionality factor $\delta_i/\vartheta$ assumes different values for particular profiles. The matter has been illustrated by several examples in R. & M. 2713[34], and it has been shown that, for instance:

(*a*) For an *ellipse*, the proportionality factor has the value 1 (this being the lowest known value by linear theory), *i.e.*, $\delta_i = \vartheta$, hence our tables and diagram apply directly, with $\delta_i$ meaning simply thickness ratio.

(*b*) For a *biconvex parabolic profile*, the proportionality factor is $\frac{4}{\pi} = 1 \cdot 273$, and $\delta_i = 1 \cdot 273\vartheta$, thus the critical Mach number will be lower than for an ellipse of the same thickness ratio.

(*c*) For *every other profile*, the proportionality factor assumes a definite value characteristic for the profile, and this may range from 1 to 2, and sometimes even higher. For example, for the profile (I.19) of R. & M. 2713[34], with maximum thickness at 1/3-chord, and with a trailing-edge cusp, we have $\delta_i \simeq 1 \cdot 667\vartheta$, and a similar value of the proportionality factor applies to the round-nosed profile (I.44) of R. & M. 2713[34] (although in this case the value is somewhat doubtful as the maximum velocity occurs so very near the leading edge). The critical Mach number will be much lower for such profiles.

How far these differences affect $M_c$, will be shown by the following figures :—

*Critical Mach numbers for different profiles and thickness ratios*

| Profile : | ellipse ($\delta_i : \vartheta = 1$) | B (biconvex parabolic) ($\delta_i : \vartheta = 1 \cdot 273$) | C (cubic of Fig 5) ($\delta_i : \vartheta = 1 \cdot 667$) | poor profile ($\delta_i : \vartheta = 2$) |
|---|---|---|---|---|
| $\vartheta = 0 \cdot 10$ | $M_c = 0 \cdot 826$ | 0·800 | 0·766 | 0·741 |
| $\vartheta = 0 \cdot 20$ | $M_c = 0 \cdot 741$ | 0·704 | 0·659 | 0·626 |

It is seen that, while the thickness ratio is of primary importance, the effect of profile shape may also be very large.

In Fig. 2, a few additional horizontal scales in $\vartheta$ are added, referring to a few particular profiles. They enable one to read critical Mach numbers directly off the diagram for a given profile with a given thickness ratio.

3. *Critical Mach Numbers for Infinite Yawed or Sheared Wings* (*quasi two-dimensional*).—The two cases to be considered here are theoretically almost equivalent, as every *infinite* yawed wing can also be viewed as sheared, and vice versa. The only difference lies in the choice of the fundamental profile of the infinite straight wing ($\varphi = 0$) to be used as a basis of comparison. If the wing in the oblique position is considered as yawed (Fig. 3, upper part), then the fundamental profile is the section normal to the leading and trailing edges; for a sheared wing (Fig. 3, lower part), it is the section parallel to the velocity $U$ of undisturbed flow.

*In both cases*, the isobars run parallel to the edges, so that it is sufficient to consider only the component flow at right-angles to them. This flow has the undisturbed velocity $U \cos \varphi$, and the corresponding 'effective' Mach number is $M_0 \cos \varphi$, while $M_0 = U/a_0$ always denotes the Mach number of the full undisturbed flow, equivalent to 'flight Mach number'. The local speed of sound in critical conditions will now be obtained from (2.3) by replacing $M_0$ by $M_0 \cos \varphi$:

$$a_c = a_0 \left(1 - \frac{\gamma - 1}{\gamma + 1}(1 - M_0^2 \cos^2 \varphi)\right)^{1/2}, \quad \ldots \quad (3.1)$$

which may also be written, as critical value of the normal component (*cf.* 2.4):

$$V_{nc} = U \cos \varphi \left(1 + \frac{2}{\gamma + 1} \frac{1 - M_0^2 \cos^2 \varphi}{M_0^2 \cos^2 \varphi}\right)^{1/2}. \quad \ldots \quad (3.2)$$

This critical value of the speed of sound, or of the local normal velocity component, must now be equated to the true maximum normal velocity for the given wing. This will take different forms for a yawed or sheared wing, if the fundamental section is the same in both cases, with thickness ratio $\vartheta = t/c$ and maximum supervelocity ratio in two dimensions $\delta_i$.

(*a*) For a *yawed wing* (Fig. 3, upper part) the fundamental section is normal to the edges, hence the maximum normal velocity in incompressible flow is $U \cos \varphi \,.\, (1 + \delta_i)$. In compressible flow, the incremental term $\delta_i$ must be divided, according to Glauert-Prandtl law, by $\sqrt{(1 - M_0^2 \cos^2 \varphi)}$, and hence:

$$V_{n\,\max} = U \left(1 + \frac{\delta_i}{(1 - M_0^2 \cos^2 \varphi)^{1/2}}\right) \cos \varphi \,. \quad \ldots \quad (3.3)$$

By equating (3.2) and (3.3), and denoting the critical value of $M_0$ by $M_{cy}$ we obtain the *fundamental formula for infinite yawed wings*:

$$\delta_i = (1 - M_{cy}^2 \cos^2 \varphi)^{1/2} \left[\left(1 + \frac{2}{\gamma + 1} \frac{1 - M_{cy}^2 \cos^2 \varphi}{M_{cy}^2 \cos^2 \varphi}\right)^{1/2} - 1\right]. \quad (3.4)$$

It is seen that this equation may be obtained directly from (2.5) by replacing $M_c$ by $M_{cy} \cos \varphi$.

(*b*) For a *sheared wing* (Fig. 3, lower part) the section normal to the edges has the same thickness $t$ as the fundamental one, but its chord is reduced from $c$ to $c \cos \varphi$, hence the thickness ratio is increased from $\vartheta$ to $\vartheta \sec \varphi$. The maximum supervelocity ratio (incompressible) varies in proportion to thickness ratio, thus it amounts now to $\delta_i \sec \varphi$, and therefore the maximum normal velocity in incompressible flow is $U \cos \varphi \, (1 + \delta_i \sec \varphi) = U (\cos \varphi + \delta_i)$. In compressible flow, the incremental term $\delta_i \sec \varphi$ must again be divided by $\sqrt{(1 - M_0^2 \cos^2 \varphi)}$, and hence:

$$V_{n\,\max} = U \left(\cos \varphi + \frac{\delta_i}{(1 - M_0^2 \cos^2 \varphi)^{1/2}}\right). \quad \ldots \quad (3.5)$$

By equating (3.2) and (3.5) and denoting the critical value of $M_0$ by $M_{cs}$, we obtain the *fundamental formula for infinite sheared wings*:

$$\delta_i = (1 - M_{cs}^2 \cos^2 \varphi)^{1/2} \left[\left(1 + \frac{2}{\gamma + 1} \frac{1 - M_{cs}^2 \cos^2 \varphi}{M_{cs}^2 \cos^2 \varphi}\right)^{1/2} - 1\right] \cos \varphi, \quad \ldots \quad (3.6)$$

and it is seen that this equation may be obtained directly from (2.5) by replacing $M_c$ by $M_{cs} \cos \varphi$, and $\delta_i$ by $\delta_i \sec \varphi$.

The two fundamental formulae give the critical Mach numbers for infinite oblique (yawed or sheared) wings, as functions of two parameters $\delta_i$ and $\varphi$; they are illustrated by two families of curves in Fig. 4, and the relevant numerical values may be found in Tables 2, 3. The computation of those tables has been greatly facilitated by the use of the previous Table 1.

For given values of $\delta_i$ and $\varphi$, critical Mach numbers for yawed wings are higher than for sheared ones. Fig. 4 shows that the differences are quite appreciable and rise quickly with both $\delta_i$ and $\varphi$. The important fact is that, with large angles $\varphi$ and not too large $\delta_i$, critical Mach numbers well above unity may be obtained. This is particularly easy for yawed wings, but also possible for sheared ones. Were it possible to design *finite* wings with similar properties, we could achieve supersonic flight with subsonic aerodynamic characteristics.

The diagrams of Fig. 4, as those of Fig. 2, apply to *all profiles*, provided the abscissa $\delta_i$ represents the true supervelocity ratio for the given profile. As $\delta_i$ is proportional to thickness ratio $\vartheta$, it again suffices to provide an additional uniform scale on the horizontal axis for the diagram to apply directly to any given profile with varying thickness ratio. A few of such additional scales are added in Fig. 4, relating to several particular profiles.

4. *Critical Mach Numbers for Untapered Swept Wings.*—4.1. *Definition of Lower and Upper Critical Mach Numbers and their Analysis Based on Studying Velocity Distributions.*—When dealing with infinite oblique wings, there was a single critical Mach number for each wing, since the flow in parallel sections of such wings was identical, and the critical conditions in all sections were reached simultaneously. When we consider other wings, such as kinked swept ones (infinite or finite), or simple sheared ones (semi-infinite or finite), the aspect of the flow is different in each section, and the sonic (and supersonic) conditions are not reached simultaneously but gradually. The problem becomes more complicated, and one of the chief difficulties is that, once a local supersonic area with shock-waves has been created, the entire velocity field undergoes changes which are difficult to predict. The local sonic conditions will be reached first at a certain single point of one particular section (' first danger section '), at some value of $M_0$ (Mach number of undisturbed flow) which will be called *' lower critical '*. When $M_0$ increases above this value, the sonic conditions penetrate progressively further portions of the wing, and the shock-wave area spreads. It seems natural to expect that, at a certain higher value of $M_0$ the sonic (or supersonic) conditions will reach every section of the wing, and that value will be called *' upper critical Mach number '*. We have now: (a) to find methods of determining both lower and upper criticals for various wings, and (b) to interpret their meaning as regards the aerodynamic properties of the wings.

For the solution of the first problem, the velocity distribution over the surface of the wing must be determined. This can be done on the lines of Refs. 34 and 48 for the case of incompressible flow. It is known that, when the Mach number of the flow increases, the velocity field changes gradually due to compressibility. At any particular (subcritical) Mach number, the field may be determined, to the first order approximation, by applying the three-dimensional similarity law (generalized Glauert-Prandtl law), *i.e.*, by correlating the compressible flow past the given wing with the incompressible flow past an ' equivalent ' wing (*see* Fig. 29), the concept originally due to Gothert[6] and later elaborated by Dickson[26].

The methods of Refs. 34 and 48 have been effectively applied only to the simplest case of the biconvex parabolic profile but they are suitable for any symmetrical profiles, expecially those represented by polynomial equations. It was thought essential to study and compare critical Mach numbers for wings with different profiles, and four profiles B, C, Q and R have been chosen as examples, *see* Fig. 5. The equations of the profiles, and detailed calculations of the velocity distributions, are given in Appendix III.

Once the wing profile has been chosen, there are two independent geometrical parameters for untapered swept wings, *i.e.*, angle of sweep and aspect ratio. But if the latter is not very small, say not below 2, its effect on velocity distribution and critical Mach numbers may be neglected, with inappreciable error. For it has been shown in R. & M. 2717[48] that, for wings of not very small aspect ratio, considerable parts of both semi-wings are ' regular ' regions, with isobars running almost parallel to the wing edges, and with velocity distributions almost the same as for infinite sheared wings; also, that the velocity field in the kink region of a finite wing differs only negligibly from that of an infinite swept wing. Similarly, the velocity field in the tip region of a finite wing is almost the same as that in the corresponding region of a semi-infinite sheared one. Similar remarks apply to finite sheared wings whose velocity fields may be regarded as consisting approximately of a central ' regular ' region and two tip regions (' upstream tip ' and ' downstream tip '). The degree of accuracy of this approximate method is shown in Figs. 8 and 9, where the isobars on finite wings of indeterminate aspect ratio (with profile B and $\varphi$ = 53 deg 8 min) have been produced by using only velocity diagrams for tip and kink regions of infinite wings (Figs. 6 and 7). Comparing Figs. 8 and 9 of this report with rigorous solutions as represented in Figs. 19 and 23 of R. & M. 2717[48], for aspect ratios 1 and 2 respectively, we see that the discrepancies are very small. Also formulae (4.1.8, 10; 4.3.2, 3) and Fig. 24 of R. & M. 2717[48] show clearly that the effect of finite aspect ratio on maximum supervelocities in kink or tip sections is negligibly small for normal wings. The only important difference between wings of large and small aspect ratio is that, on the former, the regular regions occupy major parts of the surface, while on the latter the regular regions are merely small intermediate portions between the kinks and the tips.

In view of the above reasons, it would not be justifiable to derive and use very complicated rigorous formulae for velocity distribution on finite wings (as in R. & M. 2717[48]). Therefore, only formulae referring to semi-infinite, sheared or infinite swept wings (as representatives of tip and kink regions, respectively) are given in Appendix III. The general formulae (III.18) and (III.22) apply to a wide class of profiles represented by polynomials of the 5th degree at the most (form. III.7). The profiles B, C and Q are examples of this class—of 2nd, 3rd and 4th degree respectively. Figs. 10 to 14 represent velocity diagrams and isobar patterns for the profile C, Figs. 15 to 19 for Q*. The round-nosed profile R is not one of the 'polynomial' class, and it would be more difficult to work out similar diagrams for this case. This work has not been attempted till now, more so as the material represented in Figs. 6 to 19 seems to be quite sufficient to give a general idea of the flow in various cases and of the effect of typical peculiarities of the profile shape.

Returning to the problem of critical Mach numbers, let us examine first the simplest flow pattern of Fig. 9 (for profile B) and consider three characteristic sections of the wing :—

(a) *Central kink section.*—Here the isobars cut the section at right-angles, the normal to the isobars coincides with the direction of the flow, and therefore we must reckon with the total velocity of the flow. The crucial point is A in Fig. 9, where the total velocity reaches its maximum. Conditions for critical Mach number are reached when this velocity at A becomes equal to the local velocity of sound. It is obvious that the relevant critical Mach number must always be less than 1. It is the true *lower critical* because nowhere does the velocity of the flow exceed that at A.

(b) *Section in the regular region, i.e.*, a section at a considerable distance from both the kink and the tip. The flow here is almost identical with that on an infinite sheared wing of the same profile and angle of sweep, and we assume that it is not appreciably affected by transonic changes occurring in the kink area. Only the maximum velocity component normal to the isobars (*i.e.*, normal to wing edges) must be taken into account, and the critical conditions may be defined exactly as in section 3 (formula 3.6); the relevant Mach number may be considered as *upper critical*. When the Mach number of the flow increases gradually from its lower critical value, critical conditions spread sideways from the kink section, to embrace ultimately almost the entire wing when the upper critical value is reached. The upper critical may, of course, exceed 1.

(c) *Tip section.*—In the case represented in Fig. 9, the maximum supervelocity at the tip is approximately half that at the kink section, and also appreciably lower than that in the regular region; the latter fact is due to the angle of sweepback not being very large. The isobars bend sharply in the tip area to run nearly parallel to the flow. The critical conditions are reached here much later than in the central kink, and apparently also later than in the regular region. The tip area seems not to play a significant part in this case, and there is hardly any sense in trying to define a 'tip critical Mach number'. It is true that there are points in the rear portions of the tip area, where the isobars run locally at right-angles to the main flow, and

---

* It may be mentioned that, while in Fig. 8 the two tips present identical flow patterns (only inverted) owing to the fore-and-aft symmetry of the profile, it is not so in Figs. 13 and 18, where the two tips exhibit quite different patterns. It is essential to discriminate between 'upstream tips' and 'downstream tips' in all cases when there is no fore-and-aft symmetry. For details of calculation, *see* Appendix III.

for each of such points a local critical Mach number could be determined, lying sometimes between the previously defined lower and upper critical, sometimes above the latter. However, it seems that there is little point in trying to analyse the complicated phenomena at the tips. If some local shock waves appeared in these areas before the entire regular region became shock-stalled, the effect on the performance of the whole wing would probably be insignificant. In addition, the flow in the tip areas may be strongly affected by small changes in the geometrical shaping, and the investigation of this flow would be not only difficult but also of little promise.

The above analysis of Fig. 9 leads to the simple conclusion that the lower critical Mach number should be determined from the conditions prevalent at the central kink section, while the upper critical may be taken as that corresponding to an infinite sheared wing of the same profile and angle of sweep. This would mean that the upper critical could always be obtained by a simple interpolation from our Table 3 while the calculation of the lower critical would require a complete knowledge of the velocity distribution in the kink section for the given profile and for a wide range of the angle $\varphi$. This is comparatively easy, as we possess a general formula for this velocity distribution (*see* R. & M. 2713[34], form. 7.5):

$$(v_x)_{\text{kink}} = \left( (v_x)_{\varphi=0} - \frac{U}{\pi} F'(x) \,.\, \ln \frac{1 + \sin \varphi}{1 - \sin \varphi} \right) \cos \varphi \,. \qquad \ldots \quad \ldots \quad \ldots \quad (4.1.1)$$

The formula has been used, as expounded in Appendix III, for calculating supervelocity distribution in the kink section at varying $\varphi$, for four profiles B, C, Q, R (formulae III.34, 39, 45 and 53 respectively), and the results are represented in Figs. 20 to 27. There are two diagrams for each profile, giving respectively the curves of

$$\left( - \frac{v_x}{\vartheta U \cos \varphi} \right) \text{ and } \left( - \frac{v_x}{\vartheta U} \right) \qquad \ldots \quad \ldots \quad \ldots \quad \ldots \quad \ldots \quad (4.1.2)$$

against $\xi$. The first provides a comparison of the supervelocity distribution in the kink section at any $\varphi$ to that 'at infinity' (meaning, really, in the 'regular' region); the second gives the same supervelocity distribution as compared to that on an unswept wing. The important maximum values of the quantities (4.1.2) are tabulated in Tables 5, 6, 7 and 8, illustrated in Fig. 28*.

The problem of critical Mach numbers for swept wings is not quite so simple as would appear from the above reasoning, based mainly on analysing Fig. 9. The following circumstances must be taken into consideration.

(i) The upper critical Mach numbers for *swept-back* and *swept-forward* wings, *i.e.*, for positive or negative $\varphi$'s of the same numerical value, are identical, whatever the profile. This is generally *not* true for the lower critical, unless the profile is symmetrical fore-and-aft (as, for instance, profile B). Therefore, the lower critical must usually be calculated separately for positive and negative $\varphi$'s.

(ii) Even in the case of a profile with fore-and-aft symmetry, the tips may play a more important part when $\varphi$ is large enough. The maximum supervelocity at the tip may become greater than that in the regular region; this will occur when the value of $(- v_x/\vartheta U \cos \varphi)_{\max}$ exceeds more than twice the corresponding value for $\varphi = 0$. It will be seen from Table 5 that this will occur for the profile B if $\varphi$ exceeds $\sim 78 \cdot 5$ deg. It might seem that such angles would not be used. However, the angle of sweep which matters is not that of the true wing but that (appreciably larger) of the Göthert's equivalent wing (*see* Fig. 29), hence the case may occur in practice.

* It must be mentioned that, as shown in Figs. 26 and 27, it is impossible to determine, by applying the linear perturbation method, the maximum supervelocities for negative $\varphi$'s, *i.e.*, for *swept-forward wings*, in the case of profile R. This is due to the fact that the profile possesses a *rounded leading edge*, hence $F'(x)$ becomes $(-\infty)$ at that edge (*see* form. 4.1.1). The true maxima must, of course, be finite, but undoubtedly very large. A similar behaviour is to be expected generally for profiles with rounded nose and maximum thickness well forward. Such profiles are clearly most inappropriate for swept-forward design.

If it does, the isobars in the tip area of a swept-back wing must run more or less similarly to those in the kink area of a swept-forward wing, cutting the tip section at right-angles. In such a case a '*tip critical Mach number*' may be defined. This will lie between the lower critical and unity. Its physical meaning is such that, when $M_0$ gradually increases, first the kink area becomes shock-stalled, later shock waves appear at both tips, and only afterwards the three shock wave areas coalesce. The importance of this 'intermediate' critical must not be over-estimated. However, it is interesting that, in some cases, the critical conditions may, so to speak, attack each semi-wing from both flanks.

(iii) The problem of the lower critical Mach numbers becomes more complicated if the wing *profile is not symmetrical fore-and-aft*. The reason is that, for such profiles, the point of maximum ordinate and that of maximum velocity (in two-dimensional flow) do not coincide. In typical cases, the maximum thickness will be in the front half of the chord (between 40 per cent and 25 per cent chord, say), and the point of maximum supervelocity will usually be located even further forward. For instance, the data for profiles C, Q and R are:

| Profile | Position of maximum thickness (per cent) | Position of maximum supervelocity (in two dimensions) (per cent) |
|---|---|---|
| C | 33·33 | 27·2 |
| Q | 30 | 20·1 |
| R | 30 | $\sim$0* |

* 0 per cent according to linear theory; true position very near the leading edge.

Let us now consider the supervelocity distribution in the central kink section, for a family of swept-back wings with a certain constant profile and with gradually increasing $\varphi$. At the point of maximum thickness we have $F'(x) = 0$, and hence the ratio $(-\, v_x/\vartheta U \cos \varphi)$ will not change with $\varphi$ (*see* form. 4.1.1). Ahead of or behind this point, the ratio will decrease or increase, respectively, as $\varphi$ increases. Hence, the point of maximum supervelocity in the kink will gradually move backwards (as usual), but the maximum of $(-\, v_x/\vartheta U \cos \varphi)$ will initially decrease. Only when the point of maximum supervelocity moves to behind that of maximum thickness (*see* Figs. 22, 24 and 26), will the maximum of $(-\, v_x/\vartheta U \cos \varphi)$ again increase, to reach eventually very high values. Consequently, for small angles of sweep-back within a certain range, the maximum supervelocity at the kink will be smaller than 'at infinity', so that the picture of isobars will differ greatly from that of Fig. 9, and will be similar to that in Fig. 19 (for profile Q). It is seen that some of the 'higher' isobars (*e.g.*, those marked 0·9 and 1·0 in Fig. 19) bend sharply and double back on themselves, without reaching the kink section. It does not seem legitimate in this case to base the determination of the lower critical Mach number on the maximum supervelocity in the ***kink section*** alone, while higher supervelocities occur in nearby sections of the ***kink area***; there being, in addition, points in the front parts of each section where the isobars run in the $y$-direction, so that the full velocity $U$ plus local supervelocity must be taken into account when looking for critical conditions. As all (or almost all) of these highest isobars present such points in a comparatively narrow area near the kink, it seems reasonable simply to replace the kink maximum by that at infinity. In Fig. 28, the curve of $(-\, v_x/\vartheta U \cos \varphi)_{\max}$ against $\varphi$ possesses a considerable part lying below the point K corresponding to $\varphi = 0$. This part should be replaced by a horizontal chord through K. This applies, of course, to profiles C and R as well, but in the former case the difference is insignificant while in the latter it is quite important*.

* The reader will notice that, in Tables 6, 7 and 8, the columns marked 'kink area' correspond to the horizontal chords in Fig. 28, as opposed to 'kink section'.

It is interesting that, if the lower critical Mach number is based on the kink maximum super-velocity, it may sometimes be greater than the upper critical; but this will never happen if the maximum supervelocity ' as at infinity ' is used for calculating lower $M_c$.

(iv) When the *angle of sweep-back* is *large enough* then, even in the case of a *profile with no fore-and-aft symmetry,* the maximum supervelocity at the kink will exceed that ' at infinity '; hence the former should be used for calculating lower $M_c$. However, it *may* happen for such profiles that the maximum supervelocity at the tip is even greater than that at the kink. One must keep in mind that, according to the linear theory, the maximum supervelocity at the tip of a swept-back wing should be equal to half that at the kink of a corresponding swept-forward wing. Now, examining carefully Fig. 28 (and corresponding Tables), we see that, for very large $\varphi$'s, this tip maximum supervelocity may exceed that at the kink. In such cases, the tip section becomes ' first danger spot ', and the *tip critical Mach number becomes true lower critical.* Here we find the explanation why, contrary to the original assertion by Ludwieg[23], shock-waves may start first at the tips of a swept-back wing, instead of in the centre area (*see* Ref. 40, Clarkson's contribution).

The *final conclusion* is that the calculation of lower critical Mach numbers for swept-back wings should be based either on the maximum super-velocity at the kink, or ' at infinity ', or at the tip, whichever is the highest. There will generally be no similar complications in the case of swept-forward wings, for which the kink section will be the first danger spot, unless some quite unusual profiles are used (with maximum thickness far behind 50 per cent chord).

4.2. *Method of Calculating Critical Mach Numbers.*—In Fig. 29, the sketch on the right represents the true wing, past which the compressible flow is being considered (Mach number $M_0$). The wing on the left is the fictitious or ' analogous ' (Göthert's) wing[6, 7], defined in such a way that all dimensions in $x$-direction are unaltered, while those in $y$ and $z$-directions are both reduced in the ratio $\sqrt{(1 - M_0^2)}$. Hence the thickness, thickness ratio and angle of sweep of the analogous wing will be $t'$, $\vartheta'$, $\varphi'$, related to $t$, $\vartheta$, $\varphi$ of the true wing by means of the following relationships*:

$$t' = t(1 - M_0^2)^{1/2}; \quad \ldots \quad (4.2.1)$$

$$\vartheta' = \vartheta(1 - M_0^2)^{1/2}; \quad \ldots \quad (4.2.2)$$

$$\tan \varphi' = \frac{\tan \varphi}{(1 - M_0^2)^{1/2}}\,; \cos \varphi' = \cos \varphi \left(\frac{1 - M_0^2}{1 - M_0^2 \cos^2 \varphi}\right)^{1/2}; \sin \varphi' = \frac{\sin \varphi}{(1 - M_0^2 \cos^2 \varphi)^{1/2}}\,. \quad (4.2.3)$$

If the two-dimensional maximum supervelocity ratio (in incompressible flow) for the true wing profile (in $xz$ plane) is $\delta_i$, the analogous parameter for the fictitious wing will, by linear theory, be reduced in the same ratio as $\vartheta$, *i.e.*:

$$\delta_i' = \delta_i(1 - M_0^2)^{1/2}\,. \quad \ldots \quad (4.2.4)$$

If the induced velocity components in $x$ and $y$-directions, in incompressible flow past the fictitious wing, are $v_x'$ and $v_y'$, the corresponding components on the true wing (in compressible flow) will be, respectively:

$$v_x = v_x'/(1 - M_0^2)\,, \quad \ldots \quad (4.2.5)$$

$$v_y = v_y'/(1 - M_0^2)^{1/2}\,. \quad \ldots \quad (4.2.6)$$

We shall now consider, in turn, upper and lower critical Mach numbers.

(*a*) *Upper criticals.*—Let us consider a section of the true wing in the ' regular ' region (normal section S in Fig. 29). The corresponding section of the fictitious wing will be S'. Resolving the flow at S' into components parallel and normal to the wing edges, we obtain:

$$\left.\begin{aligned} V_p' &= U \sin \varphi'\,, \\ V_n' &= U(\cos \varphi' + \delta_i')\,. \end{aligned}\right\} \quad \ldots \quad (4.2.7)$$

* This definition corresponds exactly to Göthert's original concept. Dickson[26] gave a generalized scheme in which lateral ($y$)-dimensions are reduced in the ratio $(1 - M^2)^{1/2} : 1$, while normal ($z$)-dimensions are reduced in the ratio $(1 - M^2)^{(N-1)/2} : 1$, where $N$ is an arbitrary integer. Göthert's method corresponds obviously to $N = 2$.

Resolving in $x$ and $y$-directions, we get:

$$\left.\begin{aligned} -V_x' &= V_p' \sin\varphi' + V_n' \cos\varphi' = U(1+\delta_i' \cos\varphi')\,, \\ -V_y' &= V_n' \sin\varphi' - V_p' \cos\varphi' = U\delta_i' \sin\varphi'\,. \end{aligned}\right\} \quad .. \quad .. \quad (4.2.8)$$

For the true wing, using (4.2.5) and (4.2.6):

$$\left.\begin{aligned} -V_x &= U\left(1+\frac{\delta_i' \cos\varphi'}{1-M_0^2}\right), \\ -V_y &= U\frac{\delta_i' \sin\varphi'}{(1-M_0^2)^{1/2}}\,, \end{aligned}\right| \quad .. \quad .. \quad .. \quad .. \quad .. \quad .. \quad (4.2.9)$$

or, taking into account (4.2.3) and (4.2.4):

$$\left.\begin{aligned} -V_x &= U\left(1+\frac{\delta_i \cos\varphi}{(1-M_0^2\cos^2\varphi)^{1/2}}\right), \\ -V_y &= U\frac{\delta_i \sin\varphi}{(1-M_0^2\cos^2\varphi)^{1/2}}\,. \end{aligned}\right| \quad .. \quad .. \quad .. \quad .. \quad .. \quad (4.2.10)$$

Finally, resolving the velocity at S into components normal and parallel to the wing edges, we obtain:

$$V_n = -V_x \cos\varphi - V_y \sin\varphi = U\left(\cos\varphi + \frac{\delta_i}{(1-M_0^2\cos^2\varphi)^{1/2}}\right); \quad .. \quad .. \quad (4.2.11)$$

$$V_p = V_y \cos\varphi - V_x \sin\varphi = U \sin\varphi\,. \quad .. \quad .. \quad .. \quad .. \quad .. \quad .. \quad (4.2.12)$$

It is seen that Göthert's method gives the same result as the simple method used in the section 3 of this report and illustrated in Fig. 3; formulae (3.5) and (4.2.11) are identical. That was to be expected and, as regards the regular region, the new procedure may only be looked upon as a useful check. Further, it is clear that the formula (3.6) gives the upper critical Mach number for any given $\delta_i$ and $\varphi$, and our Table 3 and Fig. 4 may be used in this connection. For every particular profile, we know the value of the ratio $\delta_i/\vartheta$, and so we may find the upper critical $M$ for any given $\vartheta$ and $\varphi$, by interpolating Table 3. Thus our Table 4 has been computed, and illustrated by (upper) curves in Figs. 30 to 33.

(*b*) *Lower criticals*.—Here, the method of 'analogous' wing is essential. Let us assume first that the maximum supervelocity occurs in the central kink section (as it always must if the profile is symmetrical fore-and-aft, *e.g.*, profile B). Suppose that we possess, for the given profile, the numerical values of

$$H = \left(-\frac{v_x}{\vartheta U}\right)_{\max} \quad .. \quad .. \quad .. \quad .. \quad .. \quad .. \quad .. \quad (4.2.13)$$

tabulated against $\varphi$ (as in our Tables 5–8 for profiles B, C, Q, R). Let us denote by $H'$ the value corresponding to the angle of sweep $\varphi'$ of the analogous wing (Fig. 29). Then the maximum velocity in the kink section of the analogous wing, in incompressible flow, is:

$$V'_{\max} = U(1+\vartheta' H')\,, \quad .. \quad .. \quad .. \quad .. \quad .. \quad .. \quad .. \quad (4.2.14)$$

and that in the kink of the true wing, in compressible flow, becomes (*see* 4.2.5 and 4.2.2):

$$V_{\max} = U\left(1+\frac{\vartheta' H'}{1-M_0^2}\right) = U\left(1+\frac{\vartheta H'}{(1-M_0^2)^{1/2}}\right). \quad .. \quad .. \quad (4.2.15)$$

It will be seen that $V_{max}$ may be made equal to the maximum velocity $V_m$ in two-dimensional flow, as given by (2.1), provided that

$$H' = \frac{\delta_i}{\vartheta} . \qquad \qquad (4.2.16)$$

This simple formula really solves our problem. Suppose we want to determine lower critical Mach numbers for a range of angles of sweep, given the profile (and the respective $H$ vs. $\varphi$ table) and thickness ratio $\vartheta$. An arbitrary value of $M_0 = M_c$ being assumed, we find $\delta_i$ from Table 1 and then $H'$ from (4.2.16). Then $\varphi'$ is found by interpolating the $H$ vs. $\varphi$ table, and $\varphi$ from (4.2.3). Thus one pair of corresponding values of $\varphi$ and $M_c$ is determined, and the procedure is repeated for several values of $M_c$ until a required range of $\varphi$ is covered. Repeating this process for several values of thickness ratio $\vartheta$, we may obtain a comprehensive diagram similar to those given in Figs. 30 to 33. The computation is easy, once the $H$ vs. $\varphi$ table is available. The method applies to both swept-back and swept-forward wings.

It has been explained in section 4.1 that the central kink is not always the first danger spot, and that the calculation of the lower critical must often be based on the maximum supervelocity 'at infinity' or at the tip, whichever the highest. The method of calculation remains unaltered, but correct values of $H$ must be used. One must bear in mind particularly that, to determine the tip criticals (for large positive $\varphi$'s only), half the values of $H$ for corresponding negative angles must be used.

4.3. *Examples.*—(*a*) *Profile* B: Formulae—*see* Appendix III (III.31 to 36)

Maximum supervelocities—Table 5

Critical Mach numbers—Tables 4 and 9

Diagrams—Figs. 6, 7, 8, 9, 20, 21, 28, 30, 34.

This case is particularly simple, the lower and upper critical Mach numbers for swept-back and swept-forward wings being the same, and the kink section being always decisive for the lower critical. The final results are represented in Fig. 30. It is seen that critical Mach numbers rise consistently with increasing angle of sweep and with decreasing thickness ratio. The differences between the upper and lower criticals are small for small $\varphi$'s but rise to very high values as $\varphi$ increases.

(*b*) *Profile* C: Formulae—*see* Appendix III (III.37 to 41)

Maximum supervelocities—Table 6

Critical Mach numbers—Tables 4, 10, 10a

Diagrams—Figs. 10, 11, 12, 13, 14, 22, 23, 28, 31, 35.

The calculation must be done separately for positive and negative $\varphi$, and the lower criticals are higher for swept-back wings than for swept-forward ones. In the interval $0 < \varphi' < 43$ deg the maximum supervelocity at infinity is greater than at the kink (*see* Fig. 28), and therefore, in this range, the former values should be used. The lower criticals have first been calculated on the basis of the conditions in the kink section, for the whole range of positive $\varphi$'s, and tabulated in Table 10. The additional (lower) values, based on supervelocities 'in the kink area' are given in Table 10a, for the interval $0 < \varphi' < 43$ deg. Fig. 31 contains the curves of upper and lower $M_c$. It is seen that the alternative solutions for moderate positive $\varphi$'s differ little in this case, the error in $M_{cl}$ being always less than $0 \cdot 01$. This is obviously due to the fore-and-aft asymmetry being not very pronounced in the neighbourhood of maximum ordinate. The tip criticals are not shown, as they are always higher than the lower criticals in the range considered.

(*c*) *Profile* Q: Formulae—*see* Appendix III (III.42 to 47)
Maximum supervelocities—Table 7
Critical Mach numbers—Tables 4, 11, 11a, 11b, 11c
Diagrams—Figs. 15, 16, 17, 18, 19, 24, 25, 28, 32, 36.

The profile has some peculiarities which make the calculation more intricate. The maximum ordinate lies as far forward as 30 per cent chord, and the fore-and-aft asymmetry is very pronounced in the region of maximum thickness. At the same time, the rear part of the profile is rather thick, with an almost imperceptible inflexion. The result is that, at zero sweep, the maximum supervelocity lies much ahead of the maximum thickness point, and the rear part of the supervelocity curve (Fig. 24) shows an unusual inflexion. With positive sweep, we have a vast region ($0 < \varphi' < 75$ deg) where the maximum supervelocities at infinity are greater than those at the kink (Fig. 28). Therefore, we have again alternative curves of $M_{cl}$ in Fig. 32, and the differences between them are quite appreciable. Obviously, the lowest curves should be considered as ' correct '. An unusual occurrence is that, at high positive values of $\varphi$, the supervelocity curves in Figs. 24 and 25 exhibit two maxima, the additional rear one being the result of the peculiar profile shape (see also Fig. 19 with the curious rear ' supervelocity peak '). If $\varphi$ is very large, the rear maximum becomes greater than the front one, which means a reduction of the lower criticals. Figs. 24 and 28 also show that, for negative $\varphi$'s, the maximum supervelocities rise to very high values which eventually become more than double those for positive $\varphi$'s. In this region the tips become ' first danger spots ', and the tip criticals should be taken as true lower criticals (*see* Fig. 32). This could be prevented by a gradual change of profile in the tip areas so that, at the very tips, the profile should be more or less similar to B.

(*d*) *Profile* R: Formulae—*see* Appendix III (III.48 to 59)
Maximum supervelocities—Table 8
Critical Mach numbers—Tables 4, 12, 12a
Diagrams—Figs. 26, 27, 28, 33, 37.

The profile possessing a rounded nose, the first-order theory is less reliable as regards the velocity field near the leading edge and—in the given case—it fails for all negative $\varphi$'s, *i.e.*, for swept-forward wing. It is clear, however, that maximum supervelocities for swept-forward wings with such a profile will be very large, and so this profile would be most inappropriate for swept-forward design. We may also expect that tip criticals will become important for comparatively low values of positive $\varphi$, but they cannot be calculated by using the pure linear method. Fig. 33 therefore shows only two sets of curves for lower critical Mach numbers (those based on maximum supervelocities in the kink section or ' in the kink area ') and, again, the lower curves are the ' correct ' ones. The differences between the alternative curves are very considerable in this case. Fig. 33 may only be considered as correct, if the tips are designed with different profiles, so as to prevent the premature shock-stall at the tips.

5. *General Discussion and Conclusions.*—The lower and upper critical Mach numbers have been defined in sub-section 4.1, the methods of calculating them given in 4.2, and several examples worked out as described in 4.3. The question now arises as to the practical meaning of both criticals and the basis they provide to a designer for predicting the characteristics and comparing the merits of particular swept wings. A complete quantitative analysis would require a solution of the formidable problem of transonic phenomena. However, we can try to clear the matter, at least qualitatively, by the following simple reasoning:—

For an *infinite straight wing* ($\varphi = 0$), there is only one critical Mach number $M_c$ (always less than 1), the same for all sections. Below this there are no shock-waves, and no wave drag. Above the critical, shock-waves appear, initially in the region of maximum velocities, and simultaneously in all sections. The flow becomes transonic (subsonic and supersonic mixed);

and a wave drag results*, the coefficient $C_D$ rising steeply up to about $M_0 = 1$ when it reaches its maximum value. For Mach numbers above 1, the flow becomes essentially supersonic (supposing the wing is thin, and there are no detached shock-waves), and $C_D$ decreases soon, following approximately the Ackeret's law, *i.e.*:

$$(C_D)_{\varphi=0} = K\vartheta^2/(M_0^2 - 1)^{1/2}, \quad \ldots \quad \ldots \quad \ldots \quad \ldots \quad (5.1)$$

where $K$ is a constant factor, depending only on the profile geometry.

If the thickness ratio were very small, $M_c$ would differ very little from 1; in such a case as $M_0$ passes through the critical value, the wave-drag coefficient would jump from 0 to its maximum value almost instantaneously, to fall afterwards according to (5.1). The transitory range of Mach numbers (approximately between $M_c$ and 1) widens considerably as the thickness ratio increases.

If the infinite wing is *sheared* through an angle $\varphi$, the fundamental behaviour remains very similar but, as only the flow component at right-angles to the wing edges counts, the critical Mach number assumes a new value $M_{cs}$. This is always greater than $M_c$; it may exceed 1, if $\varphi$ is large and $\vartheta$ not too large, but it can never exceed sec $\varphi$. In the case of vanishingly small thickness, the critical would be simply sec $\varphi$; usually, there will be a transitory range between $M_{cs}$ and sec $\varphi$, where $C_D$ rises more or less steeply. When $M_0$ exceeds sec $\varphi$, the drag coefficient will fall again, the equation (5.1) being replaced by (*see* Refs. 30 and 37) :

$$C_D = K\vartheta^2/(M_0^2 - \sec^2\varphi)^{1/2} . \quad \ldots \quad \ldots \quad \ldots \quad (5.2)$$

Considering finally a *true swept wing*, with two symmetrical halves and a kink, we have to deal with two critical Mach numbers. The lower one ($M_{cl}$) corresponds to critical conditions being reached at the first danger points, where the maximum total velocities (in flight direction) coincide with the isobars running perpendicular to that direction. These points often lie in the central kink, sometimes away from it (theoretically at infinity, practically somewhere in the kink area), and in some extreme cases at the tips. The lower critical normally increases with the angle of sweep, but always remains below 1. For the parts of the wing adjoining the first danger points, it plays a similar role to that of $M_c$ for unswept wings. The upper critical $M_{cu}$ is almost the same as that ($M_{cs}$) pertaining to infinite sheared wings with the same angle $\varphi$. There will be again a transitory range, from $M_{cu}$ to sec $\varphi$. It must be borne in mind that there is a continuous change-over from most endangered to least endangered sections, and hence there should be a continuous sequence of critical Mach numbers, and even a continuous sequence of transitory ranges. It would, of course, be futile to try to calculate ' local criticals '.

---

* The noticeable rise of the drag will normally occur for Mach numbers somewhat exceeding $M_c$. This is natural, as the intensity of the shock-waves must be very small initially, and so we must always reckon with a certain delay of the balance-measurable effects. However, when discrepancies between the ' theoretical ' and all sorts of ' practical ' critical Mach numbers were first noticed, they led to a trend of pessimism as to the significance of the former. This may be seen in some papers by Lee[29, 33], and especially by Smelt[31] who went so far as to assert that ' this critical Mach number bears no relation whatever to the Mach number at which the drag begins to rise '. The opinion was at least premature at a time, when so little was known about actually calculating critical Mach numbers.

An interesting method of accounting for the discrepancies between the calculated and observed criticals was suggested by Griffith[21] and McKinnon Wood[22]. They both interpreted the criterion for wave drag (velocity component along the *resultant* acceleration = local velocity of sound) in such an ' extremist ' way that, for particles travelling along the surface, the acceleration should include the component normal to wing surface, due to the curvature. Some two-dimensional calculations on these lines were done by Beavan and Lock[25, 42], without conclusive results. The method leads to some paradoxical consequences; *e.g.*, at the point of maximum velocity the relevant velocity component would be zero. The matter is complicated and far from clear. It seems that the interpretation has never been really adopted either in Britain or elsewhere. From the point of view of our linearized method, however, no such question arises. According to this method, the resultant velocities (and pressures) do not depend on the normal co-ordinate $z$, and the isobaric surfaces are all cylindrical. It is therefore sufficient to consider the velocity field in $xy$-plane, and the velocity components normal to the plane isobars.

It becomes clear that, as a result of the geometry of a swept wing, we have finally to deal with a vastly extended 'transitory' or transonic range of Mach numbers (from $M_{cl}$ through 1, $M_{cu}$ up to sec $\varphi$). When $M_0$ gradually increases through this range, the particular sections of the wing gradually experience their transitory stages. The flow over some sections is already essentially supersonic (with decreasing $C_D$) while that over others is still in the transonic stage (with sharply increasing $C_D$), and some may still be in the subsonic stage (with no wave drag). The entire process is intricate and may present many unexpected features. However, when $M_0$ exceeds 1, the methods of supersonic aerodynamics may help to explain the course of aerodynamic changes. Several authors[27, 28, 35, 37, 39] have given results of drag calculations for swept wings in supersonic flow, mostly for the simplest case of double-wedge profile. The most enlightening are perhaps von Kármán's results[37]. In connection with Fig. 13 of his paper, he shows how the wave-drag coefficient of an 'arrowhead' swept-back wing (of considerable aspect ratio) varies with Mach number, on the basis of an approximate calculation. It appears that $C_D$ starts with a very small value at $M_0 = 1$ and then rises, first slowly and then at a strongly increasing rate, until it reaches a finite maximum at $M_0 = \sec \varphi$; finally, it decreases again, soon following the formula (5.2). The approximate method, as used by von Kármán, clearly does not take into account the incremental velocities ($v_x$) due to thickness, and therefore, in his picture, the lower critical Mach number is 1 and the upper one sec $\varphi$ (*cf.* Fig. 9 of Ref. 37). Between these values, the 'regular' region of the wing is in subsonic conditions ($M_0 \cos \varphi < 1$), and almost the entire wave drag originates in the kink area (*see* Fig. 11 of Ref. 37, where the drag distribution on a finite sheared wing is shown). It is interesting that, according to von Kármán, the resultant wave drag of the downstream tip is zero, and this seems to confirm our suggestion (section 4.1) that the seemingly critical conditions in the tip areas are of little importance*.

In reality, the variation of the wave-drag coefficient with Mach number should differ somewhat from the simplified von Kármán's picture. Its first appearance should not occur at $M_0 = 1$ but at $M_{cl}$ (or somewhat higher, if we look for clearly appreciable effects). Similarly, the maximum drag should take place not at $M_0 = \sec \varphi$ but rather at $M_{cu}$ (or possibly at some value between $M_{cu}$ and sec $\varphi$). If we aim at utilizing the swept-wing design in order to avoid wave drag completely, then the flight Mach number must clearly not exceed $M_{cl}$, and then the only important thing would be to raise this lower critical as high as possible. If, however, a small wave drag can be tolerated, then the flight Mach number may exceed $M_{cl}$ to a certain extent; in such a case, we should aim at as low rate of increase of $C_D$ as possible, and also keep well below $M_{cu}$. From this point of view, the upper critical may be quite important, and it should be as high as possible. The best formulation perhaps would be, that the difference $(M_{cu} - M_{cl})$ should be as large as possible. It must be stressed, however, that this reasoning applies fully to wings of fairly large aspect ratio only, where the regular regions embrace a major part of the wing surface, thus the wave drag caused by the small kink region is of comparatively little significance. As the aspect ratio decreases, the regular regions gradually dwindle and almost disappear, so that little but the kink and tip areas remain. Hence, at small aspect ratios, the upper critical becomes less and less important. This is corroborated by Fig. 14 of Ref. 37 which shows that in such cases, the values of $C_D$ at $M_0 \simeq 1$ are very much larger than at large aspect ratios, while the peaks (at $M_0 \simeq \sec \varphi$) are considerably reduced.

The *most important question for a designer* is to know how the critical Mach numbers depend on the main design factors which are: thickness ratio, angle of sweep, and profile†. This is what our Figs. 30 to 33 aim at showing, for four representative profiles. It is seen that, although the four pictures are qualitatively similar, the numerical differences are considerable. Ludwieg[23] expected that at least the gains in the (lower) critical Mach numbers due to sweep should be

* At least as long as the maximum supervelocities at the tip do not exceed those in the regular part. If they do, we should expect wave drag at the tips, and therefore our 'tip critical Mach numbers' in the case of large $\varphi$ and profiles strongly asymmetrical fore-and-aft (*see* section 4.1 (iii)) should have some practical significance. One must realise that von Kármán's graphs apply to the double-wedge profile only; for other profiles the results may differ, but the calculation would be laborious.

† It is hoped to describe the effects of taper in a later report.

practically the same for different profiles. To check this, we have replotted the values of $M_{cl}$ at varying $\varphi$ against $M_c$ for $\varphi = 0$, for all four profiles, in Figs. 34 to 37. It is seen that Ludwieg's prediction was not correct, the four diagrams differing very appreciably. The differences in the effect of *sweep-forward* are particularly striking: for the profiles strongly asymmetrical fore-and-aft, small or moderate sweep-forward may often be detrimental for $M_{cl}$, and only for very large negative $\varphi$'s there is some, rather disappointing, gain*. It is obvious that, if swept-forward wings are to be used, their profiles should be nearly symmetrical fore-and-aft, perhaps even with maximum thickness slightly further back than 50 per cent chord—if compatible with other requirements.

As to the *swept-back wings*, the following point should be stressed, with reference to Figs. 38 and 39 containing comparative diagrams of $M_{cu}$ and $M_{cl}$ for different profiles and thickness ratios $0 \cdot 1$ and $0 \cdot 2$. At small $\varphi$'s, the decisive factor for the lower criticals (as always for the upper ones), is the maximum supervelocity ratio: the lower the value of $\delta_i$, the higher that of $M_{cl}$. Hence, in this range, B seems the best, C and Q follow next, and R is the worst of the four profiles considered. The position alters considerably for large $\varphi$'s. At about 45 deg, there is little difference in the performance of the profiles, and above that, the order of precedence is partly inverted. However, at quite large $\varphi$'s, the wings with profiles Q and R will be severely handicapped by their 'tip criticals'. To avoid this, the simple method is to change the profiles spanwise towards the tips, so as to have nearly fore-and-aft symmetry there.

Another interesting question may now be considered. It has been suggested[38] that a considerable improvement in the (lower) critical Mach number could be obtained by such a change in the geometry of the kink and possibly also by such fuselage interference effects, which would result in artificial straightening of the isobars in the kink area. It might be said that it is hoped to impart the properties of an infinite sheared wing to the (less fortunate) kink area. The idea may seem promising, but the matter is not so simple.

Even if it is possible to straighten the isobars so that the supervelocities become constant along the $\xi$-parallels almost down to the central kink section, it does not follow that the critical conditions in the kink area will be the same as in the regular regions of the wing. The isobars must cut the central kink plane at right-angles[34, 43], and thus the lower critical will depend on the total velocity $U$ (not on $U \cos \varphi$) plus an appropriate supervelocity. Therefore the lower critical will always be less than one, while the upper critical may exceed unity. The only possible gain is an increase in the lower critical (to a value always less than one), due to a certain decrease in the supervelocity, as in the case of profile B. But, in many cases, especially if the profile is strongly asymmetrical fore-and-aft, and if the angle of sweep-back $\varphi$ is not very large, the maximum supervelocity in the original kink may be less than that in the regular region. In such cases, the effect of straightening the isobars would be to increase the supervelocities in the kink area.

The magnitude of the maximum supervelocity in the kink section is of more importance for the lower critical Mach number than the shape of the isobars. In addition, it is difficult to obtain even approximately rectilinear isobars in the kink area—and even if this were achieved at a certain Mach number, the shape of the isobars would alter with the Mach number.

---

* This is shown in Fig. 36 for the profile Q, but not in Fig. 37, because the lower criticals cannot be determined for the profile R and negative $\varphi$ by the first-order method. The effect should, of course, be even more pronounced for the profile R.

## LIST OF SYMBOLS

| | | |
|---|---|---|
| $A$ | | Coefficient, *see* (III.7) |
| $a$ | | Speed of sound |
| $a_0$ | | Speed of sound in undisturbed flow |
| $a_c$ | | Speed of sound in critical conditions (local Mach number = 1) |
| $B$ | | Coefficient, *see* (III.7) |
| $b$ | | Half-chord of wing section |
| $b_1$ | | Coefficient, *see* (III.31) |
| $C$ | | Coefficient, *see* (III.7) |
| $C_p$ | = | $\frac{2(p - p_0)}{\rho V^2}$ Pressure coefficient |
| $C_{pc}$ | | Pressure coefficient in critical conditions (local Mach number = 1) |
| $C_{pi}$ | | Pressure coefficient in incompressible flow |
| $c$ | = | $2b$ Chord of the wing section |
| $F(x)$, $F(x + y \tan \varphi)$ | | Function determining the wing section or surface |

$$\left.\begin{aligned} F_1 &= \frac{1 + \xi + (r_1 - \eta) \tan \varphi}{1 - \xi - (r_2 - \eta) \tan \varphi} = \sqrt{(F_2 F_5)} \\ F_2 &= \frac{r_1 + (1 + \xi) \sin \varphi \cos \varphi + \eta \cos 2\varphi}{r_2 - (1 - \xi) \sin \varphi \cos \varphi + \eta \cos 2\varphi} \\ F_4 &= \frac{r_1 + (1 + \xi) \cos \varphi - \eta \sin \varphi}{r_2 - (1 - \xi) \cos \varphi - \eta \sin \varphi} \\ F_5 &= \frac{r_1 + (1 + \xi) \sin \varphi \cos \varphi - \eta}{r_2 - (1 - \xi) \sin \varphi \cos \varphi - \eta} \end{aligned}\right\} \text{ see table of auxiliary functions, Ref. 48, p. 32}$$

| | | |
|---|---|---|
| $H$ | = | $\left(-\frac{v_x}{\vartheta U}\right)_{\max}$ Maximum supervelocity ratio per unit thickness ratio |
| $k$ | | Coefficient, *see* (III.7, 8) and (III.31, 32) |
| ln | | Natural logarithm |
| $M$ | = | $V/a$ Local Mach number |
| $M_0$ | = | $U/a_0$ Mach number of undisturbed flow |
| $M_c$ | | Critical Mach number (critical value of $M_0$) |
| $M_{cl}$, $M_{cu}$ | | Lower and upper critical Mach number for a swept wing |
| $M_{cs}$, $M_{cy}$ | | Critical Mach numbers for an infinite wing, sheared or yawed |
| $m_0, m_1, m_2, m_3$ | | Polynomials in $\xi$, *see* (III.19) |
| $n_0, n_1, n_2, n_3, n_4$ | | Polynomials in $\xi$, *see* (III.11) |
| $P$ | | Auxiliary variable, *see* (III.4) |
| $p$ | | Pressure |
| $p_0$ | | Pressure in undisturbed flow |

| | | |
|---|---|---|
| $r$ | | *see* (III.5) |
| $r_1$ | $=$ | $\sqrt{[(1+\xi)^2 \cos^2 \varphi - 2(1+\xi) \sin \varphi \cos \varphi + \eta^2]}$ |
| $r_2$ | $=$ | $\sqrt{[(1-\xi)^2 \cos^2 \varphi + 2(1-\xi) \sin \varphi \cos \varphi + \eta^2]}$ |
| $T$ | | Auxiliary function of $\xi$, *see* (III.26, 27) |
| $T_m$ | | Value of $T$ for $\xi = \xi_m$ |
| $t$ | | Thickness of wing section |
| $t'$ | | Thickness of section of analogous (Göthert's) wing (*see* Fig. 29) |
| $U$ | | Velocity of undisturbed flow |
| $V$ | | Local velocity of the flow |
| $V_c$ | | Local velocity in critical conditions |
| $V_m$ | | Maximum value of $V$ in compressible two-dimensional flow |
| $V_n$ | | Local velocity component normal to the edges of a sheared or yawed wing |
| $V_{nc}$ | | Critical value of $V_n$ |
| $v_x$ | | $x$-component of the induced velocity, or supervelocity |
| $x$ | | Chordwise co-ordinate, positive forwards |
| $\bar{x}$ | | Chordwise co-ordinate of the source filament |
| $y$ | | Spanwise co-ordinate, positive to starboard |
| $z$ | | Vertical co-ordinate |
| $\gamma$ | | Adiabatic constant |
| $\delta$ | $=$ | $\left(-\frac{v_x}{U}\right)_{\max}$ Maximum supervelocity ratio in two-dimensional flow |
| $\delta_i$ | | Value of $\delta$ in incompressible flow |
| $\delta_i'$ | | Value of $\delta_i$ for analogous (Göthert's) wing |
| $\vartheta$ | $=$ | $t/c$ Thickness ratio of wing section |
| $\eta$ | $=$ | $y/b$ Non-dimensional spanwise co-ordinate |
| $\mu$ | $=$ | $1 - M_c^2$ Auxiliary variable, *see* (I.25) |
| $\mu_0$ | | First approximate value of $\mu$, *see* (I.28) |
| $\xi$ | $=$ | $(x + y \tan \varphi)/b$ Non-dimensional chordwise co-ordinate on a sheared or swept wing |
| $\xi_m$ | | Value of $\xi$ corresponding to maximum supervelocity |
| $\xi_n$ | | Value of $\xi$ corresponding to $z_{\max}$ of the profile |
| $\rho$ | | Air density |
| $\rho_0$ | | Air density in undisturbed flow |
| $\varphi$ | | Angle of sweep (positive for sweep-back, negative for sweep-forward) |
| $\varphi'$ | | Angle of sweep of analogous (Göthert's) wing, *see* Fig. 29 |

# REFERENCES


| No. | Author | Title, etc. |
|---|---|---|
| 1 | H. Glauert .. .. .. .. .. | The Effect of Compressibility on the Lift of Aerofoils. *Proc. Roy. Soc.* A, Vol. 118, p. 113. 1927. |
| 2 | L. Prandtl .. .. .. .. .. | Über Strömungen deren Geschwindigkeiten mit der Schallgeschwindigkeit vergleichbar sind. *Journal of the Aeronautical Research Institute of the University of Tokyo.* No. 6. 1930. |
| 3 | A. Busemann .. .. .. .. | Aerodynamischer Auftrieb bei Überschallgeschwindigkeiten. Proceedings, Volta Congress. Reale Accademia d'Italia. October, 1935. |
| 4 | L. Prandtl .. .. .. .. .. | Allgemeine Überlegungen über die Strömung zusammendrückbarer Flüssigkeiten. Para. 3. Proceedings, Volta Congress. Reale Accademia d'Italia. October, 1935. |
| 5 | F. Ringleb .. .. .. .. .. | Exakte Lösungen der Differentialgleichungen einer adiabatischen Gasströmung. *Z.A.M.M.* 1940. (*cf.* A.R.C. 6598, also Temple and Yarwood, A.R.C. 6347.) |
| 6 | B. Göthert .. .. .. .. .. | Ebene und räumliche Strömung bei hohen Unterschallgeschwindigkeiten (Erweiterung der Prandtlschen Regel). Meeting 'Hochgeschwindigkeit'. Braunschweig, 3.9.1940. *Lilienthal-Gesellschaft.* Bericht 127, p. 97. |
| 7 | B. Göthert .. .. .. .. .. | Berechnung des Geschwindigkeitsfeldes von Pfeilflügeln bei hohen Unterschallgeschwindigkeiten. Meeting 'Hochgeschwindigkeit'. Göttingen, 26–27.9.1940. *Lilienthal-Gesellschaft.* Bericht 127, p. 52. |
| 8 | H. Ludwieg .. .. .. .. | Pfeilflügeln bei hohen Geschwindigkeiten. Meeting 'Hochgeschwindigkeit'. Göttingen, 26.7.9.1940. *Lilienthal-Gesellschaft.* Bericht 127, p. 44. |
| 9 | Th. von Kármán .. .. .. .. | Compressibility Effects in Aerodynamics. *J.Ae.Sci.*, Vol. 8, No. 9. July, 1941. |
| 10 | R. C. Pankhurst and J. F. C. Conn .. | Physical Properties of the Standard Atmosphere. R. & M. 1891. January, 1941. |
| 11 | A. D. Young .. .. .. .. | A Survey of Compressibility Effects in Aeronautics. A.R.C. 5749. (Unpublished.) |
| 12 | W. G. Bickley .. .. .. .. | Note on Conditions for the Breakdown of Steady Continuous Irrotational Isentropic Flow of a Gas. A.R.C. 5649. February, 1942. (Unpublished.) |
| 13 | G. Temple and J. Yarwood .. .. | The Approximate Solution of the Hodograph Equations for Compressible Flow. A.R.C. 6107. (Unpublished.) |
| 14 | S. Goldstein and A. D. Young .. .. | The Linear Perturbation Theory of Compressible Flow with Applications to Wind-Tunnel Interference. R. & M. 1909. July, 1943. |
| 15 | M. G. Scherberg .. .. .. .. | Regions of Infinite Acceleration and Flow Realms in a Compressible Fluid. *J.Ae.Sci.*, Vol. 10, No. 3. July, 1943. |
| 16 | W. G. Bickley .. .. .. .. | Note on the Acceleration in the Two-dimensional Irrotational Motion in a Compressible Fluid. A.R.C. 7414. (Unpublished.) |
| 17 | L. M. Greene .. .. .. .. | The Attenuated Flow of Compressible Fluids. *J.Ae.Sci.*, Vol. 12, No. 3. July, 1945. |
| 18 | C. N. H. Lock and R. G. Fowler .. .. | Yaw and Sweepback at High Mach Number. A.R.C. 8718. May, 1945. (Unpublished.) |
| 19 | R. Smelt .. .. .. .. .. | Notes on Discussion with the Staff of Focke-Wulf Ltd. Para. 2.4. R.A.E. Technical Note Aero. 1644. May, 1945. |
| 20 | R. McKinnon Wood .. .. .. | Notes on Sweptback Wings for High Speeds. A.R.C. 8806. September, 1945. (Unpublished.) |
| 21 | A. A. Griffith .. .. .. .. | Note on the Criterion for Wave-Drag in Supersonic Flight. A.R.C. 9463. January, 1946. (Unpublished.) |

| No. | Author | Title, etc. |
|---|---|---|
| 22 | R. McKinnon Wood .. .. .. | A Note on the Critical Mach Number. A.R.C. 9435. February, 1946. (Unpublished.) |
| 23 | H. Ludwieg .. .. .. .. | Improvement on the Critical Mach Numbers of Aerofoils by Sweep-back. M.A.P. Völkenrode. R. & T. 84. May, 1946. |
| 24 | W. G. Bickley .. .. .. .. | Critical Conditions for Compressible Flow. R. & M. 2330. May, 1946. |
| 25 | J. A. Beavan .. .. .. .. | Application of a New Definition of Critical Mach Number to a Profile. A.R.C. 9787. July, 1946. (Unpublished.) |
| 26 | R. Dickson .. .. .. .. | The Relationship between the Compressible Flow round a Swept-back Aerofoil and the Incompressible Flow round Equivalent Aerofoils. A.R.C. 9986. August, 1946. |
| 27 | R. T. Jones .. .. .. .. | Thin Oblique Airfoils at Supersonic Speed. N.A.C.A. Technical Note 1107. September, 1946. |
| 28 | A. E. Puckett .. .. .. .. | Supersonic Wave Drag of Thin Airfoils. *J.Ae.Sci.*, Vol. 13, No. 9. September, 1946. |
| 29 | G. Lee .. .. .. .. .. | The Case for the Tailless Aircraft. *J.R.Ae.S.* November, 1946. Pp. 884–5. |
| 30 | S. B. Gates .. .. .. .. | Swept Wings in Supersonic Flight. R. & M. 2818. December, 1946. |
| 31 | R. Smelt .. .. .. .. .. | A Critical Review of German Research on High-Speed Flow. *J.R.Ae.S.* December, 1946. Pp. 911–915; *see also* contribution in discussion by A. Robinson, ibidem, p. 929. |
| 32 | H. W. Liepmann and A. E. Puckett .. | Introduction to Aerodynamics of a Compressible Fluid. *Galcit* Aeronautical Series. N. York and London. 1947. Chapters 9 and 15, esp. form. (9.3). |
| 33 | G. Lee .. .. .. .. .. | Tailless Aircraft Design Problems. *J.R.Ae.S.* February, 1947. |
| 34 | S. Neumark .. .. .. .. | Velocity Distribution on Straight and Swept-back Wings of Small Thickness and Infinite Aspect Ratio at Zero Incidence. R. & M. 2713. May, 1947. |
| 35 | S. M. Harmon and M. D. Swanson .. | Calculations of the Supersonic Wave Drag of Non-lifting Wings with Arbitrary Sweepback and Aspect Ratio. N.A.C.A. Technical Note 1319. May, 1947. |
| 36 | R. T. Jones .. .. .. .. | Subsonic Flow over Thin Oblique Airfoils at Zero Lift. N.A.C.A. Report 902. 1948. |
| 37 | Th. von Kármán .. .. .. .. | Supersonic Aerodynamics—Principles and Applications. *J.Ae.Sci.*, Vol. 14, No. 7. July, 1947. |
| 38 | D. Küchemann .. .. .. .. | Design of Wing Junction, Fuselage and Nacelles to Obtain the Full Benefit of Swept-back Wings at High Mach Number. A.R.C. 11,035. August, 1947. (To be published.) |
| 39 | W. G. A. Perring .. .. .. .. | High Speed Performance. Anglo-American Aeronautical Conference, London, 3–5 September, 1947; *Proceedings*, published by R.Ae.S. London. 1948. Pp. 197–209. |
| 40 | E. J. Richards .. .. .. .. | Practical Design Problems arising from Sweep-back. Anglo-American Aeronautical Conference, London 3–5 September, 1947; *Proceedings*, published by R.Ae.S. London. 1948. Pp. 381 *et seq.*, *see also* contributions in discussion by G. H. Lee, R. M. Clarkson, S. Neumark, L. W. Rosenthal, C. N. H. Lock, ibidem, pp. 397–402. |
| 41 | A. D. Young and S. Kirkby .. .. | Application of the Linear Perturbation Theory to Compressible Flow about Bodies of Revolution. R. & M. 2624. September, 1947. |
| 42 | C. N. H. Lock and J. A. Beavan .. | The Higher Critical Mach Number. A.R.C. 11,106. December, 1947. (Unpublished.) |
| 43 | F. Ursell .. .. .. .. .. | Notes on the Linear Theory of Incompressible Flow Round Symmetrical Swept-back Wing at Zero Lift. A.R.C. 11,679. July, 1948 (also: The *Aeronautical Quarterly*. R.Ae.S. Vol. I, Part 1. May, 1949). |

## REFERENCES—*continued*

| No. | Author | Title, etc. |
|---|---|---|
| 44 | J. Weber .. .. .. .. .. | Application of Theory of Incompressible Flow around a Swept Wing at High Subsonic Mach Numbers. A.R.C. 11,774. July, 1948. (To be published.) |
| 45 | M. J. Lighthill .. .. .. .. | Methods for Predicting Phenomena in the High-speed Flow of Gases. Paper presented to the 7th International Congress of Applied Mechanics, London, September, 1948, and published in the *J.Ae.Sci.*, Vol. 16, No. 2. February, 1949. |
| 46 | S. Neumark .. .. .. .. | Critical Mach Numbers for Swept-back Wings. Paper presented to the 7th International Congress of Applied Mechanics, London, September, 1948, and published in the *Aeronautical Quarterly*. R.Ae.S. Vol. II. August, 1950. |
| 47 | R. V. Hess and C. S. Gardner .. .. | Study by the Prandtl-Glauert Method of Compressibility Effects and Critical Mach Number for Ellipsoids of Various Aspect Ratios and Thickness Ratios. N.A.C.A. Technical Note 1792. January, 1949. |
| 48 | S. Neumark and J. Collingbourne .. | Velocity Distribution on Untapered Sheared and Swept-back Wings of Small Thickness and Finite Aspect Ratio at Zero Incidence. R. & M. 2717. March, 1949. |
| 49 | J. Weber .. .. .. .. .. | Low-Speed Measurements of Pressure Distribution near Tips of Swept-back Wings at No Lift. A.R.C. 12,421. March, 1949. (Unpublished.) |
| 50 | J. Weber .. .. .. .. .. | Design of Wing Junction, Fuselage and Nacelles to Obtain the Full Benefit of Swept-back Wings at High Mach Number. A.R.C. 12,493. May, 1949. (To be published.) |
| 51 | A. Busemann .. .. .. .. | The Drag Problem at High Supersonic Speeds. *J.Ae.Sci.*, Vol. 16, No. 6. June, 1949. |

## APPENDIX I (to Section 2)

*Derivation and Analysis of Formulae for Critical Mach Numbers in Two-dimensional Flow*

Let us consider a two-dimensional compressible flow past an arbitrary profile (Fig. 1a). The velocity of undisturbed flow is denoted by $U$, while $p_0$, $\rho_0$, $a_0$, $M_0$ are the corresponding values of pressure, density, speed of sound, and Mach number. At a certain point A of the profile, the velocity will be:—

$$V = U(1 + \delta) , \qquad \text{(I.1)}$$

and $p$, $\rho$, $a$, $M$ will denote the corresponding (local) values of the respective quantities. It will suffice to consider only that point where $V$ (and hence $\delta$) has its maximum value, so that $\delta$ is the maximum supervelocity ratio.

If $V$ (or $\delta$) is known, we may determine all other physical variables at A, in particular:—

from Bernoulli's equation:
$$a^2 = a_0^2 - \frac{\gamma - 1}{2} (V^2 - U^2) , \qquad \text{(I.2)}$$

from adiabatic relationship:
$$\frac{p}{p_0} = \left(1 - \frac{\gamma - 1}{2} \frac{V^2 - U^2}{a_0^2}\right)^{\frac{\gamma}{\gamma-1}}, \qquad \text{(I.3)}$$

hence the pressure coefficient:—

$$C_p = -\frac{2a_0^2}{\gamma U^2}\left[1 - \left(1 - \frac{\gamma - 1}{2} \frac{V^2 - U^2}{a_0^2}\right)^{\frac{\gamma}{\gamma-1}}\right], \qquad \text{(I.4)}$$

and the local Mach number:—

$$M^2 = \frac{V^2}{a_0^2 - \dfrac{\gamma - 1}{2} (V^2 - U^2)} . \qquad \text{(I.5)}$$

The quantities $a$, $V$ and $C_p$ may also be represented in terms of the local Mach number $M$, as follows:—

$$a^2 = a_0^2 \frac{1 + \frac{1}{2}(\gamma - 1)M_0^2}{1 + \frac{1}{2}(\gamma - 1)M^2} , \qquad \text{(I.6)}$$

$$V^2 = U^2 \frac{\frac{1}{2}(\gamma - 1) + 1/M_0^2}{\frac{1}{2}(\gamma - 1) + 1/M^2} , \qquad \text{(I.7)}$$

$$C_p = -\frac{2}{\gamma M_0^2}\left[1 - \left(1 - \frac{\gamma - 1}{2} \frac{M^2 - M_0^2}{1 + \frac{1}{2}(\gamma - 1)M^2}\right)^{\frac{\gamma}{\gamma-1}}\right] . \qquad \text{(I.8)}$$

Suppose now that the local Mach number $M$ becomes $= 1$, which means that $M_0$ is critical for the given profile, or alternatively: that $V$ and $C_p$ assume critical values for the given $M_0$. Then (I.6, 7, 8) become:—

$$V_c^2 = a_c^2 = U^2\left(1 + \frac{2}{\gamma + 1} \frac{1 - M_0^2}{M_0^2}\right) = a_0^2\left(1 - \frac{\gamma - 1}{\gamma + 1} (1 - M_0^2)\right), \qquad \text{(I.9)}$$

(*cf.* 2.3), and:—

$$C_{pc} = -\frac{2}{\gamma M_0^2}\left[1 - \left(1 - \frac{\gamma - 1}{\gamma + 1} (1 - M_0^2)\right)^{\frac{\gamma}{\gamma-1}}\right], \qquad \text{(I.10)}$$

while the critical value of the supervelocity ratio $\delta$ becomes:—

$$\delta_c = \left(1 + \frac{2}{\gamma + 1} \frac{1 - M_0^2}{M_0^2}\right)^{1/2} - 1 . \qquad \text{(I.11)}$$

Suppose now that the Mach number $M_0$ is small, so that the flow may be considered as incompressible (Fig. 1b). The formula (I.4) may then be expanded and yields:—

$$C_{p\,i} = -(V_i^2/U^2 - 1) = -(2\delta_i + \delta_i^2)\,, \quad \ldots \qquad \text{(I.12)}$$

which is the known relationship between $C_{p\,i}$ and $\delta_i$ in incompressible flow. If $\delta_i$ is small, then, to the first order:—

$$C_{p\,i} \simeq -2\delta_i\,. \qquad \ldots \qquad \text{(I.13)}$$

It is now interesting to determine how far an approximate relationship analogous to (I.13) applies in compressible flow. Let us expand (I.4) in powers of

$$\frac{V^2 - U^2}{a_0^2} = (2\delta + \delta^2)M_0^2\,;$$

we obtain the following series:—

$$C_p = -2\delta - (1 - M_0^2)\delta^2 + M_0^2\left(1 - \frac{2-\gamma}{3}M_0^2\right)\delta^3$$

$$+ M_0^2\left\{\frac{1}{4} - \frac{2-\gamma}{2}M_0^2 + \frac{(2-\gamma)(3-2\gamma)}{12}M_0^4\right\}\delta^4 \ldots, \qquad \ldots \qquad \text{(I.14)}$$

the inversion of which is*:—

$$\delta = -\tfrac{1}{2}C_p - \tfrac{1}{8}(1 - M_0^2)C_p^2 - \tfrac{1}{16}\left(1 - M_0^2 + \frac{1+\gamma}{3}M_0^4\right)C_p^3$$

$$- \tfrac{1}{128}\left(5 - 6M_0^2 + \frac{7+4\gamma}{3}M_0^4 - \frac{(\gamma+1)(2\gamma+1)}{3}M_0^6\right)C_p^4 \ldots \qquad \text{(I.15)}$$

It is seen that, again, to the first order:—

$$C_p \simeq -2\delta\,, \qquad \ldots \qquad \text{(I.16)}$$

and that the error due to the use of this approximate relationship, is rather smaller than in the incompressible case, but still appreciable.

To calculate the critical Mach number for a given profile, there is a choice between the formulae (I.10) and (I.11), *i.e.*, between basing the calculation on the pressure ratio $C_p$ or on the supervelocity ratio $\delta$. Both formulae are exact†. In theoretical work, it seems greatly preferable to use (I.11), not only because it is so much simpler, but also because all theories of potential flow lead directly to supervelocity ratio, not to pressure ratio‡. However, the theory of potential incompressible flow gives only $\delta_i$ (and hence $C_{p\,i}$), and one more relationship is needed to connect

---

* Assuming $\gamma = 1{\cdot}4$, we may rewrite the expansions (I.14, 15) as follows:—

$$C_p = -2\delta - (1 - M_0^2)\delta^2 + (M_0^2 - 0{\cdot}2M_0^4)\delta^3 + (0{\cdot}25M_0^2 - 0{\cdot}3M_0^4 + 0{\cdot}01M_0^6)\delta^4 \ldots,$$

$$\delta = -0{\cdot}5C_p - (0{\cdot}125 - 0{\cdot}125M_0^2)C_p^2 - (0{\cdot}0625 - 0{\cdot}0625M_0^2 + 0{\cdot}05M_0^4)C_p^3$$
$$- (0{\cdot}0390625 - 0{\cdot}046875M_0^2 + 0{\cdot}0328125M_0^4 - 0{\cdot}02375M_0^6)C_p^4 \ldots.$$

† On the assumption of Bernoulli's equation and adiabatic law.

‡ When analysing experimental results (pressure plottings), the values of $C_p$ are given, and then the formula (I.10) is preferable, but a great care is needed, especially to avoid illusory claims as to the accuracy of deductions.

$\delta$ with $\delta_i$ (or $C_p$ with $C_{pi}$). Such a relationship is provided, to the first-order approximation, by the *Glauert-Prandtl rule* which is expressed by:—

$$\delta = \delta_i/\sqrt{(1 - M_0^2)}\,, \qquad \text{(I.17)}$$

or

$$C_p = C_{pi}/\sqrt{(1 - M_0^2)}\,. \qquad \text{(I.18)}$$

It should be noticed that (I.17) and (I.18) are *not strictly equivalent.* They lead to slightly different results, as shown by the following table (calculated with $\gamma = 1\cdot4$):—

| (1) | (2) | (3) | (4) | (5) | (6) | Difference between (5) and (6) | |
|---|---|---|---|---|---|---|---|
| $M_0$ | $\delta_i$ | $C_{pi}$ (from I.12) | $\delta$ (from I.17) | $C_p$ (from I.4) | $C_p$ (from I.18) | absolute | per cent |
| 0·9 | 0·039230 | −0·079999 | 0·09 | −0·181044 | −0·183531 | 0·0025 | 1·4 |
| 0·8 | 0·12 | −0·2544 | 0·20 | −0·409890 | −0·424000 | 0·0141 | 3·4 |
| 0·7 | 0·275091 | −0·580279 | 0·36 | −0·764819 | −0·812553 | 0·0477 | 6·2 |

In this table, $\delta_i$ has been chosen for every $M_0$ in such a way as to give a predetermined round value of $\delta$, near to the critical value from (I.11). Hence the differences (shown in the two last columns) represent the maxima to be expected at the given Mach numbers. It is seen that, for large values of $M_0$, the errors are negligible; they increase, however, with falling $M_0$, and become appreciable for $M_0 < 0\cdot8$. If the entire calculation is based on the linear perturbation method, the formulae (I.17) and (I.18) may be considered as interchangeable.

Some efforts have been made[9, 13, 17, 44] to improve on the Glauert-Prandtl rule so as to achieve higher accuracy. The alternative formulae are all based on theoretical considerations, but the final recommendation is usually based on a claim of better agreement with experimental data. They therefore usually refer to $C_p$, not to $\delta$. The earliest and most known correction was suggested by von Kármán[9] in the form:—

$$C_p = \frac{C_{pi}}{(1 - M_0^2)^{1/2} + \frac{1}{2}C_{pi}\,[1 - (1 - M_0^2)^{1/2}]}\,. \qquad \text{(I.19)}$$

The formula involves second-order correction in $C_{pi}$ (as do all other alternative formulae), and therefore its use in connection with linear theories is doubtful if not outright rejectable*.

It may seem that von Kármán's correction is most significant when $[1 - \sqrt{(1 - M_0^2)}]$ is large, *i.e.*, when $M_0$ is nearly 1. However, the admissible sub-critical values of $C_{pj}$ are then so small that the entire correction is negligible. The correction assumes appreciable values for smaller Mach numbers, *i.e.*, for thicker profiles, as shown below.

A corrected formula for $\delta$, equivalent (to the second order of accuracy) to (I.19), cannot be simply obtained by introducing (I.13) and (I.16) into (I.19). To ensure the accuracy required, we must rather replace $C_{pi}$ in (I.19) by (I.12), and then use the expansion (I.15)—with two terms only. We thus obtain:—

$$\delta = \frac{\delta_i}{(1 - M_0^2)^{1/2} - \frac{1}{2}\delta_i[1 + M_0^2 - (1 - M_0^2)^{1/2}]}\,. \qquad \text{(I.20)}$$

* This does not preclude, naturally, on von Kármán's formula (or any alternatives) being studied and applied in connection with experimental data, or with theories of higher order of accuracy.

The formulae (I.19) and (I.20) are not exactly equivalent, but the differences between their numerical results are negligible, as shown by the following table:—

| | | | | |
|---|---|---|---|---|
| (1) | $M_0$ | 0·9 | 0·8 | 0·7 |
| (2) | $\delta_i$ | 0·036946 | 0·108696 | 0·225587 |
| (3) | $C_{pi}$ (from I.12) | −0·075256 | −0·229206 | −0·502064 |
| (4) | $\delta$ (from I.20) | 0·09 | 0·20 | 0·36 |
| (5) | $C_p$ (from I.4) | −0·181044 | −0·409890 | −0·764819 |
| (6) | $C_p$ (from I.19) | −0·181487 | −0·413611 | −0·781564 |
| Difference | Absolute | 0·00044 | 0·00372 | 0·01674 |
| between (5) and (6) | Per cent | 0·24 | 0·91 | 2·19 |
| (7) | $C_p$ (from I.18) | −0·172649 | −0·382010 | −0·703030 |
| Difference | Absolute | 0·00884 | 0·03160 | 0·07853 |
| between (6) and (7) | Per cent | 4·9 | 7·6 | 10·0 |

In this table, $\delta_i$ has again been chosen for every $M_0$ so as to give predetermined values of $\delta$ (same as in the previous table). The interchangeability of (I.19) and (I.20) is clearly shown by the negligible differences between (5) and (6), which are small of the third order. As to the magnitude of von Kármán's correction itself, it is illustrated by the last two lines of the table, and it is seen to be appreciable, although obviously of the second order.

It is now clear how the critical Mach numbers should be calculated for given profiles, *i.e.*, for given $\delta_i$. For first-order accuracy (expecially if $\delta_i$ is only approximately known), we use (I.11) and (I.17), and replace the symbol $M_0$ by $M_c$, thus obtaining:—

$$\delta_i = (1 - M_c^2)^{1/2}\left[\left(1 + \frac{2}{\gamma+1}\,\frac{1-M_c^2}{M_c^2}\right)^{1/2} - 1\right] \quad \ldots \quad \ldots \quad \ldots \quad \text{(I.21)}$$

(*cf.* 2.5 and Fig. 2). If, however, the second-order accuracy is aimed at (which requires at least such an accuracy in $\delta_i$), and we apply von Kármán's correction, then we must use (I.11) and (I.20), and obtain:—

$$\delta_i = \frac{(1 - M_c^2)^{1/2}\left[\left(1 + \frac{2}{\gamma+1}\,\frac{1-M_c^2}{M_c^2}\right)^{1/2} - 1\right]}{1 + \frac{1}{2}\left[\left(1 + \frac{2}{\gamma+1}\,\frac{1-M_c^2}{M_c^2}\right)^{1/2} - 1\right]\left[1 + M_c^2 - (1 - M_c^2)^{1/2}\right]} \quad \text{(I.22)}$$

The differences between (I.21) and (I.22) are not negligible, especially for smaller values of $M_0$, *i.e.*, for thicker profiles, as shown in the following table.

| $M_c$ | $\delta_i$ from (I.21) (simple Glauert-Prandtl rule) | $\delta_i$ from (I.22) (with von Kármán's correction) | Difference | |
|---|---|---|---|---|
| | | | absolute | per cent |
| 1 | 0 | 0 | 0 | 0 |
| 0·95 | 0·0137 | 0·0133 | 0·0004 | 3·4 |
| 0·9 | 0·0407 | 0·0382 | 0·0024 | 6·0 |
| 0·85 | 0·0784 | 0·0720 | 0·0064 | 8·2 |
| 0·8 | 0·1210 | 0·1095 | 0·0115 | 9·5 |
| 0·75 | 0·1875 | 0·1663 | 0·0212 | 11·3 |
| 0·7 | 0·2615 | 0·2289 | 0·0325 | 12·4 |
| 0·65 | 0·3511 | 0·3045 | 0·0466 | 13·3 |
| 0·6 | 0·4597 | 0·3960 | 0·0637 | 13·9 |

In Fig. 2, the thick curve of $M_c$ corresponds to (I.21), the thin one to (I.22).

It would undoubtedly be preferable to obtain higher accuracy, which seems to be possible by using von Kármán's correction (or any alternative one, whichever deemed most reliable). If, however, the supervelocity ratio $\delta_i$ itself is determined only with the first order accuracy, then using any of the corrections would only give an illusory improvement, and serve no useful purpose. In this report, the two-dimensional case is treated only as the introduction to the more complex case of swept wings. And, as the only method available for predicting flow characteristics on such wings is the linear perturbation theory, the simpler formula (I.21) is used. This seems to be in line with other similar efforts, *e.g.*, those relating to critical Mach numbers for ellipsoids, where the simple Glauert-Prandtl rule is applied[47]. Hence, the fundamental Table 1 is based on that rule, and thus on the formula (I.21).

It may be noted that the formula (I.21) would become simpler for one particular value of the adiabatic constant, *i.e.*, for $\gamma = 1$, in which case:—

$$\delta_i = \frac{(1 - M_c)(1 - M_c^2)^{1/2}}{M_c} . \quad \ldots \quad (I.23)$$

An equivalent formula was given by von Kármán (Ref. 9, form. 68). The assumption $\gamma = 1$ means that all changes of the speed of sound are neglected. This sort of simplification does not seem quite legitimate. The error involved can be easily estimated by expanding (I.21) on assumption of $(\gamma - 1)$ being small; we then get:—

$$\delta_i = \frac{(1 - M_c)(1 - M_c^2)^{1/2}}{M_c}\left(1 - \frac{\gamma - 1}{\gamma + 1}\frac{1 + M_c}{2} \ldots\right), \quad \ldots \quad (I.24)$$

and it is seen that the error on $\delta_i$ amounts to about 13 to 17 per cent. There is no reason for such an unnecessary error, the more so as the formulae (I.21) and (I.23) are almost equally easy for computation. The simpler formula is just as insoluble for $M_c$, as the more accurate one.

This brings us to the problem of inverting the formula (I.21), *i.e.*, solving it for $M_c$. The equation being of the fourth degree in $M_c^2$, no simple explicit solution is likely to be found, and only a series expansion may be tried. This should be done preferably in the neighbourhood of the singular point ($M_c = 1$, $\delta = 0$) of the curve in Fig. 2, where both $\delta$ and $1 - M_c^2 = \mu$ may be considered as small, but not of the same order. The singularity is easily recognised as a 'semi-cubic' cusp, and the equation (I.21) can be rewritten thus:—

$$\delta_i = \sqrt{\mu}\left[\left(1 + \frac{2}{\gamma + 1}\frac{\mu}{1 - \mu}\right)^{1/2} - 1\right], \quad \ldots \quad (I.25)$$

or

$$\delta_i = \sqrt{\mu}\left[\left(1 + \frac{2}{\gamma + 1}\mu + \frac{2}{\gamma + 1}\mu^2 + \frac{2}{\gamma + 1}\mu^3 \ldots\right)^{1/2} - 1\right], \quad \ldots \quad (I.26)$$

or expanded:—

$$\delta_i(\gamma + 1) = \mu^{3/2}\left(1 + \frac{\gamma + \frac{1}{2}}{\gamma + 1}\mu + \frac{\gamma^2 + \gamma + \frac{1}{2}}{(\gamma + 1)^2}\mu^2 \ldots\right). \quad \ldots \quad (I.27)$$

Let us put:—

$$[\delta_i(\gamma + 1)]^{2/3} = \mu_0 , \quad \ldots \quad (I.28)$$

then

$$\mu_0 = \mu\left(1 + \frac{\gamma + \frac{1}{2}}{\gamma + 1}\mu + \frac{\gamma^2 + \gamma + \frac{1}{2}}{(\gamma + 1)^2}\mu^2 \ldots\right)^{2/3}, \quad \ldots \quad (I.29)$$

or

$$\mu_0 = \mu + \frac{2\gamma + 1}{3(\gamma + 1)}\mu^2 + \frac{5\gamma^2 + 5\gamma + 2{\cdot}75}{9(\gamma + 1)^2}\mu^3 \ldots \quad \ldots \quad (I.30)$$

Inverting this series, we obtain:—

$$\mu = \mu_0 - \frac{2\gamma + 1}{3(\gamma + 1)}\mu_0^2 + \frac{4\gamma^2 + 4\gamma - 1}{12(\gamma + 1)^2}\mu_0^3 \dots, \qquad \text{(I.31)}$$

whence:—

$$M_c = \sqrt{(1 - \mu)} = 1 - \tfrac{1}{2}\mu_0 + \frac{5\gamma + 1}{24(\gamma + 1)}\mu_0^2 - \frac{3\gamma^2 + 2\gamma - 3}{48(\gamma + 1)^2}\mu_0^3 \dots, \qquad \text{(I.32)}$$

or finally:—

$$M_c = 1 - \tfrac{1}{2}[\delta_i(\gamma + 1]^{2/3} + \frac{5\gamma + 1}{24(\gamma + 1)}[\delta_i(\gamma + 1)]^{4/3} - \frac{3\gamma^2 + 2\gamma - 3}{48(\gamma + 1)^2}[\delta_i(\gamma + 1]^2 \dots \qquad \text{(I.33)}$$

By a similar procedure, $M_c$ may be expressed in terms of $C_{pi}$. Using formulae (I.10) and (I.18) we obtain:—

$$C_{pi} = -\frac{2(1 - M_c^2)^{1/2}}{\gamma M_c^2}\left[1 - \left(1 - \frac{\gamma - 1}{\gamma + 1}(1 - M_c^2)\right)^{\frac{\gamma}{\gamma - 1}}\right]; \qquad \text{(I.34)}$$

this relation corresponds to (I.21). The solution for $M_c$ in the form of an infinite series may be obtained by following the lines of the previous transformation, and we obtain:—

$$M_c = 1 - \tfrac{1}{2}\left(-\frac{\gamma + 1}{2}C_{pi}\right)^{2/3} + \frac{5\gamma + 1}{24(\gamma + 1)}\left(-\frac{\gamma + 1}{2}C_{pi}\right)^{4/3}$$
$$- \frac{9\gamma^2 + 8\gamma - 25}{144(\gamma + 1)^2}\left(-\frac{\gamma + 1}{2}C_{pi}\right)^2 \dots \qquad \text{(I.35)}$$

The two series (I.33) and (I.35) converge satisfactorily for moderate values of $\delta_i$ or $C_{pi}$, but they are not convenient for computation*.

Bearing in mind that the entire theory is only approximate, one is strongly tempted to keep only two terms in each of the two series, thus:—

$$M_c \simeq 1 - \tfrac{1}{2}[\delta_i(\gamma + 1)]^{2/3}, \qquad \text{(I.36)}$$

or

$$M_c \simeq 1 - \tfrac{1}{2}\left(-\frac{\gamma + 1}{2}C_{pi}\right)^{2/3}. \qquad \text{(I.37)}$$

The formula (I.37) was derived by Liepmann and Puckett[32]. However, both (I.36) and (I.37) involve appreciable errors. A linear approximation is based on neglecting second and higher powers of the quantity originally assumed as small, but in this approximation the 4/3rd power of $\delta_i$ or $C_{pi}$ is neglected. Liepmann and Puckett's approximation leads to the lowest curve in our Fig. 2, and it is seen that it considerably under-estimates the critical $M$; it may therefore be used only for very rough estimates. Using three terms of our series (I.33), we should obtain the upper curve in Fig. 2; this curve follows the main one rather closely, but it slightly over-estimates the critical $M$. The curve representing $M_c$ according to von Kármán's correction lies *below* our main curve, and the results would be similar if Temple's, Greene's or Weber's corrections were used instead. It is seen that the series solutions in this case have some rather unfortunate features, and should only be used with great care.

---

* As mentioned in section 2, it was found more expedient to calculate $\delta_i$ for assumed values of $M_c$ (Table 1), and then to interpolate to tabulate $M_c$ against $\delta_i$ (Table 2).

## APPENDIX II (to Section 3)

*Approximate Expressions for Critical Mach Numbers of Infinite Yawed and Sheared Wings*

The approximate formula (I.33) for the critical Mach number of an infinite straight wing can be modified so as to give similar expressions in the cases of infinite yawed, or infinite sheared wings. In the former case, as shown in section 3, it is sufficient to replace $M_c$ by $M_{cy} \cos \varphi$ in the relationship pertaining to the two-dimensional case. Hence, for *infinite yawed wings* :—

$$M_{cy} = \Big\{ 1 - \tfrac{1}{2}[\delta_i(\gamma + 1)]^{2/3} + \frac{5\gamma + 1}{24(\gamma + 1)} [\delta_i(\gamma + 1)]^{4/3} - \frac{3\gamma^2 + 2\gamma - 3}{48(\gamma + 1)^2} [\delta_i(\gamma + 1)]^2 \ldots \Big\} \sec \varphi . \qquad \text{(II.1)}$$

Similarly, in the latter case, $M_c$ must be replaced by $M_{cs} \cos \varphi$ and, at the same time, $\delta_i$ by $\delta_i \sec \varphi$. Thus we obtain, for *infinite sheared wings* :—

$$M_{cs} = \Big\{ 1 - \tfrac{1}{2}[\delta_i(\gamma + 1) \sec \varphi]^{2/3} + \frac{5\gamma + 1}{24(\gamma + 1)} [\delta_i(\gamma + 1) \sec \varphi]^{4/3} - \frac{3\gamma^2 + 2\gamma - 3}{48(\gamma + 1)^2} [\delta_i(\gamma + 1) \sec \varphi]^2 \ldots \Big\} \sec \varphi . \qquad \text{(II.2)}$$

Both formulae are subject to the same reservations as the original expansion (I.33). With all four terms of the series taken into account, they are accurate enough, but rather inconvenient. With only three or two terms, they are not sufficiently accurate, and may only be used for rough estimates.

## APPENDIX III (to Sub-Section 4.1)

*Supervelocity Distributions over Swept and Sheared Wings with Various Profiles*

(A) *General.*—In this Appendix, we consider the distribution of the incremental velocity $v_x$ on semi-infinite sheared and infinite swept wings with various profiles. The general theory was given in previous reports (R. & M. 2713[34] and 2717[48]) and applied in the simplest case of the biconvex parabolic profile. It will therefore suffice here to show how the method can be applied to other profiles.

For a semi-infinite sheared wing with arbitrary section, defined by the equation:

$$z = F(x + y \tan \varphi) \qquad (0 < y < +\infty)$$
$$(-b < x + y \tan \varphi < +b) \qquad \text{(III.1)}$$

the general formula for $v_x$ at an arbitrary point $(x, y)$ is, according to R. & M. 2717[48], form. (3.5.3):

$$\frac{2\pi v_x}{U \cos \varphi} = -\int_{-b}^{b} \frac{F'(\bar{x})}{x - \bar{x} + y \tan \varphi}\left(1 + \frac{y \sec \varphi}{[(x - \bar{x})^2 + y^2]^{1/2}}\right) d\bar{x}\,. \qquad \text{(III.2)}$$

Introducing non-dimensional co-ordinates:

$$\xi = \frac{x + y \tan \varphi}{b}, \quad \eta = \frac{y}{b}, \qquad \text{(III.3)}$$

the new non-dimensional variable of integration:

$$P = \frac{\bar{x} - x - y \tan \varphi}{b}, \qquad \text{(III.4)}$$

and denoting for abbreviation:

$$r = (P^2 \cos^2 \varphi + 2P\eta \sin \varphi \cos \varphi + \eta^2)^{1/2}, \qquad \text{(III.5)}$$

we may reduce (I.2) to the following form:

$$\frac{2\pi v_x}{U \cos \varphi} = \int_{-1-\xi}^{1-\xi} \frac{F'[b(P + \xi)]}{P}\left(1 + \frac{\eta}{r}\right) dP\,. \qquad \text{(III.6)}$$

Suppose now that $F$ is a polynomial of any degree. The integral (III.6) will be always calculable by elementary methods, and the only functions required, apart from simple polynomials, will be some of those given in the ' Table of auxiliary functions ' of Ref. 48 (page 25).

We shall limit ourselves to the polynomial of 5th degree, but higher degrees will involve only additional algebra. Let us put:

$$z = F(b\xi) = k\vartheta b(1 - \xi^2)(1 + A\xi + B\xi^2 + C\xi^3), \qquad \text{(III.7)}$$

where $\vartheta$ is thickness ratio, and $k$ a non-dimensional coefficient chosen in such a way that $z_{\max} = \vartheta b$, *i.e.*,

$$k = \frac{1}{(1 - \xi_n^2)(1 + A\xi_n + B\xi_n^2 + C\xi_n^3)}, \qquad \text{(III.8)}$$

$\xi_n$ denoting the value of $\xi$ corresponding to $z_{\max}$.

The first derivative of (III.8) becomes:

$$F'(b\xi) = k\vartheta[A - 2(1 - B)\xi - 3(A - C)\xi^2 - 4B\xi^3 - 5C\xi^4] , \quad \ldots \quad \ldots \quad \text{(III.9)}$$

and hence:

$$F'[b(\xi + P)] = k\vartheta(n_0 - n_1P - n_2P^2 - n_3P^3 - n_4P^4) , \quad \ldots \quad \ldots \quad \text{(III.10)}$$

where:

$$\left.\begin{aligned} n_0 &= A - 2(1 - B)\xi - 3(A - C)\xi^2 - 4B\xi^3 - 5C\xi^4 , \\ n_1 &= 2(1 - B) + 6(A - C)\xi + 12B\xi^2 + 20C\xi^3 , \\ n_2 &= 3(A - C) + 12B\xi + 30C\xi^2 , \\ n_3 &= 4B + 20C\xi , \\ n_4 &= 5C . \end{aligned}\right| \quad \ldots \quad \ldots \quad \text{(III.11)}$$

The formula (III.6) then becomes:

$$-\frac{2\pi v_x}{k\vartheta U \cos\varphi} = \int_{-1-\xi}^{1-\xi} (n_1 + n_2P + n_3P^2 + n_4P^3)dP - n_0\int_{-1-\xi}^{1-\xi} \frac{r + \eta}{Pr}dP$$

$$+ \eta\int_{-1-\xi}^{1-\xi} (n_1 + n_2P + n_3P^2 + n_4P^3)\frac{dP}{r} . \quad \ldots \quad \ldots \quad \text{(III.12)}$$

The first two integrals in (III.12) are easily determined as follows:—

$$\int_{-1-\xi}^{1-\xi} (n_1 + n_2P + n_3P^2 + n_4P^3)dP = 2n_1 - 2n_2\xi + \tfrac{2}{3}n_3(1 + 3\xi^2) - 2n_4(\xi + \xi^3) , \quad \ldots \quad \text{(III.13)}$$

and (*cf.* R. & M. 2717[48] form. II.7 and table on p. 25):

$$\int_{-1-\xi}^{1-\xi} \frac{r + \eta}{Pr}dP = -\ln F_5 . \quad \ldots \quad \ldots \quad \text{(III.14)}$$

The third integral in (III.12) is somewhat more complicated. By applying the usual reduction formulae, we obtain the following expression for the indefinite integral:

$$\int(n_1 + n_2P + n_3P^2 + n_4P^3)\frac{dP}{r} =$$

$$\frac{r}{\cos^2\varphi}\{[n_2 - \tfrac{3}{2}n_3\eta \tan\varphi + n_4\eta^2(\tfrac{11}{6} \tan^2\varphi - \tfrac{2}{3})] + (\tfrac{1}{2}n_3 - \tfrac{5}{6}n_4\eta \tan\varphi)P + \tfrac{1}{3}n_4P^2\}$$

$$+ [n_1 - n_2\eta \tan\varphi + n_3\eta^2(\tan^2\varphi - \tfrac{1}{2}) + n_4\eta^3(\tfrac{3}{2} \tan\varphi - \tan^3\varphi)] \int\frac{dP}{r} , \quad \ldots \quad \ldots \quad \text{(III.15)}$$

which may be easily checked by differentiation. Introducing the limits, and taking into account the formula (II.6) of R. & M. 2717[48]

$$\int_{-1-\xi}^{1-\xi} \frac{dP}{r} = \frac{\ln F_4}{\cos\varphi} \quad \ldots \quad \ldots \quad \text{(III.16)}$$

we find the definite integral as follows:

$$\int_{-1-\xi}^{1-\xi} (n_1 + n_2P + n_3P^2 + n_4P^3)\frac{dP}{r} = \frac{r_1 + r_2}{\cos^2\varphi}(2B + \tfrac{20}{3}C\xi - \tfrac{25}{6}C\eta \tan\varphi)$$

$$+ \frac{r_2 - r_1}{\cos^2\varphi}[(3A - \tfrac{4}{3}C + 10B\xi + \tfrac{65}{3}C\xi^2) - (6B + \tfrac{155}{6}C\xi)\eta \tan\varphi + 5C\eta^2(\tfrac{11}{6} \tan^2\varphi - \tfrac{2}{3})]$$

$$+ \frac{\ln F_4}{\cos\varphi}[n_1 - n_2\eta \tan\varphi + n_3\eta^2(\tan^2\varphi - \tfrac{1}{2}) + n_4\eta^3(\tfrac{3}{2} \tan\varphi - \tan^3\varphi)] . \quad \ldots \quad \ldots \quad \text{(III.17)}$$

Introducing (III.13), (III.14), and (III.17) into (III.12), we finally obtain, for a *semi-infinite sheared wing:*

$$-\frac{2\pi v_x}{k\vartheta U\cos\varphi} = m_0 + n_0 \ln F_5 + \frac{\eta}{\cos\varphi}\,[n_1 - n_2\eta\tan\varphi + n_3\eta^2(\tan^2\varphi - \tfrac{1}{2})$$

$$+ n_4\eta^3(\tfrac{3}{2}\tan\varphi - \tan^3\varphi)]\ln F_4 + \frac{\eta(r_2 - r_1)}{\cos^2\varphi}\,[m_1 - m_2\eta\tan\varphi + n_4\eta^2(\tfrac{11}{6}\tan^2\varphi - \tfrac{2}{3})]$$

$$+ \frac{\eta(r_1 + r_2)}{\cos^2\varphi}\,(m_3 - \tfrac{5}{6}n_4\eta\tan\varphi) \qquad \text{(III.18)}$$

where:

$$\left.\begin{aligned} m_0 &= 4\left(1 - \frac{B}{3}\right) + 6(A - \tfrac{4}{9}C)\xi + 8B\xi^2 + 10C\xi^3\,,\\ m_1 &= (3A - \tfrac{4}{3}C) + 10B\xi + \tfrac{65}{3}C\xi^2\,,\\ m_2 &= 6B + \tfrac{155}{6}C\xi\,,\\ m_3 &= 2B + \tfrac{20}{3}C\xi\,, \end{aligned}\right\} \qquad \text{(III.19)}$$

and $n_0$, $n_1$, $n_2$, $n_3$, $n_4$ are given by (III.11).

Two special cases deserve attention. Putting $\eta = 0$, we get, for the *upstream tip section:*

$$\left|-\frac{\pi v_x}{k\vartheta U\cos\varphi}\right|_{\eta=0} = \tfrac{1}{2}m_0 + \tfrac{1}{2}n_0\ln\left(\frac{1+\xi}{1-\xi}\,\frac{1+\sin\varphi}{1-\sin\varphi}\right), \qquad \text{(III.20)}$$

and, when $\eta \to \infty$, we obtain (taking into account the expansions T.19, 20, 24, 25 of R. & M. 2717[48]) for a *section far away from the tip:*

$$\left|-\frac{\pi v_x}{k\vartheta U\cos\varphi}\right|_{\eta\to\infty} = m_0 + n_0\ln\frac{1+\xi}{1-\xi}. \qquad \text{(III.21)}$$

The formula (III.21) can be obtained directly by using the general method for two-dimensional aerofoils, described in Ref. 34 (form. I.14). The formula (III.20) represents one half of (III.21), with the kink correction term $\ln(1 + \sin\varphi)/(1 - \sin\varphi)$ included. The two cases provide useful checks of the general formula (III.18).

The next step is to work out the general formula for $v_x$-distribution over an *infinite swept-back wing* (*with a central kink*). As shown in R. & M. 2717[48] (section 4.1), the right procedure is to find the contribution of the left half-wing, by replacing $\eta$ by $(-\eta)$, and $\xi$ by $(\xi - 2\eta\tan\varphi)$, in (III.18), and then to add together the contributions for both half-wings. This is a simple algebraical operation, but rather long in the given case. The final result for an *infinite swept-back wing* is:

$$-\frac{\pi v_x}{k\vartheta U\cos\varphi} = [m_0 - 2(m_1 - m_3\xi)\eta\tan\varphi + 4(n_3 - n_4\xi)\eta^2\tan^2\varphi - 8n_4\eta^3\tan^3\varphi] + n_0\ln F_1$$

$$+ \eta\tan\varphi(n_1 - 2n_2\eta\tan\varphi + 4n_3\eta^2\tan^2\varphi - 8n_4\eta^3\tan^3\varphi)\ln F_2$$

$$+ \frac{\eta^2\sin\varphi}{\cos^2\varphi}\,[n_2 - 3n_3\eta\tan\varphi + n_4\eta^2(7\tan^2\varphi - \tfrac{1}{2})]\ln F_4$$

$$+ \frac{\eta^2\sin\varphi}{2\cos^3\varphi}\,(2n_3 - n_4\xi - 7n_4\eta\tan\varphi)(r_2 - r_1) + \frac{n_4\eta^2(r_1 + r_2)\sin\varphi}{2\cos^3\varphi}\,. \qquad \text{(III.22)}$$

There are again two important special cases. Putting $\eta = 0$, we obtain, for the *central kink section :*

$$\left| - \frac{\pi v_x}{k\vartheta U \cos \varphi} \right|_{\eta=0} = m_0 + n_0 \ln \left( \frac{1+\xi}{1-\xi} \frac{1+\sin \varphi}{1-\sin \varphi} \right), \quad \ldots \quad \ldots \quad \ldots \quad \ldots \quad \text{(III.23)}$$

which is exactly twice (III.20), as it should be. Letting $\eta \rightarrow \infty$ in (III.22), we get, after a long transformation:

$$\left| - \frac{\pi v_x}{k\vartheta U \cos \varphi} \right|_{\eta\rightarrow\infty} = m_0 + n_0 \ln \frac{1+\xi}{1-\xi}, \quad \ldots \quad \ldots \quad \ldots \quad \ldots \quad \ldots \quad \ldots \quad \text{(III.24)}$$

*i.e.*, the same result as (III.21), as it should be.

It must be intimated now that the formulae (III.18) and (III.22) apply directly only if $\varphi > 0$, *i.e.*, in the cases of a semi-infinite sheared wing with an *upstream tip*, or of an infinite *swept-back* wing, respectively. However, both formulae can also be used when $\varphi < 0$, *i.e.*, in the cases of *downstream tip*, or a *swept-forward wing*, but then special pains must be taken to avoid errors. Examining carefully the formulae, together with expressions T.1, 2, 7, 8, 10, 11 of R. & M. 2717[48], we come to the conclusion that following rules must be observed:—

(1) tan $\varphi$ and sin $\varphi$ should be replaced by $(-\tan \varphi)$ and $(-\sin \varphi)$ in (III.18) and (III.22);

(2) values of $r_1$, $r_2$, $F_4$ corresponding to the given $\xi$, $\eta$, $\varphi$ should be replaced by those of $r_2$, $r_1$, $F_4$ corresponding to $(-\xi)$, $\eta$, $\varphi$;

(3) values of $\ln F_1$, $\ln F_2$, $\ln F_5$ corresponding to the given $\xi$, $\eta$, $\varphi$ should be replaced by those of $(-\ln F_1)$, $(-\ln F_2)$. $(-\ln F_5)$ corresponding to $(-\xi)$, $\eta$, $\varphi$.

The *supervelocity distribution in the kink section,* given by (III.23), is of paramount interest, and the maximum value of the supervelocity is particularly important. This maximum can be determined by equating to zero the first derivative of (III.23) with respect to $\xi$. This leads to the equation:

$$m_0' - n_1 \ln \left( \frac{1+\xi}{1-\xi} \frac{1+\sin \varphi}{1-\sin \varphi} \right) + \frac{2n_0}{1-\xi^2} = 0\,, \quad \ldots \quad \ldots \quad \ldots \quad \text{(III.25)}$$

where $m_0'$ and $(-n_1)$ are first derivatives of the polynomials $m_0$ and $n_0$ respectively. The equation (III.25) cannot generally be solved for $\xi$. However, it may be solved for $\varphi$ when the value of $\xi$ is assumed. We get from (III.25) :

$$\ln \left( \frac{1+\xi}{1-\xi} \frac{1+\sin \varphi}{1-\sin \varphi} \right) = 2T\,, \quad \ldots \quad \ldots \quad \ldots \quad \ldots \quad \text{(III.26)}$$

where:

$$T = \frac{m_0'}{2n_1} + \frac{n_0}{n_1(1-\xi^2)} \,. \quad \ldots \quad \ldots \quad \ldots \quad \ldots \quad \ldots \quad \ldots \quad \ldots \quad \ldots \quad \text{(III.27)}$$

Hence, denoting by $\xi_m$ the value of $\xi$ corresponding to the maximum supervelocity in the central kink, and by $T_m$ the corresponding value of $T$, we obtain:

$$\sin \varphi = \frac{(1-\xi_m)\, e^{2T_m} - (1+\xi_m)}{(1-\xi_m)\, e^{2T_m} + (1+\xi_m)}\,,$$

or alternatively:

$$\cos \varphi = \frac{(1-\xi_m^{\,2})^{1/2}}{\cosh T_m - \xi_m \sinh T_m} \,. \quad \ldots \quad \ldots \quad \ldots \quad \ldots \quad \ldots \quad \text{(III.28)}$$

The maximum value of the supervelocity may be found from (III.23) and (III.26):

$$\left| -\frac{v_x}{\vartheta U \cos\varphi} \right|_{\max} = \frac{k}{\pi}\,(m_{0m} + 2n_{0m}T_m)\,, \quad \ldots \quad \text{(III.29)}$$

where $p_{0m}$, $n_{0m}$ denote the values of the polynomials $p_0$, $n_0$ for $\xi = \xi_m$.

The normal procedure will be to tabulate $T_m$, $\varphi$, (III.29), and

$$H = \left| -\frac{v_x}{\vartheta U} \right|_{\max} = \frac{k}{\pi}\,(m_{0m} + 2n_{0m}T_m)\cos\varphi \quad \ldots \quad \text{(III.30)}$$

for a range of values of $\xi_m$. If required, the table may be interpolated in order to produce a table of $\xi_m$, (III.29), and $H$, against $\varphi$. In such a way our Tables 5, 6, 7 and 8 have been prepared.

(B) *Particular cases.*—The above general results are now applied to four particular cases, for the profiles B, C, Q and R.

*Profile* B (biconvex parabolic), Figs. 5, 6 to 9, 20 to 21.

Coefficients: $A = B = C = 0\,,\quad \xi_n = 0\,,\quad k = 1\,.$

Profile equation (III.7):

$$z = \vartheta b(1 - \xi^2)\,. \quad \ldots \quad \text{(III.31)}$$

Velocity distribution over semi-infinite sheared wing (III.18):

$$-\frac{2\pi v_x}{\vartheta U \cos\varphi} = 4 + \frac{2\eta}{\cos\varphi}\ln F_4 - 2\xi \ln F_5\,, \quad \ldots \quad \text{(III.32)}$$

and over infinite swept-back wing (III.22):

$$-\frac{\pi v_x}{\vartheta U \cos\varphi} = 4 - 2\xi \ln F_1 + 2\eta \tan\varphi \ln F_2\,. \quad \ldots \quad \text{(III.33)}$$

Velocity distribution in the kink section (III.23):

$$-\frac{v_x}{\vartheta U \cos\varphi} = \frac{2}{\pi}\left[2 - \xi \ln\left(\frac{1+\xi}{1-\xi}\,\frac{1+\sin\varphi}{1-\sin\varphi}\right)\right]. \quad \ldots \quad \text{(III.24)}$$

Auxiliary quantity $T_m$ (*cf.* III.27):

$$T_m = -\frac{\xi_m}{1 - \xi_m^{\,2}}\,. \quad \ldots \quad \text{(III.35)}$$

Maximum supervelocity in the kink section (III.29):

$$\left| -\frac{v_x}{\vartheta U \cos\varphi} \right|_{\max} = \frac{4}{\pi}\,\frac{1}{1 - \xi_m^{\,2}}\,. \quad \ldots \quad \text{(III.36)}$$

All these results have been given in Refs. 34 and 48, and are repeated here only for the sake of check and comparison.

*Profile* C (cubic with cusped tail), Figs. 5, 10 to 14, 22 to 23.

Maximum thickness at $33\frac{1}{3}$ per cent.

Coefficients: $A = 1$, $B = C = 0$, $\xi_n = \dfrac{1}{3}$, $k = \dfrac{27}{32} = 0{\cdot}84375$.

Profile equation (III.7): $z = k\vartheta b(1 - \xi)(1 + \xi)^2\,.$ .. .. .. .. .. (III.37)

Velocity distribution over semi-infinite sheared wing (III.18):

$$-\frac{2\pi v_x}{k\vartheta U\cos\varphi} = (4+6\xi) + (1+\xi)(1-3\xi)\ln F_5 + \frac{\eta}{\cos\varphi}(2+6\xi-3\eta\tan\varphi)\ln F_4 + \frac{3\eta(r_2-r_1)}{\cos^2\varphi}, \quad \text{(III.38)}$$

and over infinite swept-back wing (III.22):

$$-\frac{\pi v_x}{k\vartheta U\cos\varphi} = (4+6\xi-6\eta\tan\varphi) + (1+\xi)(1-3\xi)\ln F_1 + \eta\tan\varphi\,(2+6\xi-6\eta\tan\varphi)\ln F_2 + \frac{3\eta^2\sin\varphi}{\cos^2\varphi}\ln F_4 \ldots \quad \text{(III.38a)}$$

Velocity distribution in the kink section (III.23):

$$-\frac{v_x}{\vartheta U\cos\varphi} = \frac{27}{32\pi}\left[(4+6\xi) + (1+\xi)(1-3\xi)\ln\left(\frac{1+\xi}{1-\xi}\frac{1+\sin\varphi}{1-\sin\varphi}\right)\right]. \quad \text{(III.39)}$$

Auxiliary quantity $T_m$ (*cf.* III.27):

$$T_m = \frac{2-3\xi_m}{(1+3\xi_m)(1-\xi_m)}, \quad \text{(III.40)}$$

$\xi_m$ being confined to the range $-\frac{1}{3} < \xi_m < 1$, and being $\sim 0\cdot4555$ for $\varphi = 0$.

Maximum supervelocity in the kink section (III.29):

$$\left|-\frac{v_x}{\vartheta U\cos\varphi}\right|_{\max} = \frac{27}{4\pi}\frac{1}{(1-\xi_m)(1+3\xi_m)}. \quad \text{(III.41)}$$

*Profile* Q (quartic with max. thickness at 30 per cent), Figs. 5, 15 to 19, 24 to 25.

Coefficients: $A = 0\cdot712$, $B = 0\cdot79$, $C = 0$, $\xi_n = 0\cdot4$, $k = 0\cdot8435914$.

Profile equation (III.7): $z = k\vartheta b(1-\xi^2)(1+0\cdot712\xi+0\cdot79\xi^2)$. (III.42)

Velocity distribution over semi-infinite sheared wing (III.18):

$$-\frac{2\pi v_x}{k\vartheta U\cos\varphi} = (2\cdot946\dot{6} + 4\cdot272\xi + 6\cdot32\xi^2) + (0\cdot712 - 0\cdot42\xi - 2\cdot136\xi^2 - 3\cdot16\xi^3)\ln F_5 + \frac{\eta}{\cos\varphi}[(0\cdot42 + 4\cdot272\xi + 9\cdot48\xi^2) - (2\cdot136 + 9\cdot48\xi)\eta\tan\varphi + 3\cdot16\eta^2(\tan^2\varphi - \tfrac{1}{2})]\ln F_4 + \frac{\eta(r_2-r_1)}{\cos^2\varphi}[(2\cdot136+7\cdot9\xi) - 4\cdot74\eta\tan\varphi] + \frac{1\cdot58\eta(r_1+r_2)}{\cos^2\varphi}. \quad \text{(III.43)}$$

and over infinite swept-back wing (III.22):

$$-\frac{\pi v_x}{k\vartheta U\cos\varphi} = [(2\cdot946\dot{6} + 4\cdot272\xi + 6\cdot32\xi^2) - (4\cdot272 + 10\cdot64\xi)\eta\tan\varphi + 12\cdot64\eta^2\tan^2\varphi] + (0\cdot712 - 0\cdot42\xi - 2\cdot136\xi^2 - 3\cdot16\xi^3)\ln F_1 + \eta\tan\varphi[(0\cdot42 + 4\cdot272\xi + 9\cdot48\xi^2) - (4\cdot272 + 18\cdot96\xi)\eta\tan\varphi + 12\cdot64\eta^2\tan^2\varphi]\ln F_2 + \frac{\eta^2\sin\varphi}{\cos^2\varphi}[(2\cdot136+9\cdot48\xi) - 9\cdot48\eta\tan\varphi]\ln F_4 + \frac{3\cdot16\eta^2\sin\varphi(r_2-r_1)}{\cos^3\varphi}. \quad \text{(III.44)}$$

Velocity distribution in the kink section (III.23):

$$-\frac{v_x}{\vartheta U \cos\varphi} = 0\cdot2685235\Big[(2\cdot946\dot{6} + 4\cdot272\xi + 6\cdot32\xi^2) + (0\cdot712 - 0\cdot42\xi - 2\cdot136\xi^2 - 3\cdot16\xi^3)\ln\left(\frac{1+\xi}{1-\xi}\frac{1+\sin\varphi}{1-\sin\varphi}\right)\Big] . \quad .. \quad \text{(III.45)}$$

Auxiliary quantity $T_m$ (*cf.* III.27):

$$T_m = \frac{2\cdot848 + 5\cdot9\xi_m - 4\cdot272\xi_m^{\ 2} - 9\cdot48\xi_m^{\ 3}}{(1-\xi_m^{\ 2})(0\cdot42 + 4\cdot272\xi_m + 9\cdot48\xi_m^{\ 2})} . \quad .. \quad .. \quad .. \quad .. \quad \text{(III.46)}$$

Maximum supervelocity in the kink section (III.29):

$$\left|-\frac{v_x}{\vartheta U \cos\varphi}\right|_{\max} = 0\cdot2685235[(2\cdot9466 \ldots + 4\cdot272\xi_m + 6\cdot32\xi_m^{\ 2}) + 2(0\cdot712 - 0\cdot42\xi_m - 2\cdot136\xi_m^{\ 2} - 3\cdot16\xi_m^{\ 3})T_m] . \quad .. \quad .. \quad \text{(III.47)}$$

*Profile* R (simplest profile with rounded nose, max. thickness at 30 per cent chord), Figs. 5, 26, 27.

This profile is *not* a special case of (III.7), and its equation is:

$$z = F(b\xi) = k\vartheta b(1-\xi)^{1/2}(1+\xi)(1+b_1\xi) , \quad .. \quad .. \quad .. \quad .. \quad \text{(III.48)}$$

where $k$ is a non-dimensional coefficient chosen so that $F_{\max} = \vartheta b$, *i.e.*:

$$k = \frac{1}{(1-\xi_n)^{1/2}(1+\xi_n)(1+b_1\xi_n)} . \quad .. \quad .. \quad .. \quad .. \quad .. \quad \text{(III.49)}$$

The first derivative of (III.48) becomes:

$$F'(b\xi) = k\vartheta\,\frac{-5b_1\xi^2 - (3-b_1)\xi + (1+2b_1)}{2(1-\xi)^{1/2}} . \quad .. \quad .. \quad .. \quad .. \quad \text{(III.50)}$$

and hence:

$$b_1 = \frac{3\xi_n - 1}{2 + \xi_n - 5\xi_n^{\ 2}} . \quad .. \quad .. \quad .. \quad .. \quad .. \quad .. \quad .. \quad \text{(III.51)}$$

In the given case:

$$\xi_n = 0\cdot4,\ b_1 = 0\cdot125;\ k = \frac{\sqrt{(15)}}{4\cdot41} = 0\cdot8782275.$$

The velocity distribution over the entire sheared or swept-back wing with this profile has not been worked out, this requiring a formidable array of elliptic integrals. However, a formula for velocity distribution in the *kink section* may be easily derived by using methods of R. & M.2713[34] (App. I, form. I.8, example VII, also form. 7.5), and the result is:

$$-\frac{2\pi v_x}{k\vartheta U\cos\varphi} = 2\sqrt{2}(3 + \tfrac{2}{3}b_1 + 5b_1\xi) + \frac{5b_1\xi^2 + (3-b_1)\xi - (1+2b_1)}{(1-\xi)^{1/2}}\left(\ln\frac{\sqrt{2}+(1-\xi)^{1/2}}{\sqrt{2}-(1-\xi)^{1/2}} - \ln\frac{1+\sin\varphi}{1-\sin\varphi}\right) . \quad \text{(III.52)}$$

In the given case ($b_1 = 0\cdot125$):

$$-\frac{v_x}{\vartheta U\cos\varphi} = \frac{5k}{16\pi}\Big[2\sqrt{2}(\tfrac{74}{15} + \xi) + \frac{(\xi - 0\cdot4)(\xi + 5)}{(1-\xi)^{1/2}}\left(\ln\frac{\sqrt{2}+(1-\xi)^{1/2})}{\sqrt{2}-(1-\xi)^{1/2}} - \ln\frac{1+\sin\varphi}{1-\sin\varphi}\right)\Big] . \quad .. \quad \text{(III.53)}$$

$$\left(\frac{5k}{16\pi} = 0\cdot0873589\right)$$

The maximum supervelocity is, again, the most important. Equating to zero the first derivative of (III.52), we obtain, after a rather long transformation:

$$\ln\frac{1+\sin\varphi}{1-\sin\varphi} = 2W = \ln\frac{\sqrt{2}+(1-\xi_m)^{1/2}}{\sqrt{2}-(1-\xi_m)^{1/2}} + \frac{2[2(1-\xi_m)]^{1/2}}{1+\xi_m}\,\frac{(1+12b_1)-(3-b_1)\xi_m-15b_1\xi_m^2}{(5-4b_1)+(21b_1-3)\xi_m-15b_1\xi_m^2}, \qquad \text{(III.54)}$$

and

$$\sin\varphi = \tanh W. \qquad \text{(III.55)}$$

Substituting from (III.54) into (III.53), we obtain:

$$H = \left(-\frac{v_x}{U}\right)_{\max} = \frac{16k\sqrt{2}}{3\pi(1+\xi_m)}\cdot\frac{(3+b_1+4b_1^2)+(7b_1+b_1^2)\xi_m}{(5-4b_1)+(21b_1-3)\xi_m-15b_1\xi_m^2}\cos\varphi. \qquad \text{(III.56)}$$

The formulae (III.54, 55, 56) enable us to tabulate $\varphi$ and $H$ against $\xi_m$, and then, by applying interpolation, to re-tabulate $\xi_m$ and $H$ against $\varphi$.

In the given case ($b_1 = 0{\cdot}125$):

$$2W = \ln\frac{\sqrt{2}+(1-\xi_m)^{1/2}}{\sqrt{2}-(1-\xi_m)^{1/2}} + \frac{2[2(1-\xi_m)]^{1/2}}{1+\xi_m}\cdot\frac{20-23\xi_m-15\xi_m^2}{36-3\xi_m-15\xi_m^2}; \qquad \text{(III.57)}$$

$$H = 0{\cdot}263561\,\frac{68+19\xi_m}{(1+\xi_m)(12-\xi_m-5\xi_m^2)}\cos\varphi. \qquad \text{(III.58)}$$

In particular, for $\varphi = 0$ (unswept wing), we have $\xi_m = 1$, and then:

$$H_{\varphi=0} = \frac{4k\sqrt{2}(3+5b_1)}{3\pi} = 1{\cdot}9108\,, \text{ hence } \delta_i = 1{\cdot}9108\vartheta. \qquad \text{(III.59)}$$

It should be mentioned that the formula for $H$ is valid only for positive $\varphi$ and $\xi_m < 1$, *i.e.*, for *swept-back* wings. If $\varphi$ is negative, then the expression (III.53) becomes $(+\infty)$ at $\xi = 1$ (see Figs. 26 and 27), and the true maximum cannot be determined by the 1st order method. There is some doubt about the validity of the general formula at $\varphi = 0$ and $\xi_m = 1$. In this case the maximum certainly occurs near the leading edge, but not at the edge itself, and we may only hope that the value obtained in this case differs little from the true maximum.

## TABLES 1 and 1a

*Critical Mach numbers $M_c$ in Two-dimensional Flow, for Varying Supervelocity Ratio $\delta_i$ (incompressible), according to Formula* (2.5)

Table 1. $\delta_i$ against $M_c$

| $M_c$ | $\delta_i$ |
|---|---|
| 1·00 | 0·0000 |
| 0·99 | 0·0012 |
| 0·98 | 0·0034 |
| 0·97 | 0·0063 |
| 0·96 | 0·0097 |
| 0·95 | 0·0137 |
| 0·94 | 0·0182 |
| 0·93 | 0·0232 |
| 0·92 | 0·0286 |
| 0·91 | 0·0344 |
| 0·90 | 0·0407 |
| 0·89 | 0·0473 |
| 0·88 | 0·0545 |
| 0·87 | 0·0620 |
| 0·86 | 0·0700 |
| 0·85 | 0·0784 |
| 0·84 | 0·0872 |
| 0·83 | 0·0965 |
| 0·82 | 0·1062 |
| 0·81 | 0·1164 |
| 0·80 | 0·1270 |
| 0·79 | 0·1381 |
| 0·78 | 0·1497 |
| 0·77 | 0·1618 |
| 0·76 | 0·1744 |
| 0·75 | 0·1875 |
| 0·74 | 0·2012 |
| 0·73 | 0·2154 |
| 0·72 | 0·2301 |
| 0·71 | 0·2455 |
| 0·70 | 0·2615 |
| 0·69 | 0·2780 |
| 0·68 | 0·2953 |
| 0·67 | 0·3132 |
| 0·66 | 0·3318 |
| 0·65 | 0·3511 |
| 0·64 | 0·3712 |
| 0·63 | 0·3921 |
| 0·62 | 0·4138 |
| 0·61 | 0·4363 |
| 0·60 | 0·4597 |
| 0·59 | 0·4841 |
| 0·58 | 0·5094 |
| 0·57 | 0·5358 |
| 0·56 | 0·5632 |
| 0·55 | 0·5917 |
| 0·54 | 0·6215 |

Table 1a. $M_c$ against $\delta_i$

| $\delta_i$ | $M_c$ | $\delta_i$ | $M_c$ |
|---|---|---|---|
| 0 | 1·0000 | 0·30 | 0·6773 |
| 0·01 | 0·9593 | 0·31 | 0·6718 |
| 0·02 | 0·9363 | 0·32 | 0·6663 |
| 0·03 | 0·9175 | 0·33 | 0·6609 |
| 0·04 | 0·9010 | 0·34 | 0·6557 |
| 0·05 | 0·8862 | 0·35 | 0·6506 |
| 0·06 | 0·8726 | 0·36 | 0·6455 |
| 0·07 | 0·8600 | 0·37 | 0·6406 |
| 0·08 | 0·8481 | 0·38 | 0·6357 |
| 0·09 | 0·8369 | 0·39 | 0·6310 |
| 0·10 | 0·8263 | 0·40 | 0·6263 |
| 0·11 | 0·8162 | 0·41 | 0·6217 |
| 0·12 | 0·8066 | 0·42 | 0·6172 |
| 0·13 | 0·7973 | 0·43 | 0·6128 |
| 0·14 | 0·7883 | 0·44 | 0·6084 |
| 0·15 | 0·7797 | 0·45 | 0·6041 |
| 0·16 | 0·7715 | 0·46 | 0·5999 |
| 0·17 | 0·7635 | 0·47 | 0·5958 |
| 0·18 | 0·7557 | 0·48 | 0·5917 |
| 0·19 | 0·7482 | 0·49 | 0·5877 |
| 0·20 | 0·7408 | 0·50 | 0·5837 |
| 0·21 | 0·7337 | 0·51 | 0·5798 |
| 0·22 | 0·7268 | 0·52 | 0·5760 |
| 0·23 | 0·7201 | 0·53 | 0·5722 |
| 0·24 | 0·7135 | 0·54 | 0·5685 |
| 0·25 | 0·7071 | 0·55 | 0·5648 |
| 0·26 | 0·7009 | 0·56 | 0·5612 |
| 0·27 | 0·6948 | 0·57 | 0·5576 |
| 0·28 | 0·6888 | 0·58 | 0·5541 |
| 0·29 | 0·6830 | 0·59 | 0·5506 |
| 0·30 | 0·6773 | 0·60 | 0·5472 |

## TABLE 2

*Critical Mach Numbers for Yawed Infinite Wings $M_{cy}$ for Varying Angle $\varphi$ and Varying Supervelocity Ratio $\delta_i$, according to Formula* (3.4)

| $\delta_i$ | $\varphi$ (degrees) | | | | | |
|---|---|---|---|---|---|---|
| | 10 | 20 | 30 | 40 | 50 | 60 |
| 0 | 1·0154 | 1·0642 | 1·1547 | 1·3054 | 1·5557 | 2·0000 |
| 0·01 | 0·9741 | 1·0209 | 1·1077 | 1·2523 | 1·4924 | 1·9186 |
| 0·02 | 0·9507 | 0·9964 | 1·0811 | 1·2223 | 1·4566 | 1·8726 |
| 0·03 | 0·9317 | 0·9764 | 1·0594 | 1·1977 | 1·4274 | 1·8350 |
| 0·04 | 0·9149 | 0·9588 | 1·0404 | 1·1762 | 1·4017 | 1·8020 |
| 0·05 | 0·8999 | 0·9431 | 1·0233 | 1·1569 | 1·3787 | 1·7724 |
| 0·06 | 0·8861 | 0·9286 | 1·0076 | 1·1391 | 1·3575 | 1·7452 |
| 0·07 | 0·8733 | 0·9152 | 0·9930 | 1·1227 | 1·3379 | 1·7200 |
| 0·08 | 0·8612 | 0·9025 | 0·9793 | 1·1071 | 1·3194 | 1·6962 |
| 0·09 | 0·8498 | 0·8906 | 0·9664 | 1·0925 | 1·3020 | 1·6738 |
| 0·10 | 0·8390 | 0·8793 | 0·9541 | 1·0787 | 1·2855 | 1·6526 |
| 0·11 | 0·8288 | 0·8686 | 0·9425 | 1·0655 | 1·2698 | 1·6324 |
| 0·12 | 0·8190 | 0·8584 | 0·9314 | 1·0529 | 1·2548 | 1·6132 |
| 0·13 | 0·8096 | 0·8485 | 0·9206 | 1·0408 | 1·2404 | 1·5946 |
| 0·14 | 0·8005 | 0·8389 | 0·9103 | 1·0291 | 1·2264 | 1·5766 |
| 0·15 | 0·7917 | 0·8297 | 0·9003 | 1·0178 | 1·2130 | 1·5594 |
| 0·16 | 0·7834 | 0·8210 | 0·8909 | 1·0071 | 1·2002 | 1·5430 |
| 0·17 | 0·7753 | 0·8125 | 0·8816 | 0·9967 | 1·1878 | 1·5270 |
| 0·18 | 0·7674 | 0·8042 | 0·8726 | 0·9865 | 1·1757 | 1·5114 |
| 0·19 | 0·7597 | 0·7962 | 0·8639 | 0·9767 | 1·1640 | 1·4964 |
| 0·20 | 0·7522 | 0·7883 | 0·8554 | 0·9670 | 1·1525 | 1·4816 |
| 0·21 | 0·7450 | 0·7808 | 0·8472 | 0·9578 | 1·1414 | 1·4674 |
| 0·22 | 0·7380 | 0·7734 | 0·8392 | 0·9488 | 1·1307 | 1·4536 |
| 0·23 | 0·7312 | 0·7663 | 0·8315 | 0·9400 | 1·1203 | 1·4402 |
| 0·24 | 0·7245 | 0·7593 | 0·8239 | 0·9314 | 1·1100 | 1·4270 |
| 0·25 | 0·7180 | 0·7525 | 0·8165 | 0·9231 | 1·1001 | 1·4142 |
| 0·26 | 0·7117 | 0·7459 | 0·8093 | 0·9150 | 1·0904 | 1·4018 |
| 0·27 | 0·7055 | 0·7394 | 0·8023 | 0·9070 | 1·0809 | 1·3896 |
| 0·28 | 0·6994 | 0·7330 | 0·7954 | 0·8992 | 1·0716 | 1·3776 |
| 0·29 | 0·6935 | 0·7268 | 0·7887 | 0·8916 | 1·0626 | 1·3660 |
| 0·30 | 0·6877 | 0·7208 | 0·7821 | 0·8842 | 1·0537 | 1·3546 |
| 0·31 | 0·6822 | 0·7149 | 0·7757 | 0·8770 | 1·0451 | 1·3436 |
| 0·32 | 0·6766 | 0·7091 | 0·7694 | 0·8698 | 1·0366 | 1·3326 |
| 0·33 | 0·6711 | 0·7033 | 0·7631 | 0·8627 | 1·0282 | 1·3218 |
| 0·34 | 0·6658 | 0·6978 | 0·7571 | 0·8560 | 1·0201 | 1·3114 |
| 0·35 | 0·6606 | 0·6924 | 0·7512 | 0·8493 | 1·0122 | 1·3012 |
| 0·36 | 0·6555 | 0·6869 | 0·7454 | 0·8426 | 1·0042 | 1·2910 |
| 0·37 | 0·6505 | 0·6817 | 0·7397 | 0·8362 | 0·9966 | 1·2812 |
| 0·38 | 0·6455 | 0·6765 | 0·7340 | 0·8298 | 0·9890 | 1·2714 |
| 0·39 | 0·6407 | 0·6715 | 0·7286 | 0·8237 | 0·9817 | 1·2620 |
| 0·40 | 0·6360 | 0·6665 | 0·7232 | 0·8176 | 0·9743 | 1·2526 |
| 0·41 | 0·6313 | 0·6616 | 0·7179 | 0·8116 | 0·9672 | 1·2434 |
| 0·42 | 0·6267 | 0·6568 | 0·7127 | 0·8057 | 0·9602 | 1·2344 |
| 0·43 | 0·6223 | 0·6521 | 0·7076 | 0·8000 | 0·9533 | 1·2256 |
| 0·44 | 0·6178 | 0·6474 | 0·7025 | 0·7962 | 0·9465 | 1·2168 |
| 0·45 | 0·6134 | 0·6429 | 0·6976 | 0·7886 | 0·9398 | 1·2082 |

## TABLE 3

*Critical Mach Numbers for Sheared Infinite Wings $M_{cs}$ for Varying Angle $\varphi$ and Varying Supervelocity Ratio $\delta_i$, according to Formula* (3.6)

| $\delta_i$ | $\varphi$ (degrees) | | | | | |
|---|---|---|---|---|---|---|
| | 10 | 20 | 30 | 40 | 50 | 60 |
| 0 | 1·0154 | 1·0642 | 1·1547 | 1·3054 | 1·5557 | 2·0000 |
| 0·01 | 0·9737 | 1·0191 | 1·1031 | 1·2423 | 1·4714 | 1·8726 |
| 0·02 | 0·9502 | 0·9937 | 1·0740 | 1·2068 | 1·4244 | 1·8021 |
| 0·03 | 0·9308 | 0·9729 | 1·0503 | 1·1780 | 1·3862 | 1·7453 |
| 0·04 | 0·9139 | 0·9547 | 1·0297 | 1·1529 | 1·3530 | 1·6963 |
| 0·05 | 0·8989 | 0·9383 | 1·0111 | 1·1303 | 1·3234 | 1·6527 |
| 0·06 | 0·8849 | 0·9234 | 0·9940 | 1·1097 | 1·2965 | 1·6132 |
| 0·07 | 0·8719 | 0·9095 | 0·9783 | 1·0907 | 1·2716 | 1·5768 |
| 0·08 | 0·8598 | 0·8964 | 0·9636 | 1·0728 | 1·2483 | 1·5430 |
| 0·09 | 0·8484 | 0·8841 | 0·9496 | 1·0560 | 1·2265 | 1·5117 |
| 0·10 | 0·8375 | 0·8724 | 0·9363 | 1·0402 | 1·2059 | 1·4817 |
| 0·11 | 0·8272 | 0·8613 | 0·9238 | 1·0251 | 1·1866 | 1·4537 |
| 0·12 | 0·8173 | 0·8507 | 0·9118 | 1·0107 | 1·1678 | 1·4272 |
| 0·13 | 0·8078 | 0·8405 | 0·9003 | 0·9971 | 1·1501 | 1·4018 |
| 0·14 | 0·7986 | 0·8307 | 0·8893 | 0·9839 | 1·1331 | 1·3777 |
| 0·15 | 0·7898 | 0·8213 | 0·8789 | 0·9711 | 1·1169 | 1·3547 |
| 0·16 | 0·7813 | 0·8124 | 0·8685 | 0·9589 | 1·1012 | 1·3327 |
| 0·17 | 0·7733 | 0·8036 | 0·8586 | 0·9472 | 1·0862 | 1·3115 |
| 0·18 | 0·7653 | 0·7950 | 0·8490 | 0·9358 | 1·0717 | 1·2914 |
| 0·19 | 0·7575 | 0·7867 | 0·8398 | 0·9248 | 1·0576 | 1·2719 |
| 0·20 | 0·7500 | 0·7787 | 0·8308 | 0·9141 | 1·0441 | 1·2527 |
| 0·21 | 0·7428 | 0·7710 | 0·8221 | 0·9038 | 1·0310 | 1·2345 |
| 0·22 | 0·7357 | 0·7634 | 0·8137 | 0·8938 | 1·0184 | 1·2169 |
| 0·23 | 0·7289 | 0·7561 | 0·8054 | 0·8841 | 1·0062 | 1·1998 |
| 0·24 | 0·7221 | 0·7490 | 0·7974 | 0·8746 | 0·9944 | 1·1834 |
| 0·25 | 0·7156 | 0·7420 | 0·7896 | 0·8654 | 0·9825 | 1·1675 |
| 0·26 | 0·7092 | 0·7352 | 0·7820 | 0·8564 | 0·9712 | 1·1520 |
| 0·27 | 0·7030 | 0·7286 | 0·7746 | 0·8477 | 0·9602 | 1·1369 |
| 0·28 | 0·6969 | 0·7220 | 0·7674 | 0·8394 | 0·9495 | 1·1223 |
| 0·29 | 0·6910 | 0·7157 | 0·7603 | 0·8311 | 0·9391 | 1·1082 |
| 0·30 | 0·6852 | 0·7095 | 0·7534 | 0·8227 | 0·9290 | 1·0944 |
| 0·31 | 0·6795 | 0·7034 | 0·7467 | 0·8148 | 0·9190 | 1·0810 |
| 0·32 | 0·6739 | 0·6976 | 0·7402 | 0·8071 | 0·9094 | 1·0680 |
| 0·33 | 0·6685 | 0·6917 | 0·7337 | 0·7995 | 0·9000 | 1·0553 |
| 0·34 | 0·6631 | 0·6862 | 0·7272 | 0·7921 | 0·8908 | 1·0429 |
| 0·35 | 0·6579 | 0·6807 | 0·7210 | 0·7848 | 0·8818 | 1·0309 |
| 0·36 | 0·6529 | 0·6751 | 0·7149 | 0·7778 | 0·8730 | 1·0191 |
| 0·37 | 0·6479 | 0·6696 | 0·7090 | 0·7708 | 0·8644 | 1·0077 |
| 0·38 | 0·6428 | 0·6644 | 0·7032 | 0·7640 | 0·8560 | 0·9964 |
| 0·39 | 0·6379 | 0·6592 | 0·6975 | 0·7573 | 0·8478 | 0·9855 |
| 0·40 | 0·6331 | 0·6542 | 0·6918 | 0·7508 | 0·8397 | 0·9748 |
| 0·41 | 0·6284 | 0·6492 | 0·6863 | 0·7444 | 0·8319 | 0·9644 |
| 0·42 | 0·6238 | 0·6443 | 0·6809 | 0·7381 | 0·8241 | 0·9542 |
| 0·43 | 0·6193 | 0·6395 | 0·6756 | 0·7319 | 0·8166 | 0·9442 |
| 0·44 | 0·6149 | 0·6348 | 0·6703 | 0·7259 | 0·8091 | 0·9344 |
| 0·45 | 0·6105 | 0·6301 | 0·6653 | 0·7199 | 0·8019 | 0·9249 |

TABLE 4

*Upper Critical Mach Numbers for Untapered Swept Wings with Four Different Profiles, for Varying Angle $\varphi$ and Thickness Ratio $\vartheta$ (obtained by interpolation from Table 3)*

(1) Profile B $\delta_i = \frac{4}{\pi}\vartheta = 1\cdot2732\vartheta$; $\vartheta = 0\cdot7854\delta_i$

| $\pm\varphi$ (deg) | $\vartheta$ | | | | | |
|---|---|---|---|---|---|---|
| | 0·05 | 0·10 | 0·15 | 0·20 | 0·25 | 0·30 |
| 0 | 0·868 | 0·800 | 0·748 | 0·704 | 0·667 | 0·635 |
| 10 | 0·880 | 0·810 | 0·757 | 0·713 | 0·675 | 0·642 |
| 20 | 0·918 | 0·843 | 0·786 | 0·739 | 0·699 | 0·663 |
| 30 | 0·988 | 0·903 | 0·839 | 0·786 | 0·741 | 0·702 |
| 40 | 1·103 | 1·001 | 0·924 | 0·861 | 0·808 | 0·763 |
| 50 | 1·287 | 1·155 | 1·056 | 0·977 | 0·911 | 0·854 |
| 60 | 1·600 | 1·409 | 1·270 | 1·160 | 1·070 | 0·994 |

(2) Profile C $\delta_i = 1\cdot6674\vartheta$; $\vartheta = 0\cdot5997\delta_i$

| $\pm\varphi$ (deg) | $\vartheta$ | | | | | |
|---|---|---|---|---|---|---|
| | 0·05 | 0·10 | 0·15 | 0·20 | 0·25 | 0·30 |
| 0 | 0·844 | 0·766 | 0·707 | 0·659 | 0·619 | 0·584 |
| 10 | 0·856 | 0·776 | 0·716 | 0·667 | 0·625 | 0·590 |
| 20 | 0·892 | 0·807 | 0·742 | 0·690 | 0·646 | 0·608 |
| 30 | 0·959 | 0·862 | 0·790 | 0·731 | 0·683 | 0·641 |
| 40 | 1·067 | 0·951 | 0·865 | 0·797 | 0·740 | 0·692 |
| 50 | 1·241 | 1·091 | 0·982 | 0·897 | 0·827 | 0·767 |
| 60 | 1·532 | 1·318 | 1·167 | 1·051 | 0·957 | 0·876 |

(3) Profile Q $\delta_i = 1\cdot7214\vartheta$; $\vartheta = 0\cdot5809\delta_i$

| $\pm\varphi$ (deg) | $\vartheta$ | | | | | |
|---|---|---|---|---|---|---|
| | 0·05 | 0·10 | 0·15 | 0·20 | 0·25 | 0·30 |
| 0 | 0·841 | 0·762 | 0·702 | 0·654 | 0·613 | 0·577 |
| 10 | 0·853 | 0·772 | 0·710 | 0·661 | 0·619 | 0·583 |
| 20 | 0·889 | 0·802 | 0·736 | 0·684 | 0·639 | 0·601 |
| 30 | 0·955 | 0·856 | 0·783 | 0·725 | 0·675 | 0·633 |
| 40 | 1·063 | 0·945 | 0·858 | 0·789 | 0·732 | 0·683 |
| 50 | 1·235 | 1·083 | 0·973 | 0·887 | 0·816 | 0·757 |
| 60 | 1·524 | 1·307 | 1·155 | 1·038 | 0·944 | — |

(4) Profile R $\delta_i = 1\cdot9108\vartheta$; $\vartheta = 0\cdot5233\delta_i$

| $\pm\varphi$ (deg) | $\vartheta$ | | | | | |
|---|---|---|---|---|---|---|
| | 0·05 | 0·10 | 0·15 | 0·20 | 0·25 | 0·30 |
| 0 | 0·831 | 0·747 | 0·685 | 0·635 | 0·593 | 0·557 |
| 10 | 0·842 | 0·757 | 0·693 | 0·642 | 0·599 | 0·562 |
| 20 | 0·878 | 0·786 | 0·718 | 0·663 | 0·618 | 0·579 |
| 30 | 0·942 | 0·839 | 0·763 | 0·702 | 0·652 | 0·609 |
| 40 | 1·047 | 0·924 | 0·834 | 0·763 | 0·704 | 0·655 |
| 50 | 1·215 | 1·056 | 0·943 | 0·854 | 0·782 | 0·722 |
| 60 | 1·495 | 1·269 | 1·113 | 0·994 | — | — |

TABLE 5

*Maximum Supervelocities in the Kink Section of a Swept Wing, Profile* B

| $\pm\varphi$ (deg) | $\mp\,\xi_m$ | $\left(-\dfrac{v_x}{\vartheta U\cos\varphi}\right)_{\max}$ | $H=\left(-\dfrac{v_x}{\vartheta U}\right)_{\max}$ |
|---|---|---|---|
| 0 | 0·000 | 1·273 | 1·273 |
| 1 | 0·009 | 1·273 | 1·273 |
| 2 | 0·018 | 1·274 | 1·273 |
| 3 | 0·026 | 1·274 | 1·272 |
| 4 | 0·035 | 1·275 | 1·272 |
| 5 | 0·044 | 1·276 | 1·271 |
| 6 | 0·052 | 1·277 | 1·270 |
| 7 | 0·061 | 1·278 | 1·269 |
| 8 | 0·070 | 1·279 | 1·267 |
| 9 | 0·079 | 1·281 | 1·265 |
| 10 | 0·087 | 1·283 | 1·264 |
| 11 | 0·096 | 1·285 | 1·262 |
| 12 | 0·105 | 1·287 | 1·259 |
| 13 | 0·113 | 1·290 | 1·257 |
| 14 | 0·122 | 1·293 | 1·254 |
| 15 | 0·131 | 1·295 | 1·251 |
| 16 | 0·140 | 1·299 | 1·248 |
| 17 | 0·148 | 1·302 | 1·245 |
| 18 | 0·157 | 1·305 | 1·242 |
| 19 | 0·166 | 1·309 | 1·238 |
| 20 | 0·175 | 1·313 | 1·234 |
| 21 | 0·183 | 1·318 | 1·230 |
| 22 | 0·192 | 1·322 | 1·226 |
| 23 | 0·201 | 1·327 | 1·221 |
| 24 | 0·210 | 1·332 | 1·217 |
| 25 | 0·218 | 1·337 | 1·212 |
| 26 | 0·227 | 1·342 | 1·207 |
| 27 | 0·236 | 1·348 | 1·201 |
| 28 | 0·244 | 1·354 | 1·196 |
| 29 | 0·253 | 1·360 | 1·190 |
| 30 | 0·262 | 1·367 | 1·184 |
| 31 | 0·271 | 1·374 | 1·178 |
| 32 | 0·279 | 1·381 | 1·171 |
| 33 | 0·288 | 1·388 | 1·165 |
| 34 | 0·297 | 1·396 | 1·158 |
| 35 | 0·306 | 1·404 | 1·150 |
| 36 | 0·314 | 1·413 | 1·143 |
| 37 | 0·323 | 1·422 | 1·135 |
| 38 | 0·332 | 1·431 | 1·128 |
| 39 | 0·341 | 1·440 | 1·119 |
| 40 | 0·350 | 1·450 | 1·111 |
| 41 | 0·358 | 1·461 | 1·102 |
| 42 | 0·367 | 1·471 | 1·093 |

| $\pm\varphi$ (deg) | $\mp\,\xi_m$ | $\left(-\dfrac{v_x}{\vartheta U\cos\varphi}\right)_{\max}$ | $H$ |
|---|---|---|---|
| 43 | 0·376 | 1·483 | 1·084 |
| 44 | 0·385 | 1·494 | 1·074 |
| 45 | 0·393 | 1·506 | 1·065 |
| 46 | 0·402 | 1·519 | 1·055 |
| 47 | 0·411 | 1·532 | 1·045 |
| 48 | 0·420 | 1·546 | 1·034 |
| 49 | 0·429 | 1·560 | 1·024 |
| 50 | 0·438 | 1·575 | 1·012 |
| 51 | 0·447 | 1·590 | 1·001 |
| 52 | 0·455 | 1·606 | 0·989 |
| 53 | 0·464 | 1·623 | 0·977 |
| 54 | 0·473 | 1·641 | 0·964 |
| 55 | 0·482 | 1·659 | 0·952 |
| 56 | 0·491 | 1·678 | 0·938 |
| 57 | 0·500 | 1·698 | 0·925 |
| 58 | 0·509 | 1·719 | 0·911 |
| 59 | 0·518 | 1·741 | 0·897 |
| 60 | 0·527 | 1·764 | 0·882 |
| 61 | 0·537 | 1·788 | 0·867 |
| 62 | 0·546 | 1·813 | 0·851 |
| 63 | 0·555 | 1·839 | 0·835 |
| 64 | 0·564 | 1·867 | 0·819 |
| 65 | 0·573 | 1·897 | 0·802 |
| 66 | 0·583 | 1·928 | 0·784 |
| 67 | 0·592 | 1·960 | 0·766 |
| 68 | 0·602 | 1·995 | 0·747 |
| 69 | 0·611 | 2·032 | 0·728 |
| 70 | 0·621 | 2·071 | 0·708 |
| 71 | 0·630 | 2·113 | 0·688 |
| 72 | 0·640 | 2·157 | 0·667 |
| 73 | 0·650 | 2·205 | 0·645 |
| 74 | 0·660 | 2·256 | 0·622 |
| 75 | 0·670 | 2·311 | 0·598 |
| 76 | 0·681 | 2·371 | 0·574 |
| 77 | 0·691 | 2·437 | 0·548 |
| 78 | 0·702 | 2·508 | 0·522 |
| 79 | 0·713 | 2·587 | 0·494 |
| 80 | 0·724 | 2·675 | 0·464 |
| 81 | 0·735 | 2·773 | 0·434 |
| 82 | 0·747 | 2·885 | 0·401 |
| 83 | 0·760 | 3·013 | 0·367 |
| — | — | — | — |
| 90 | 1·000 | $\infty$ | 0 |

# TABLE 6

*Maximum Supervelocities in the Kink Section and Kink Area of Swept Wings, Profile* C

| $\varphi$ (deg) | Kink section | | |
|---|---|---|---|
| | $\xi_m$ | $\left(-\dfrac{v_x}{\vartheta U \cos\varphi}\right)_{\max}$ | $H$ |
| 90 | —0·333 | $\infty$ | 0 |
| — | — | — | — |
| 84 | —0·090 | 2·704 | 0·283 |
| 83 | —0·079 | 2·609 | 0·318 |
| 82 | —0·068 | 2·527 | 0·352 |
| 81 | —0·058 | 2·457 | 0·384 |
| 80 | —0·048 | 2·395 | 0·416 |
| 79 | —0·039 | 2·339 | 0·446 |
| 78 | —0·029 | 2·288 | 0·476 |
| 77 | —0·020 | 2·243 | 0·505 |
| 76 | —0·012 | 2·202 | 0·533 |
| 75 | —0·004 | 2·164 | 0·560 |
| 74 | 0·005 | 2·129 | 0·587 |
| 73 | 0·013 | 2·096 | 0·613 |
| 72 | 0·021 | 2·066 | 0·638 |
| 71 | 0·028 | 2·038 | 0·664 |
| 70 | 0·036 | 2·012 | 0·688 |
| 69 | 0·044 | 1·987 | 0·712 |
| 68 | 0·051 | 1·964 | 0·736 |
| 67 | 0·058 | 1·943 | 0·759 |
| 66 | 0·065 | 1·922 | 0·782 |
| 65 | 0·072 | 1·903 | 0·804 |
| 64 | 0·079 | 1·885 | 0·826 |
| 63 | 0·086 | 1·868 | 0·848 |
| 62 | 0·093 | 1·852 | 0·869 |
| 61 | 0·100 | 1·836 | 0·890 |
| 60 | 0·107 | 1·822 | 0·911 |
| 59 | 0·113 | 1·808 | 0·931 |
| 58 | 0·120 | 1·795 | 0·951 |
| 57 | 0·127 | 1·783 | 0·971 |
| 56 | 0·133 | 1·771 | 0·990 |
| 55 | 0·140 | 1·760 | 1·009 |
| 54 | 0·146 | 1·750 | 1·028 |
| 53 | 0·153 | 1·739 | 1·047 |
| 52 | 0·159 | 1·730 | 1·065 |
| 51 | 0·165 | 1·721 | 1·083 |
| 50 | 0·172 | 1·712 | 1·101 |
| 49 | 0·178 | 1·704 | 1·118 |
| 48 | 0·184 | 1·697 | 1·135 |
| 47 | 0·190 | 1·689 | 1·152 |
| 46 | 0·196 | 1·683 | 1·169 |
| 45 | 0·202 | 1·676 | 1·185 |
| 44 | 0·209 | 1·670 | 1·201 |

| $\varphi$ (deg) | Kink section | | | Kink area ($\xi_m \simeq 0{\cdot}456$) |
|---|---|---|---|---|
| | $\xi_m$ | $\left(-\dfrac{v_x}{\vartheta U \cos\varphi}\right)_{\max}$ | $H$ | $H$ |
| 43 | 0·215 | 1·664 | 1·217 | 1·220 |
| 42 | 0·221 | 1·659 | 1·233 | 1·239 |
| 41 | 0·227 | 1·654 | 1·248 | 1·258 |
| 40 | 0·233 | 1·649 | 1·263 | 1·277 |
| 39 | 0·238 | 1·645 | 1·278 | 1·296 |
| 38 | 0·244 | 1·641 | 1·293 | 1·314 |
| 37 | 0·250 | 1·637 | 1·307 | 1·332 |
| 36 | 0·256 | 1·633 | 1·321 | 1·349 |
| 35 | 0·262 | 1·630 | 1·335 | 1·366 |
| 34 | 0·268 | 1·627 | 1·349 | 1·382 |
| 33 | 0·274 | 1·625 | 1·362 | 1·398 |
| 32 | 0·279 | 1·622 | 1·376 | 1·414 |
| 31 | 0·285 | 1·620 | 1·389 | 1·429 |
| 30 | 0·291 | 1·618 | 1·401 | 1·444 |
| 29 | 0·297 | 1·616 | 1·414 | 1·458 |
| 28 | 0·302 | 1·615 | 1·426 | 1·472 |
| 27 | 0·308 | 1·614 | 1·438 | 1·486 |
| 26 | 0·314 | 1·613 | 1·450 | 1·499 |
| 25 | 0·319 | 1·612 | 1·461 | 1·511 |
| 24 | 0·325 | 1·612 | 1·472 | 1·523 |
| 23 | 0·331 | 1·612 | 1·483 | 1·535 |
| 22 | 0·336 | 1·612 | 1·494 | 1·546 |
| 21 | 0·342 | 1·612 | 1·505 | 1·557 |
| 20 | 0·347 | 1·612 | 1·515 | 1·567 |
| 19 | 0·353 | 1·613 | 1·525 | 1·577 |
| 18 | 0·358 | 1·614 | 1·535 | 1·586 |
| 17 | 0·364 | 1·615 | 1·544 | 1·595 |
| 16 | 0·369 | 1·616 | 1·554 | 1·603 |
| 15 | 0·375 | 1·618 | 1·563 | 1·611 |
| 14 | 0·380 | 1·620 | 1·571 | 1·618 |
| 13 | 0·386 | 1·622 | 1·580 | 1·625 |
| 12 | 0·391 | 1·624 | 1·588 | 1·631 |
| 11 | 0·397 | 1·626 | 1·596 | 1·637 |
| 10 | 0·402 | 1·629 | 1·604 | 1·642 |
| 9 | 0·408 | 1·632 | 1·612 | 1·647 |
| 8 | 0·413 | 1·635 | 1·619 | 1·651 |
| 7 | 0·418 | 1·638 | 1·626 | 1·655 |
| 6 | 0·424 | 1·642 | 1·633 | 1·658 |
| 5 | 0·429 | 1·645 | 1·639 | 1·661 |
| 4 | 0·434 | 1·649 | 1·645 | 1·663 |
| 2 | 0·440 | 1·654 | 1·651 | 1·665 |
| 2 | 0·445 | 1·658 | 1·657 | 1·666 |
| 1 | 0·450 | 1·663 | 1·662 | 1·667 |
| 0 | 0·456 | 1·667 | 1·667 | 1·667 |

TABLE 6—*continued*

| $\varphi$ (deg) | Kink section | | |
|---|---|---|---|
| | $\xi_m$ | $\left(-\dfrac{v_x}{\vartheta U \cos\varphi}\right)_{\max}$ | $H$ |
| 0 | 0·456 | 1·667 | 1·667 |
| —1 | 0·461 | 1·673 | 1·672 |
| —2 | 0·466 | 1·678 | 1·677 |
| —3 | 0·471 | 1·684 | 1·681 |
| —4 | 0·477 | 1·689 | 1·685 |
| —5 | 0·482 | 1·695 | 1·689 |
| —6 | 0·487 | 1·702 | 1·692 |
| —7 | 0·492 | 1·708 | 1·696 |
| —8 | 0·497 | 1·715 | 1·699 |
| —9 | 0·502 | 1·722 | 1·701 |
| —10 | 0·508 | 1·730 | 1·703 |
| —11 | 0·513 | 1·737 | 1·705 |
| —12 | 0·518 | 1·745 | 1·707 |
| —13 | 0·523 | 1·753 | 1·709 |
| —14 | 0·528 | 1·762 | 1·710 |
| —15 | 0·533 | 1·771 | 1·710 |
| —16 | 0·538 | 1·780 | 1·711 |
| —17 | 0·543 | 1·789 | 1·711 |
| —18 | 0·548 | 1·799 | 1·711 |
| —19 | 0·554 | 1·809 | 1·710 |
| —20 | 0·559 | 1·819 | 1·710 |
| —21 | 0·564 | 1·830 | 1·708 |
| —22 | 0·569 | 1·841 | 1·707 |
| —23 | 0·574 | 1·852 | 1·705 |
| —24 | 0·579 | 1·864 | 1·703 |
| —25 | 0·584 | 1·876 | 1·700 |
| —26 | 0·589 | 1·889 | 1·698 |
| —27 | 0·594 | 1·902 | 1·694 |
| —28 | 0·599 | 1·915 | 1·691 |
| —29 | 0·604 | 1·929 | 1·687 |
| —30 | 0·609 | 1·943 | 1·682 |
| —31 | 0·614 | 1·957 | 1·678 |
| —32 | 0·619 | 1·972 | 1·673 |
| —33 | 0·623 | 1·988 | 1·667 |
| —34 | 0·628 | 2·004 | 1·661 |
| —35 | 0·633 | 2·020 | 1·655 |
| —36 | 0·638 | 2·038 | 1·648 |
| —37 | 0·643 | 2·055 | 1·641 |
| —38 | 0·648 | 2·074 | 1·634 |
| —39 | 0·653 | 2·092 | 1·626 |
| —40 | 0·658 | 2·112 | 1·618 |
| —41 | 0·663 | 2·132 | 1·609 |
| —42 | 0·668 | 2·152 | 1·600 |
| —43 | 0·672 | 2·174 | 1·590 |
| —44 | 0·677 | 2·196 | 1·580 |
| —45 | 0·682 | 2·219 | 1·569 |
| —46 | 0·687 | 2·243 | 1·558 |
| —47 | 0·692 | 2·268 | 1·546 |
| —48 | 0·697 | 2·293 | 1·534 |
| —49 | 0·702 | 2·319 | 1·522 |
| —50 | 0·707 | 2·347 | 1·508 |
| —51 | 0·711 | 2·375 | 1·495 |
| —52 | 0·716 | 2·405 | 1·480 |
| —53 | 0·721 | 2·435 | 1·466 |
| —54 | 0·726 | 2·467 | 1·450 |
| —55 | 0·731 | 2·500 | 1·434 |
| —56 | 0·736 | 2·534 | 1·417 |
| —57 | 0·740 | 2·570 | 1·400 |
| —58 | 0·745 | 2·607 | 1·382 |
| —59 | 0·750 | 2·647 | 1·363 |
| —60 | 0·755 | 2·687 | 1·344 |
| —61 | 0·760 | 2·730 | 1·324 |
| —62 | 0·765 | 2·775 | 1·303 |
| —63 | 0·770 | 2·822 | 1·281 |
| —64 | 0·775 | 2·871 | 1·259 |
| —65 | 0·780 | 2·922 | 1·235 |
| —66 | 0·785 | 2·977 | 1·211 |
| —67 | 0·790 | 3·034 | 1·186 |
| —68 | 0·795 | 3·094 | 1·159 |
| —69 | 0·800 | 3·158 | 1·132 |
| —70 | 0·805 | 3·226 | 1·103 |
| —71 | 0·810 | 3·298 | 1·074 |
| —72 | 0·815 | 3·375 | 1·043 |
| —73 | 0·820 | 3·457 | 1·011 |
| —74 | 0·826 | 3·546 | 0·977 |
| —75 | 0·831 | 3·641 | 0·943 |
| —76 | 0·837 | 3·746 | 0·906 |
| —77 | 0·842 | 3·858 | 0·868 |
| —78 | 0·848 | 3·981 | 0·828 |
| —79 | 0·853 | 4·117 | 0·786 |
| —80 | 0·859 | 4·266 | 0·741 |
| —81 | 0·865 | 4·434 | 0·694 |
| —82 | 0·871 | 4·623 | 0·643 |
| —83 | 0·878 | 4·844 | 0·590 |
| — | — | — | — |
| —90 | 1·000 | $\infty$ | 0 |

TABLE 7

*Maximum Supervelocities in the Kink Section and Kink Area of Swept Wings, Profile Q*

| $\varphi$ (deg) | Front of the kink section | | | Rear of the kink section | | |
|---|---|---|---|---|---|---|
| | $\xi_m$ | $\left(-\frac{v_x}{\vartheta U \cos\varphi}\right)_{max}$ | $H = \left(-\frac{v_x}{\vartheta U}\right)_{max}$ | $\xi_m$ | $\left(-\frac{v_x}{\vartheta U \cos\varphi}\right)_{max}$ | $H = \left(-\frac{v_x}{\vartheta U}\right)_{max}$ |
| 90 | | | | —1 | ∞ | 0 |
| — | — | — | — | — | — | — |
| 84 | | | | —0·909 | 2·459 | 0·257 |
| 83 | | | | —0·904 | 2·318 | 0·283 |
| 82 | | | | —0·899 | 2·198 | 0·306 |
| 81 | | | | —0·894 | 2·093 | 0·327 |
| 80 | 0·175 | 1·826 | 0·317 | —0·889 | 2·000 | 0·347 |
| 79 | 0·184 | 1·797 | 0·343 | —0·884 | 1·917 | 0·366 |
| 78 | 0·193 | 1·772 | 0·368 | —0·879 | 1·842 | 0·383 |
| 77 | 0·201 | 1·749 | 0·393 | —0·874 | 1·774 | 0·399 |
| 76 | 0·209 | 1·728 | 0·418 | —0·870 | 1·711 | 0·414 |
| | | | | front of the kink area | | |
| 75 | 0·216 | 1·710 | 0·443 | 0·598 | 1·722 | 0·446 |
| 74 | 0·224 | 1·693 | 0·467 | 0·598 | 1·722 | 0·475 |
| 73 | 0·231 | 1·677 | 0·490 | 0·598 | 1·722 | 0·503 |
| 72 | 0·238 | 1·663 | 0·514 | 0·598 | 1·722 | 0·532 |
| 71 | 0·245 | 1·650 | 0·537 | 0·598 | 1·722 | 0·561 |
| 70 | 0·252 | 1·638 | 0·560 | 0·598 | 1·722 | 0·589 |
| 69 | 0·258 | 1·627 | 0·583 | 0·598 | 1·722 | 0·617 |
| 68 | 0·265 | 1·617 | 0·606 | 0·598 | 1·722 | 0·645 |
| 67 | 0·271 | 1·607 | 0·628 | 0·598 | 1·722 | 0·673 |
| 66 | 0·278 | 1·598 | 0·650 | 0·598 | 1·722 | 0·700 |
| 65 | 0·284 | 1·590 | 0·672 | 0·598 | 1·722 | 0·728 |
| 64 | 0·290 | 1·583 | 0·694 | 0·598 | 1·722 | 0·755 |
| 63 | 0·296 | 1·576 | 0·716 | 0·598 | 1·722 | 0·782 |
| 62 | 0·302 | 1·570 | 0·737 | 0·598 | 1·722 | 0·808 |
| 61 | 0·308 | 1·564 | 0·758 | 0·598 | 1·722 | 0·835 |
| 60 | 0·314 | 1·559 | 0·779 | 0·598 | 1·722 | 0·861 |
| 59 | 0·319 | 1·554 | 0·800 | 0·598 | 1·722 | 0·887 |
| 58 | 0·325 | 1·549 | 0·821 | 0·598 | 1·722 | 0·912 |
| 57 | 0·331 | 1·545 | 0·841 | 0·598 | 1·722 | 0·938 |
| 56 | 0·336 | 1·541 | 0·862 | 0·598 | 1·722 | 0·963 |
| 55 | 0·342 | 1·538 | 0·882 | 0·598 | 1·722 | 0·987 |
| 54 | 0·347 | 1·535 | 0·902 | 0·598 | 1·722 | 1·012 |
| 53 | 0·353 | 1·532 | 0·922 | 0·598 | 1·722 | 1·036 |
| 52 | 0·358 | 1·530 | 0·942 | 0·598 | 1·722 | 1·060 |
| 51 | 0·364 | 1·528 | 0·962 | 0·598 | 1·722 | 1·083 |
| 50 | 0·369 | 1·526 | 0·981 | 0·598 | 1·722 | 1·107 |
| 49 | 0·374 | 1·525 | 1·000 | 0·598 | 1·722 | 1·129 |
| 48 | 0·379 | 1·524 | 1·020 | 0·598 | 1·722 | 1·152 |
| 47 | 0·384 | 1·523 | 1·039 | 0·598 | 1·722 | 1·174 |
| 46 | 0·390 | 1·522 | 1·057 | 0·598 | 1·722 | 1·196 |
| 45 | 0·395 | 1·522 | 1·076 | 0·598 | 1·722 | 1·217 |

TABLE 7—*continued*

| $\varphi$ (deg) | Front of the kink section | | | Front of the kink area | | |
|---|---|---|---|---|---|---|
| | $\xi_m$ | $\left(-\frac{v_x}{\vartheta U \cos\varphi}\right)_{\max}$ | $H=\left(-\frac{v_x}{\vartheta U}\right)_{\max}$ | $\xi_m$ | $\left(-\frac{v_x}{\vartheta U \cos\varphi}\right)_{\max}$ | $H=\left(-\frac{v_x}{\vartheta U}\right)_{\max}$ |
| 44 | 0·400 | 1·522 | 1·095 | 0·598 | 1·722 | 1·238 |
| 43 | 0·405 | 1·522 | 1·113 | 0·598 | 1·722 | 1·259 |
| 42 | 0·410 | 1·522 | 1·131 | 0·598 | 1·722 | 1·279 |
| 41 | 0·415 | 1·522 | 1·149 | 0·598 | 1·722 | 1·299 |
| 40 | 0·420 | 1·524 | 1·167 | 0·598 | 1·722 | 1·319 |
| 39 | | 1·525 | 1·185 | 0·598 | 1·722 | 1·338 |
| 38 | | 1·526 | 1·202 | 0·598 | 1·722 | 1·357 |
| 37 | | 1·527 | 1·220 | 0·598 | 1·722 | 1·375 |
| 36 | | 1·529 | 1·237 | 0·598 | 1·722 | 1·393 |
| 35 | | 1·531 | 1·254 | 0·598 | 1·722 | 1·410 |
| 34 | | 1·533 | 1·271 | 0·598 | 1·722 | 1·427 |
| 33 | | 1·535 | 1·288 | 0·598 | 1·722 | 1·444 |
| 32 | | 1·538 | 1·304 | 0·598 | 1·722 | 1·460 |
| 31 | | 1·541 | 1·321 | 0·598 | 1·722 | 1·476 |
| 30 | 0·467 | 1·543 | 1·337 | 0·598 | 1·722 | 1·491 |
| 29 | | 1·546 | 1·352 | 0·598 | 1·722 | 1·506 |
| 28 | | 1·549 | 1·368 | 0·598 | 1·722 | 1·520 |
| 27 | | 1·553 | 1·384 | 0·598 | 1·722 | 1·534 |
| 26 | | 1·557 | 1·399 | 0·598 | 1·722 | 1·547 |
| 25 | | 1·560 | 1·414 | 0·598 | 1·722 | 1·560 |
| 24 | | 1·564 | 1·429 | 0·598 | 1·722 | 1·573 |
| 23 | | 1·569 | 1·444 | 0·598 | 1·722 | 1·585 |
| 22 | | 1·573 | 1·459 | 0·598 | 1·722 | 1·596 |
| 21 | | 1·578 | 1·473 | 0·598 | 1·722 | 1·607 |
| 20 | 0·513 | 1·582 | 1·487 | 0·598 | 1·722 | 1·618 |
| 19 | | 1·587 | 1·501 | 0·598 | 1·722 | 1·628 |
| 18 | | 1·593 | 1·515 | 0·598 | 1·722 | 1·637 |
| 17 | | 1·598 | 1·528 | 0·598 | 1·722 | 1·646 |
| 16 | | 1·604 | 1·541 | 0·598 | 1·722 | 1·655 |
| 15 | | 1·609 | 1·555 | 0·598 | 1·722 | 1·663 |
| 14 | | 1·615 | 1·567 | 0·598 | 1·722 | 1·670 |
| 13 | | 1·622 | 1·580 | 0·598 | 1·722 | 1·677 |
| 12 | | 1·628 | 1·592 | 0·598 | 1·722 | 1·684 |
| 11 | | 1·635 | 1·605 | 0·598 | 1·722 | 1·690 |
| 10 | 0·556 | 1·641 | 1·617 | 0·598 | 1·722 | 1·695 |
| 9 | | 1·648 | 1·628 | 0·598 | 1·722 | 1·700 |
| 8 | | 1·656 | 1·640 | 0·598 | 1·722 | 1·705 |
| 7 | | 1·663 | 1·651 | 0·598 | 1·722 | 1·709 |
| 6 | | 1·671 | 1·662 | 0·598 | 1·722 | 1·712 |
| 5 | | 1·679 | 1·672 | 0·598 | 1·722 | 1·715 |
| 4 | | 1·687 | 1·683 | 0·598 | 1·722 | 1·717 |
| 3 | | 1·695 | 1·693 | 0·598 | 1·722 | 1·719 |
| 2 | | 1·703 | 1·702 | 0·598 | 1·722 | 1·721 |
| 1 | | 1·712 | 1·712 | 0·598 | 1·722 | 1·722 |
| 0 | 0·598 | 1·722 | 1·722 | 0·598 | 1·722 | 1·722 |

TABLE 7—*continued*

| $\varphi$ (deg) | Front of the kink section | | |
|---|---|---|---|
| | $\xi_m$ | $\left(-\dfrac{v_x}{\vartheta U \cos\varphi}\right)_{\max}$ | $H=\left(-\dfrac{v_x}{\vartheta U}\right)_{\max}$ |
| −1 | | 1·730 | 1·730 |
| −2 | | 1·741 | 1·739 |
| −3 | | 1·750 | 1·748 |
| −4 | | 1·760 | 1·756 |
| −5 | | 1·771 | 1·764 |
| −6 | | 1·781 | 1·771 |
| −7 | | 1·792 | 1·779 |
| −8 | | 1·803 | 1·786 |
| −9 | | 1·815 | 1·792 |
| −10 | 0·638 | 1·826 | 1·799 |
| −11 | | 1·838 | 1·805 |
| −12 | | 1·851 | 1·811 |
| −13 | | 1·863 | 1·816 |
| −14 | | 1·877 | 1·821 |
| −15 | | 1·890 | 1·825 |
| −16 | | 1·903 | 1·830 |
| −17 | | 1·917 | 1·834 |
| −18 | | 1·932 | 1·837 |
| −19 | | 1·947 | 1·841 |
| −20 | 0·677 | 1·962 | 1·843 |
| −21 | | 1·977 | 1·846 |
| −22 | | 1·993 | 1·848 |
| −23 | | 2·009 | 1·850 |
| −24 | | 2·026 | 1·851 |
| −25 | | 2·043 | 1·852 |
| −26 | | 2·061 | 1·852 |
| −27 | | 2·079 | 1·853 |
| −28 | | 2·098 | 1·852 |
| −29 | | 2·117 | 1·851 |
| −30 | 0·715 | 2·137 | 1·850 |
| −31 | | 2·156 | 1·848 |
| −32 | | 2·177 | 1·847 |
| −31 | | 2·199 | 1·844 |
| −34 | | 2·220 | 1·841 |
| −35 | | 2·243 | 1·837 |
| −36 | | 2·266 | 1·833 |
| −37 | | 2·290 | 1·829 |
| −38 | | 2·315 | 1·824 |
| −39 | | 2·340 | 1·818 |
| −40 | 0·752 | 2·365 | 1·812 |
| −41 | | 2·392 | 1·805 |
| −42 | | 2·419 | 1·798 |
| −43 | | 2·448 | 1·790 |
| −44 | | 2·478 | 1·782 |
| −45 | | 2·508 | 1·773 |
| −46 | | 2·540 | 1·764 |
| −47 | | 2·572 | 1·754 |
| −48 | | 2·605 | 1·743 |
| −49 | | 2·640 | 1·732 |
| −50 | 0·788 | 2·675 | 1·720 |
| −51 | | 2·713 | 1·707 |
| −52 | | 2·752 | 1·694 |
| −53 | | 2·791 | 1·679 |
| −54 | | 2·832 | 1·665 |
| −55 | | 2·875 | 1·649 |
| −56 | | 2·918 | 1·632 |
| −57 | | 2·966 | 1·616 |
| −58 | | 3·015 | 1·597 |
| −59 | | 3·063 | 1·578 |
| −60 | 0·824 | 3·117 | 1·559 |
| −61 | | 3·171 | 1·537 |
| −62 | | 3·228 | 1·515 |
| −63 | | 3·289 | 1·493 |
| −64 | | 3·351 | 1·469 |
| −65 | | 3·417 | 1·444 |
| −66 | | 3·488 | 1·419 |
| −67 | | 3·559 | 1·391 |
| −68 | | 3·639 | 1·363 |
| −60 | | 3·720 | 1·333 |
| −70 | 0·860 | 3·803 | 1·301 |
| −71 | | 3·900 | 1·270 |
| −72 | | 3·996 | 1·235 |
| −73 | | 4·100 | 1·199 |
| −74 | | 4·215 | 1·162 |
| −75 | | 4·330 | 1·121 |
| −76 | | 4·466 | 1·080 |
| −77 | | 4·607 | 1·036 |
| −78 | | 4·759 | 0·989 |
| −79 | | 4·937 | 0·942 |
| −80 | 0·900 | 5·115 | 0·888 |
| −81 | | 5·343 | 0·836 |
| −82 | | 5·578 | 0·776 |
| −83 | | 5·866 | 0·715 |
| −84 | 0·918 | 6·183 | 0·646 |
| | — | — | — |
| −90 | 1·000 | ∞ | 0 |

## TABLE 8

*Maximum Supervelocities in the Kink Section and Kink Area of Swept-back Wings, Profile* R

| $\varphi$ (deg) | Kink section $\xi_m$ | Kink section $\left(-\frac{v_x}{\vartheta U \cos\varphi}\right)_{max}$ | Kink section $H$ | Kink area ($\xi_m \simeq 1$) $H$ |
|---|---|---|---|---|
| 0 | 1·000 | 1·911 | 1·911 | 1·911 |
| 1 | | 1·821 | 1·821 | 1·910 |
| 2 | | 1·773 | 1·771 | 1·910 |
| 3 | | 1·733 | 1·730 | 1·908 |
| 4 | | 1·699 | 1·695 | 1·906 |
| 5 | | 1·670 | 1·663 | 1·903 |
| 6 | | 1·643 | 1·634 | 1·900 |
| 7 | | 1·619 | 1·607 | 1·897 |
| 8 | | 1·597 | 1·581 | 1·892 |
| 9 | | 1·576 | 1·556 | 1·887 |
| 10 | 0·826 | 1·557 | 1·533 | 1·882 |
| 11 | | 1·539 | 1·511 | 1·876 |
| 12 | | 1·522 | 1·489 | 1·869 |
| 13 | | 1·507 | 1·468 | 1·862 |
| 14 | | 1·492 | 1·448 | 1·854 |
| 15 | | 1·478 | 1·428 | 1·846 |
| 16 | | 1·465 | 1·408 | 1·837 |
| 17 | | 1·453 | 1·389 | 1·827 |
| 18 | | 1·442 | 1·371 | 1·817 |
| 19 | | 1·431 | 1·353 | 1·807 |
| 20 | 0·695 | 1·420 | 1·335 | 1·796 |
| 21 | | 1·411 | 1·317 | 1·784 |
| 22 | | 1·402 | 1·300 | 1·772 |
| 23 | | 1·393 | 1·283 | 1·759 |
| 24 | | 1·385 | 1·266 | 1·746 |
| 25 | | 1·378 | 1·249 | 1·732 |
| 26 | | 1·371 | 1·232 | 1·717 |
| 27 | | 1·365 | 1·216 | 1·702 |
| 28 | | 1·359 | 1·200 | 1·687 |
| 29 | | 1·353 | 1·183 | 1·671 |
| 30 | 0·566 | 1·348 | 1·167 | 1·655 |
| 31 | | 1·343 | 1·151 | 1·638 |
| 32 | | 1·339 | 1·136 | 1·620 |
| 33 | | 1·335 | 1·120 | 1·602 |
| 34 | | 1·332 | 1·104 | 1·584 |
| 35 | | 1·328 | 1·088 | 1·565 |
| 36 | | 1·326 | 1·073 | 1·546 |
| 37 | | 1·323 | 1·057 | 1·526 |
| 38 | | 1·322 | 1·041 | 1·506 |
| 39 | | 1·320 | 1·026 | 1·485 |
| 40 | 0·433 | 1·319 | 1·010 | 1·464 |
| 41 | | 1·318 | 0·995 | 1·442 |
| 42 | | 1·318 | 0·979 | 1·420 |

| $\varphi$ (deg) | Kink section $\xi_m$ | Kink section $\left(-\frac{v_x}{\vartheta U \cos\varphi}\right)_{max}$ | Kink section $H$ | Kink area ($\xi_m \simeq 1$) $H$ |
|---|---|---|---|---|
| 43 | | 1·318 | 0·964 | 1·397 |
| 44 | | 1·318 | 0·948 | 1·374 |
| 45 | | 1·319 | 0·933 | 1·351 |
| 46 | | 1·320 | 0·917 | 1·327 |
| 47 | | 1·322 | 0·902 | 1·303 |
| 48 | | 1·324 | 0·886 | 1·279 |
| 49 | | 1·327 | 0·870 | 1·254 |
| 50 | 0·293 | 1·330 | 0·855 | 1·228 |
| 51 | | 1·333 | 0·839 | 1·202 |
| 52 | | 1·337 | 0·823 | 1·176 |
| 53 | | 1·341 | 0·807 | 1·150 |
| 54 | | 1·346 | 0·791 | 1·123 |
| 55 | | 1·352 | 0·775 | 1·096 |
| 56 | | 1·358 | 0·759 | 1·068 |
| 57 | | 1·364 | 0·743 | 1·041 |
| 58 | | 1·371 | 0·727 | 1·013 |
| 59 | | 1·379 | 0·710 | 0·984 |
| 60 | 0·143 | 1·387 | 0·694 | 0·955 |
| 61 | | 1·397 | 0·677 | 0·926 |
| 62 | | 1·406 | 0·660 | 0·897 |
| 63 | | 1·417 | 0·643 | 0·867 |
| 64 | | 1·428 | 0·626 | 0·838 |
| 65 | | 1·441 | 0·609 | 0·808 |
| 66 | | 1·454 | 0·591 | 0·777 |
| 67 | | 1·468 | 0·574 | 0·747 |
| 68 | | 1·483 | 1·556 | 0·716 |
| 69 | | 1·500 | 0·538 | 0·685 |
| 70 | −0·025 | 1·518 | 0·519 | 0·654 |
| 71 | | 1·538 | 0·501 | 0·622 |
| 72 | | 1·559 | 0·482 | 0·590 |
| 73 | | 1·581 | 0·462 | 0·559 |
| 74 | | 1·606 | 0·443 | 0·527 |
| 75 | | 1·633 | 0·423 | 0·495 |
| 76 | | 1·663 | 0·402 | 0·462 |
| 77 | | 1·695 | 0·381 | 0·430 |
| 78 | | 1·731 | 0·360 | 0·397 |
| 79 | | 1·772 | 0·338 | 0·365 |
| 80 | −0·228 | 1·816 | 0·315 | 0·332 |
| 81 | | 1·867 | 0·292 | 0·299 |
| 82 | | 1·925 | 0·268 | 0·266 |
| — | — | — | — | — |
| 90 | −1·000 | $\infty$ | 0 | 0 |



(57974) D

## TABLE 9

*Lower Critical Mach Numbers for Untapered Swept Wings, Profile* B, *Based on Maximum Supervelocities in the Kink Section*

$\vartheta = 0 \cdot 05$

| $M_{cl}$ | $\pm\varphi$ (deg) |
|---|---|
| 0·94 | 70·4 |
| 0·93 | 64·4 |
| 0·92 | 57·75 |
| 0·91 | 50·3 |
| 0·90 | 42·2 |
| 0·89 | 33·4 |
| 0·88 | 23·5 |
| 0·87 | 9·3 |
| 0·8679 | 0 |

$\vartheta = 0 \cdot 10$

| $M_{cl}$ | $\pm\varphi$ (deg) |
|---|---|
| 0·90 | 71·8 |
| 0·89 | 68·3 |
| 0·88 | 64·3 |
| 0·87 | 59·95 |
| 0·86 | 55·1 |
| 0·85 | 49·8 |
| 0·84 | 43·9 |
| 0·83 | 37·5 |
| 0·82 | 30·1 |
| 0·81 | 20·9 |
| 0·80 | 3·45 |
| 0·7997 | 0 |

$\vartheta = 0 \cdot 15$

| $M_{cl}$ | $\pm\varphi$ (deg) |
|---|---|
| 0·87 | 73·4 |
| 0·86 | 70·8 |
| 0·85 | 68·0 |
| 0·84 | 64·8 |
| 0·83 | 61·4 |
| 0·82 | 57·6 |
| 0·81 | 53·4 |
| 0·80 | 48·8 |
| 0·79 | 43·7 |
| 0·78 | 37·9 |
| 0·77 | 31·3 |
| 0·76 | 22·9 |
| 0·75 | 10·3 |
| 0·7475 | 0 |

$\vartheta = 0 \cdot 30$

| $M_{cl}$ | $\pm\varphi$ (deg) |
|---|---|
| 0·81 | 77·2 |
| 0·80 | 75·7 |
| 0·79 | 74·2 |
| 0·78 | 72·45 |
| 0·77 | 70·6 |
| 0·76 | 68·5 |
| 0·75 | 66·4 |
| 0·74 | 64·0 |
| 0·73 | 61·3 |
| 0·72 | 58·5 |
| 0·71 | 55·3 |
| 0·70 | 51·8 |
| 0·69 | 47·9 |
| 0·68 | 43·6 |
| 0·67 | 38·6 |
| 0·66 | 32·8 |
| 0·65 | 25·5 |
| 0·64 | 14·6 |
| 0·6331 | 0 |

$\vartheta = 0 \cdot 25$

| $M_{cl}$ | $\pm\varphi$ (deg) |
|---|---|
| 0·83 | 76·6 |
| 0·82 | 75·0 |
| 0·81 | 73·2 |
| 0·80 | 71·25 |
| 0·79 | 69·1 |
| 0·78 | 66·8 |
| 0·77 | 64·2 |
| 0·76 | 61·4 |
| 0·75 | 58·4 |
| 0·74 | 55·05 |
| 0·73 | 51·35 |
| 0·72 | 47·25 |
| 0·71 | 42·6 |
| 0·70 | 37·4 |
| 0·69 | 31·1 |
| 0·68 | 23·3 |
| 0·67 | 10·85 |
| 0·6673 | 0 |

$\vartheta = 0 \cdot 20$

| $M_{cl}$ | $\pm\varphi$ (deg) |
|---|---|
| 0·85 | 75·6 |
| 0·84 | 73·6 |
| 0·83 | 71·4 |
| 0·82 | 69·1 |
| 0·81 | 66·5 |
| 0·80 | 63·6 |
| 0·79 | 60·5 |
| 0·78 | 57·1 |
| 0·77 | 53·3 |
| 0·76 | 49·05 |
| 0·75 | 44·5 |
| 0·74 | 39·3 |
| 0·73 | 33·2 |
| 0·72 | 25·9 |
| 0·71 | 15·6 |
| 0·7043 | 0 |

## TABLE 10

*Lower Critical Mach Numbers $M_{cl}$ for Untapered Swept Wings, Profile* C, *Based on Maximum Supervelocities in the Kink Section*

$\vartheta = 0{\cdot}05$

| $M_{cl}$ | $\varphi$ (deg) | |
|---|---|---|
| 0·94 | 66·6 | |
| 0·93 | 60·9 | |
| 0·92 | 54·9 | |
| 0·91 | 48·7 | −69·35 |
| 0·90 | 42·55 | −64·7 |
| 0·89 | 36·35 | −59·3 |
| 0·88 | 30·1 | −53·3 |
| 0·87 | 23·9 | −46·3 |
| 0·86 | 18·3 | −38·2 |
| 0·85 | 10·8 | −27·9 |
| 0·8443 | 0 | — |

$\vartheta = 0{\cdot}10$

| $M_{cl}$ | $\varphi$ (deg) | |
|---|---|---|
| 0·90 | 68·6 | |
| 0·89 | 65·2 | |
| 0·88 | 61·55 | |
| 0·87 | 57·75 | |
| 0·86 | 53·8 | |
| 0·85 | 49·7 | −69·8 |
| 0·84 | 45·4 | −66·8 |
| 0·83 | 41·0 | −63·35 |
| 0·82 | 36·4 | −59·5 |
| 0·81 | 31·55 | −55·2 |
| 0·80 | 27·0 | −50·25 |
| 0·79 | 22·5 | −44·5 |
| 0·78 | 17·05 | −37·5 |
| 0·77 | 9·0 | −28·1 |
| 0·7661 | 0 | — |

$\vartheta = 0{\cdot}15$

| $M_{cl}$ | $\varphi$ (deg) | |
|---|---|---|
| 0·86 | 67·9 | |
| 0·85 | 65·3 | |
| 0·84 | 62·45 | |
| 0·83 | 59·5 | |
| 0·82 | 56·4 | |
| 0·81 | 53·1 | |
| 0·80 | 49·75 | |
| 0·79 | 46·2 | −67·3 |
| 0·78 | 42·4 | −64·5 |
| 0·77 | 38·5 | −61·4 |
| 0·76 | 34·3 | −58·0 |
| 0·75 | 30·3 | −54·0 |
| 0·74 | 26·4 | −49·5 |
| 0·73 | 22·0 | −44·2 |
| 0·72 | 16·3 | −37·6 |
| 0·71 | 7·8 | −28·5 |
| 0·7070 | 0 | — |

$\vartheta = 0{\cdot}30$

| $M_{cl}$ | $\varphi$ (deg) | |
|---|---|---|
| 0·77 | 68·3 | |
| 0·76 | 66·5 | |
| 0·75 | 64·5 | |
| 0·74 | 62·5 | |
| 0·73 | 60·4 | |
| 0·72 | 58·1 | |
| 0·71 | 55·7 | |
| 0·70 | 53·2 | −71·95 |
| 0·69 | 50·55 | −70·25 |
| 0·68 | 47·7 | −68·4 |
| 0·67 | 44·7 | −66·3 |
| 0·66 | 41·5 | −64·0 |
| 0·65 | 38·1 | −61·5 |
| 0·64 | 34·75 | −58·6 |
| 0·63 | 31·6 | −55·4 |
| 0·62 | 28·05 | −51·6 |
| 0·61 | 24·0 | −47·2 |
| 0·60 | 18·9 | −41·75 |
| 0·59 | 11·9 | −34·55 |
| 0·5836 | 0 | — |
| 0·58 | −5·2 | −17·8 |

$\vartheta = 0{\cdot}25$

| $M_{cl}$ | $\varphi$ (deg) | |
|---|---|---|
| 0·80 | 68·8 | |
| 0·79 | 66·8 | |
| 0·78 | 64·7 | |
| 0·77 | 62·5 | |
| 0·76 | 60·2 | |
| 0·75 | 57·8 | |
| 0·74 | 55·25 | |
| 0·73 | 52·55 | −71·6 |
| 0·72 | 49·7 | −69·7 |
| 0·71 | 46·7 | −67·7 |
| 0·70 | 43·5 | −65·4 |
| 0·69 | 40·1 | −62·9 |
| 0·68 | 36·5 | −60·1 |
| 0·67 | 33·1 | −57·0 |
| 0·66 | 29·75 | −53·4 |
| 0·65 | 25·9 | −49·2 |
| 0·64 | 21·4 | −44·2 |
| 0·63 | 15·65 | −37·9 |
| 0·62 | 5·5 | −28·8 |
| 0·6186 | 0 | — |

$\vartheta = 0{\cdot}20$

| $M_{cl}$ | $\varphi$ (deg) | |
|---|---|---|
| 0·83 | 68·75 | |
| 0·82 | 66·5 | |
| 0·81 | 64·2 | |
| 0·80 | 61·75 | |
| 0·79 | 59·2 | |
| 0·78 | 56·4 | |
| 0·77 | 53·6 | |
| 0·76 | 50·6 | −70·3 |
| 0·75 | 47·4 | −68·1 |
| 0·74 | 44·05 | −65·75 |
| 0·73 | 40·5 | −63·1 |
| 0·72 | 36·7 | −60·2 |
| 0·71 | 32·9 | −56·9 |
| 0·70 | 29·5 | −53·1 |
| 0·69 | 25·6 | −48·7 |
| 0·68 | 21·05 | −43·45 |
| 0·67 | 15·2 | −36·9 |
| 0·66 | 4·3 | −27·2 |
| 0·6591 | 0 | — |

## TABLE 10a

*Lower Critical Mach Numbers $M_{cl}$ for Untapered Swept-Back Wings, Profile* C, *Based on Maximum Supervelocities in the Kink Area*

| $\vartheta = 0{\cdot}05$ | |
|---|---|
| $M_{cl}$ | $\varphi$ (deg) |
| 0·87 | 23·6 |
| 0·86 | 16·5 |
| 0·85 | 7·7 |
| 0·8443 | 0 |

| $\vartheta = 0{\cdot}10$ | |
|---|---|
| $M_{cl}$ | $\varphi$ (deg) |
| 0·80 | 26·4 |
| 0·79 | 20·7 |
| 0·78 | 14·0 |
| 0·77 | 5·2 |
| 0·7661 | 0 |

| $\vartheta = 0{\cdot}15$ | |
|---|---|
| $M_{cl}$ | $\varphi$ (deg) |
| 0·75 | 29·6 |
| 0·74 | 24·9 |
| 0·73 | 19·3 |
| 0·72 | 12·75 |
| 0·71 | 3·8 |
| 0·7070 | 0 |

| $\vartheta = 0{\cdot}30$ | |
|---|---|
| $M_{cl}$ | $\varphi$ (deg) |
| 0·64 | 34·3 |
| 0·63 | 30·35 |
| 0·62 | 25·9 |
| 0·61 | 20·8 |
| 0·60 | 14·8 |
| 0·59 | 7·0 |
| 0·5836 | 0 |

| $\vartheta = 0{\cdot}25$ | |
|---|---|
| $M_{cl}$ | $\varphi$ (deg) |
| 0·67 | 32·4 |
| 0·66 | 28·25 |
| 0·65 | 23·5 |
| 0·64 | 17·95 |
| 0·63 | 11·0 |
| 0·62 | 1·8 |
| 0·6186 | 0 |

| $\vartheta = 0{\cdot}20$ | |
|---|---|
| $M_{cl}$ | $\varphi$ (deg) |
| 0·71 | 32·7 |
| 0·70 | 28·3 |
| 0·69 | 23·4 |
| 0·68 | 17·8 |
| 0·67 | 10·95 |
| 0·66 | 1·2 |
| 0·6591 | 0 |

# TABLE 11

*Lower Critical Mach Numbers $M_{cl}$ for Untapered Swept Wings, Profile Q, Based on Maximum Supervelocities in the Front of the Kink Section*

$\vartheta = 0\cdot05$

| $M_{cl}$ | $\varphi$ (deg) | |
|---|---|---|
| 0·94 | 58·4 | |
| 0·93 | 52·3 | |
| 0·92 | 47·9 | |
| 0·91 | 40·6 | −74·4 |
| 0·90 | 35·3 | −70·8 |
| 0·89 | 30·05 | −66·7 |
| 0·88 | 24·85 | −61·9 |
| 0·87 | 19·6 | −56·4 |
| 0·86 | 13·95 | −49·8 |
| 0·85 | 7·5 | −41·9 |
| 0·8413 | 0 | — |
| 0·84 | −1·3 | −31·0 |

$\vartheta = 0\cdot30$

| $M_{cl}$ | $\varphi$ (deg) | |
|---|---|---|
| 0·83 | 72·15 | |
| 0·82 | 70·5 | |
| 0·81 | 68·85 | |
| 0·80 | 67·1 | |
| 0·79 | 65·3 | |
| 0·78 | 63·45 | |
| 0·77 | 61·5 | |
| 0·76 | 59·5 | |
| 0·75 | 57·5 | |
| 0·74 | 55·35 | −80·6 |
| 0·73 | 53·15 | −79·75 |
| 0·72 | 50·4 | −78·8 |
| 0·71 | 48·6 | −77·7 |
| 0·70 | 46·1 | −76·5 |
| 0·69 | 43·6 | −75·35 |
| 0·68 | 40·8 | −74·0 |
| 0·67 | 38·25 | −72·5 |
| 0·66 | 35·4 | −70·8 |
| 0·65 | 32·3 | −69·0 |
| 0·64 | 29·15 | −67·0 |
| 0·63 | 25·7 | −64·7 |
| 0·62 | 22·0 | −62·1 |
| 0·61 | 18·0 | −59·05 |
| 0·60 | 13·5 | −55·5 |
| 0·59 | 8·3 | −51·3 |
| 0·58 | 2·0 | −45·9 |
| 0·5773 | 0 | — |
| 0·57 | −6·7 | −38·2 |

$\vartheta = 0\cdot10$

| $M_{cl}$ | $\varphi$ (deg) | |
|---|---|---|
| 0·91 | 64·8 | |
| 0·90 | 61·1 | |
| 0·89 | 57·35 | |
| 0·88 | 53·6 | |
| 0·87 | 49·8 | |
| 0·86 | 46·0 | −76·9 |
| 0·85 | 42·1 | −74·85 |
| 0·84 | 38·3 | −72·55 |
| 0·83 | 34·4 | −70·0 |
| 0·82 | 30·4 | −67·1 |
| 0·81 | 26·3 | −63·9 |
| 0·80 | 22·1 | −60·1 |
| 0·79 | 17·45 | −55·7 |
| 0·78 | 12·3 | −50·3 |
| 0·77 | 6·3 | −44·3 |
| 0·7618 | 0 | — |
| 0·76 | −1·65 | −35·7 |

$\vartheta = 0\cdot25$

| $M_{cl}$ | $\varphi$ (deg) | |
|---|---|---|
| 0·84 | 69·6 | |
| 0·83 | 68·0 | |
| 0·82 | 66·05 | |
| 0·81 | 64·0 | |
| 0·80 | 61·9 | |
| 0·79 | 59·8 | |
| 0·78 | 57·55 | |
| 0·77 | 55·3 | −80·6 |
| 0·76 | 53·1 | −79·7 |
| 0·75 | 50·5 | −78·65 |
| 0·74 | 48·0 | −77·5 |
| 0·73 | 46·45 | −76·3 |
| 0·72 | 42·7 | −74·9 |
| 0·71 | 39·95 | −73·4 |
| 0·70 | 37·1 | −71·8 |
| 0·69 | 34·1 | −69·0 |
| 0·68 | 30·9 | −68·0 |
| 0·67 | 27·5 | −65·7 |
| 0·66 | 23·95 | −63·15 |
| 0·65 | 20·0 | −60·2 |
| 0·64 | 15·75 | −56·8 |
| 0·63 | 10·9 | −53·6 |
| 0·62 | 5·2 | −48·9 |
| 0·6126 | 0 | — |
| 0·61 | −2·15 | −41·15 |
| 0·60 | −15·1 | −28·8 |

$\vartheta = 0\cdot15$

| $M_c$ | $\varphi$ (deg) | |
|---|---|---|
| 0·88 | 66·25 | |
| 0·87 | 65·3 | |
| 0·86 | 60·7 | |
| 0·85 | 57·8 | |
| 0·84 | 55·1 | |
| 0·83 | 51·8 | |
| 0·82 | 48·75 | −78·1 |
| 0·81 | 45·6 | −76·5 |
| 0·80 | 42·45 | −74·9 |
| 0·79 | 39·2 | −73·1 |
| 0·78 | 35·85 | −71·0 |
| 0·77 | 32·4 | −68·7 |
| 0·76 | 28·8 | −66·2 |
| 0·75 | 25·0 | −65·25 |
| 0·74 | 21·0 | −59·9 |
| 0·73 | 16·6 | −56·1 |
| 0·72 | 11·65 | −52·35 |
| 0·71 | 5·8 | −46·35 |
| 0·7020 | 0 | — |
| 0·70 | −1·7 | −38·4 |

$\vartheta = 0\cdot20$

| $M_{cl}$ | $\varphi$ (deg) | |
|---|---|---|
| 0·86 | 68·6 | |
| 0·85 | 66·45 | |
| 0·84 | 64·15 | |
| 0·83 | 61·8 | |
| 0·82 | 59·35 | |
| 0·81 | 56·9 | |
| 0·80 | 54·3 | |
| 0·79 | 51·7 | −79·2 |
| 0·78 | 49·0 | −78·05 |
| 0·77 | 46·2 | −76·7 |
| 0·76 | 43·4 | −75·3 |
| 0·75 | 40·5 | −73·75 |
| 0·74 | 37·45 | −72·0 |
| 0·73 | 24·3 | −70·1 |
| 0·72 | 31·0 | −67·9 |
| 0·71 | 27·6 | −65·5 |
| 0·70 | 23·9 | −62·75 |
| 0·69 | 19·9 | −59·6 |
| 0·68 | 15·5 | −56·0 |
| 0·67 | 10·5 | −52·7 |
| 0·66 | 4·7 | −43·65 |
| 0·6535 | 0 | — |
| 0·65 | −3·0 | −39·0 |

## TABLE 11a

*Lower Critical Mach Numbers $M_{cl}$ for Untapered Swept-back Wings, Profile Q, Based on Maximum Supervelocities in the Kink Area*

$\vartheta = 0{\cdot}05$

| $M_{cl}$ | $\varphi$ (deg) |
|---|---|
| 0·93 | 52·75 |
| 0·92 | 48·1 |
| 0·91 | 43·6 |
| 0·90 | 39·1 |
| 0·89 | 34·7 |
| 0·88 | 30·2 |
| 0·87 | 25·4 |
| 0·86 | 20·1 |
| 0·85 | 13·45 |
| 0·8413 | 0 |

$\vartheta = 0{\cdot}10$

| $M_{cl}$ | $\varphi$ (deg) |
|---|---|
| 0·89 | 57·9 |
| 0·88 | 54·9 |
| 0·87 | 51·9 |
| 0·86 | 48·9 |
| 0·85 | 45·85 |
| 0·84 | 42·7 |
| 0·83 | 39·5 |
| 0·82 | 36·15 |
| 0·81 | 33·5 |
| 0·80 | 28·75 |
| 0·79 | 24·5 |
| 0·78 | 19·6 |
| 0·77 | 12·4 |
| 0·7618 | 0 |

$\vartheta = 0{\cdot}15$

| $M_{cl}$ | $\varphi$ (deg) |
|---|---|
| 0·86 | 61·1 |
| 0·85 | 58·8 |
| 0·84 | 56·5 |
| 0·83 | 54·2 |
| 0·82 | 51·75 |
| 0·81 | 49·3 |
| 0·80 | 46·8 |
| 0·79 | 44·1 |
| 0·78 | 41·3 |
| 0·77 | 38·4 |
| 0·76 | 35·4 |
| 0·75 | 32·05 |
| 0·74 | 28·4 |
| 0·73 | 24·3 |
| 0·72 | 19·5 |
| 0·71 | 12·9 |
| 0·7020 | 0 |

$\vartheta = 0{\cdot}30$

| $M_{cl}$ | $\varphi$ (deg) |
|---|---|
| 0·79 | 65·45 |
| 0·78 | 64·2 |
| 0·77 | 62·7 |
| 0·76 | 61·1 |
| 0·75 | 60·8 |
| 0·74 | 57·85 |
| 0·73 | 56·0 |
| 0·72 | 54·35 |
| 0·71 | 52·5 |
| 0·70 | 50·6 |
| 0·69 | 48·6 |
| 0·68 | 46·5 |
| 0·67 | 44·2 |
| 0·66 | 41·9 |
| 0·65 | 39·3 |
| 0·64 | 36·6 |
| 0·63 | 33·65 |
| 0·62 | 30·4 |
| 0·61 | 26·6 |
| 0·60 | 22·3 |
| 0·59 | 16·7 |
| 0·58 | 7·7 |
| 0·5773 | 0 |

$\vartheta = 0{\cdot}25$

| $M_{cl}$ | $\varphi$ (deg) |
|---|---|
| 0·81 | 64·4 |
| 0·80 | 62·85 |
| 0·79 | 61·1 |
| 0·78 | 59·3 |
| 0·77 | 57·55 |
| 0·76 | 55·8 |
| 0·75 | 53·8 |
| 0·74 | 51·8 |
| 0·73 | 49·8 |
| 0·72 | 47·65 |
| 0·71 | 45·4 |
| 0·70 | 43·0 |
| 0·69 | 40·5 |
| 0·68 | 37·9 |
| 0·67 | 35·0 |
| 0·66 | 31·8 |
| 0·65 | 28·3 |
| 0·64 | 24·15 |
| 0·63 | 19·4 |
| 0·62 | 12·65 |
| 0·6126 | 0 |

$\vartheta = 0{\cdot}20$

| $M_{cl}$ | $\varphi$ (deg) |
|---|---|
| 0·83 | 62·4 |
| 0·82 | 60·5 |
| 0·81 | 58·5 |
| 0·80 | 56·5 |
| 0·79 | 54·5 |
| 0·78 | 52·3 |
| 0·77 | 50·15 |
| 0·76 | 46·75 |
| 0·75 | 45·5 |
| 0·74 | 43·05 |
| 0·73 | 40·45 |
| 0·72 | 37·7 |
| 0·71 | 34·7 |
| 0·70 | 31·45 |
| 0·69 | 27·85 |
| 0·68 | 23·7 |
| 0·67 | 18·6 |
| 0·66 | 11·75 |
| 0·6535 | 0 |

## TABLE 11b

*Lower Critical Mach Number $M_{cl}$ for Untapered Swept-back Wings, Profile Q, Based on Maximum Supervelocities in the Tip Section*

| $\vartheta = 0 \cdot 05$ | |
|---|---|
| $M_{cl}$ | $\varphi$ (deg) |
| 0·94 | 69·6 |
| 0·93 | 62·75 |
| 0·92 | 54·8 |
| 0·91 | 45·1 |
| 0·90 | 33·2 |

| $\vartheta = 0 \cdot 10$ | |
|---|---|
| $M_{cl}$ | $\varphi$ (deg) |
| 0·91 | 74·6 |
| 0·90 | 70·8 |
| 0·89 | 66·7 |
| 0·88 | 61·9 |
| 0·87 | 56·4 |
| 0·86 | 49·8 |
| 0·85 | 41·9 |

| $\vartheta = 0 \cdot 15$ | |
|---|---|
| $M_{cl}$ | $\varphi$ (deg) |
| 0·88 | 75·1 |
| 0·87 | 72·5 |
| 0·86 | 69·45 |
| 0·85 | 66·0 |
| 0·84 | 62·1 |
| 0·83 | 57·5 |
| 0·82 | 52·25 |
| 0·81 | 45·8 |

| $\vartheta = 0 \cdot 30$ | |
|---|---|
| $M_{cl}$ | $\varphi$ (deg) |
| 0·82 | 78·1 |
| 0·81 | 76·5 |
| 0·80 | 74·9 |
| 0·79 | 73·0 |
| 0·78 | 71·0 |
| 0·77 | 68·7 |
| 0·76 | 66·2 |
| 0·75 | 63·25 |
| 0·74 | 59·95 |
| 0·73 | 56·1 |
| 0·72 | 51·55 |

| $\vartheta = 0 \cdot 25$ | |
|---|---|
| $M_{cl}$ | $\varphi$ (deg) |
| 0·84 | 77·7 |
| 0·83 | 76·0 |
| 0·82 | 74·1 |
| 0·81 | 72·0 |
| 0·80 | 69·6 |
| 0·79 | 66·95 |
| 0·78 | 64·0 |
| 0·77 | 60·6 |
| 0·76 | 56·6 |
| 0·75 | 52·0 |
| 0·74 | 46·4 |

| $\vartheta = 0 \cdot 20$ | |
|---|---|
| $M_{cl}$ | $\varphi$ (deg) |
| 0·86 | 76·9 |
| 0·85 | 74·85 |
| 0·84 | 72·55 |
| 0·83 | 70·0 |
| 0·82 | 67·1 |
| 0·81 | 63·9 |
| 0·80 | 60·1 |
| 0·79 | 55·7 |
| 0·78 | 50·6 |

## TABLE 11c

*Lower Critical Mach Number $M_{cl}$ for Untapered Swept-back Wings, Profile Q, Based on Maximum Supervelocities in the Rear of the Kink Section*

| $\vartheta = 0 \cdot 05$ | |
|---|---|
| $M_{cl}$ | $\varphi$ (deg) |
| 0·95 | 69·3 |
| 0·94 | 60·0 |

| $\vartheta = 0 \cdot 10$ | |
|---|---|
| $M_{cl}$ | $\varphi$ (deg) |
| 0·92 | 72·4 |
| 0·91 | 67·3 |
| 0·90 | 61·15 |

| $\vartheta = 0 \cdot 15$ | |
|---|---|
| $M_{cl}$ | $\varphi$ (deg) |
| 0·90 | 75·2 |
| 0·89 | 71·95 |
| 0·88 | 68·2 |
| 0·87 | 65·2 |

| $\vartheta = 0 \cdot 30$ | |
|---|---|
| $M_{cl}$ | $\varphi$ (deg) |
| 0·85 | 78·4 |
| 0·84 | 76·7 |
| 0·83 | 74·6 |
| 0·82 | 72·3 |
| 0·81 | 69·8 |

| $\vartheta = 0 \cdot 25$ | |
|---|---|
| $M_{cl}$ | $\varphi$ (deg) |
| 0·86 | 76·7 |
| 0·85 | 74·4 |
| 0·84 | 71·85 |
| 0·83 | 68·8 |

| $\vartheta = 0 \cdot 20$ | |
|---|---|
| $M_{cl}$ | $\varphi$ (deg) |
| 0·88 | 76·3 |
| 0·87 | 73·7 |
| 0·86 | 70·7 |
| 0·85 | 67·1 |

## TABLE 12

*Lower Critical Mach Numbers $M_{cl}$ for Untapered Swept-back Wings, Profile* R, *Based on Maximum Supervelocities in the Kink Section*

$\vartheta = 0{\cdot}05$

| $M_{cl}$ | $\varphi$ (deg) |
|---|---|
| 0·95 | 65·1 |
| 0·94 | 57·6 |
| 0·93 | 50·2 |
| 0·92 | 42·9 |
| 0·91 | 36·1 |
| 0·90 | 29·7 |
| 0·89 | 23·8 |
| 0·88 | 18·35 |
| 0·87 | 13·25 |
| 0·86 | 8·7 |
| 0·85 | 4·5 |
| 0·84 | 1·45 |
| 0·8310 | 0 |

$\vartheta = 0{\cdot}10$

| $M_{cl}$ | $\varphi$ (deg) |
|---|---|
| 0·91 | 64·3 |
| 0·90 | 59·9 |
| 0·89 | 55·2 |
| 0·88 | 50·5 |
| 0·87 | 45·8 |
| 0·86 | 41·05 |
| 0·85 | 36·4 |
| 0·84 | 31·9 |
| 0·83 | 27·6 |
| 0·82 | 23·4 |
| 0·81 | 18·8 |
| 0·80 | 14·8 |
| 0·79 | 10·9 |
| 0·78 | 7·3 |
| 0·77 | 4·4 |
| 0·76 | 1·7 |
| 0·75 | 0·3 |
| 0·7474 | 0 |

$\vartheta = 0{\cdot}15$

| $M_{cl}$ | $\varphi$ (deg) |
|---|---|
| 0·88 | 65·6 |
| 0·87 | 62·3 |
| 0·86 | 58·7 |
| 0·85 | 55·1 |
| 0·84 | 51·4 |
| 0·83 | 47·6 |
| 0·82 | 43·8 |
| 0·81 | 39·9 |
| 0·80 | 36·05 |
| 0·79 | 32·2 |
| 0·78 | 28·4 |
| 0·77 | 24·6 |
| 0·76 | 20·8 |
| 0·75 | 17·1 |
| 0·74 | 13·5 |
| 0·73 | 10·1 |
| 0·72 | 6·9 |
| 0·71 | 4·2 |
| 0·70 | 1·9 |
| 0·69 | 0·5 |
| 0·6850 | 0 |

$\vartheta = 0{\cdot}30$

| $M_{cl}$ | $\varphi$ (deg) |
|---|---|
| 0·84 | 73·8 |
| 0·83 | 72·0 |
| 0·82 | 70·05 |
| 0·81 | 68·0 |
| 0·80 | 65·9 |
| 0·79 | 63·6 |
| 0·78 | 61·3 |
| 0·77 | 58·8 |
| 0·76 | 56·3 |
| 0·75 | 53·7 |
| 0·74 | 50·95 |
| 0·73 | 48·15 |
| 0·72 | 45·3 |
| 0·71 | 42·3 |
| 0·70 | 39·3 |
| 0·69 | 36·3 |
| 0·68 | 33·1 |
| 0·67 | 30·0 |
| 0·66 | 26·8 |
| 0·65 | 23·5 |
| 0·64 | 20·3 |
| 0·63 | 17·1 |
| 0·62 | 13·9 |
| 0·61 | 10·9 |
| 0·60 | 8·05 |
| 0·59 | 5·5 |
| 0·58 | 3·2 |
| 0·57 | 1·5 |
| 0·56 | 0·3 |
| 0·5565 | 0 |

$\vartheta = 0{\cdot}25$

| $M_{cl}$ | $\varphi$ (deg) |
|---|---|
| 0·85 | 71·65 |
| 0·84 | 69·45 |
| 0·83 | 67·2 |
| 0·82 | 64·8 |
| 0·81 | 62·2 |
| 0·80 | 59·6 |
| 0·79 | 56·9 |
| 0·78 | 54·0 |
| 0·77 | 51·1 |
| 0·76 | 48·1 |
| 0·75 | 45·05 |
| 0·74 | 42·0 |
| 0·73 | 38·7 |
| 0·72 | 35·5 |
| 0·71 | 32·2 |
| 0·70 | 28·9 |
| 0·69 | 25·6 |
| 0·68 | 22·2 |
| 0·67 | 18·9 |
| 0·66 | 15·6 |
| 0·65 | 12·0 |
| 0·64 | 9·4 |
| 0·63 | 6·6 |
| 0·62 | 4·15 |
| 0·61 | 2·3 |
| 0·60 | 1·1 |
| 0·5926 | 0 |

$\vartheta = 0{\cdot}20$

| $M_{cl}$ | $\varphi$ (deg) |
|---|---|
| 0·86 | 68·2 |
| 0·85 | 65·5 |
| 0·84 | 62·7 |
| 0·83 | 59·7 |
| 0·82 | 56·7 |
| 0·81 | 53·5 |
| 0·80 | 50·25 |
| 0·79 | 46·9 |
| 0·78 | 43·55 |
| 0·77 | 40·15 |
| 0·76 | 36·7 |
| 0·75 | 33·2 |
| 0·74 | 29·7 |
| 0·73 | 26·2 |
| 0·72 | 22·7 |
| 0·71 | 18·2 |
| 0·70 | 15·8 |
| 0·69 | 12·4 |
| 0·68 | 9·8 |
| 0·67 | 6·4 |
| 0·66 | 3·9 |
| 0·65 | 1·8 |
| 0·64 | 0·5 |
| 0·6348 | 0 |

TABLE 12a

*Lower Critical Mach Numbers $M_{cl}$ for Untapered Swept-back Wings, Profile* R, *Based on Maximum Supervelocities in the Kink Area*

$\vartheta = 0{\cdot}05$

| $M_{cl}$ | $\varphi$ (deg) |
|---|---|
| 0·95 | 65·05 |
| 0·94 | 60·4 |
| 0·93 | 55·8 |
| 0·92 | 51·35 |
| 0·91 | 47·05 |
| 0·90 | 42·8 |
| 0·89 | 38·6 |
| 0·88 | 34·4 |
| 0·87 | 30·0 |
| 0·86 | 25·4 |
| 0·85 | 20·2 |
| 0·84 | 13·65 |
| 0·8310 | 0 |

$\vartheta = 0{\cdot}10$

| $M_{cl}$ | $\varphi$ (deg) |
|---|---|
| 0·91 | 65·8 |
| 0·90 | 63·45 |
| 0·89 | 60·7 |
| 0·88 | 57·9 |
| 0·87 | 55·2 |
| 0·86 | 52·35 |
| 0·85 | 49·5 |
| 0·84 | 46·6 |
| 0·83 | 43·65 |
| 0·82 | 40·6 |
| 0·81 | 37·4 |
| 0·80 | 34·0 |
| 0·79 | 30·4 |
| 0·78 | 26·4 |
| 0·77 | 21·85 |
| 0·76 | 16·2 |
| 0·75 | 7·4 |
| 0·7474 | 0 |

$\vartheta = 0{\cdot}15$

| $M_{cl}$ | $\varphi$ (deg) |
|---|---|
| 0·88 | 67·8 |
| 0·87 | 65·8 |
| 0·86 | 63·7 |
| 0·85 | 61·65 |
| 0·84 | 59·5 |
| 0·83 | 57·35 |
| 0·82 | 55·1 |
| 0·81 | 52·9 |
| 0·80 | 50·5 |
| 0·79 | 48·1 |
| 0·78 | 45·6 |
| 0·77 | 43·05 |
| 0·76 | 40·3 |
| 0·75 | 37·4 |
| 0·74 | 34·3 |
| 0·73 | 31·0 |
| 0·72 | 27·25 |
| 0·71 | 23·0 |
| 0·70 | 17·8 |
| 0·69 | 10·0 |
| 0·6850 | 0 |

$\vartheta = 0{\cdot}30$

| $M_{cl}$ | $\varphi$ (deg) |
|---|---|
| 0·84 | 74·2 |
| 0·83 | 73·0 |
| 0·82 | 71·75 |
| 0·81 | 70·5 |
| 0·80 | 69·3 |
| 0·79 | 67·95 |
| 0·78 | 66·6 |
| 0·77 | 65·2 |
| 0·76 | 63·8 |
| 0·75 | 62·4 |
| 0·74 | 60·9 |
| 0·73 | 59·35 |
| 0·72 | 57·7 |
| 0·71 | 56·05 |
| 0·70 | 53·9 |
| 0·69 | 52·5 |
| 0·68 | 50·7 |
| 0·67 | 48·6 |
| 0·66 | 46·6 |
| 0·65 | 44·4 |
| 0·64 | 42·2 |
| 0·63 | 39·6 |
| 0·62 | 36·95 |
| 0·61 | 34·0 |
| 0·60 | 30·8 |
| 0·59 | 27·1 |
| 0·58 | 22·8 |
| 0·57 | 17·35 |
| 0·56 | 8·9 |
| 0·5565 | 0 |

$\vartheta = 0{\cdot}25$

| $M_{cl}$ | $\varphi$ (deg) |
|---|---|
| 0·85 | 72·5 |
| 0·84 | 71·1 |
| 0·83 | 69·7 |
| 0·82 | 68·3 |
| 0·81 | 66·8 |
| 0·80 | 65·3 |
| 0·79 | 63·8 |
| 0·78 | 62·2 |
| 0·77 | 60·6 |
| 0·76 | 58·9 |
| 0·75 | 57·2 |
| 0·74 | 55·4 |
| 0·73 | 53·5 |
| 0·72 | 51·6 |
| 0·71 | 49·6 |
| 0·70 | 47·5 |
| 0·69 | 45·3 |
| 0·68 | 43·0 |
| 0·67 | 40·5 |
| 0·66 | 37·9 |
| 0·65 | 35·0 |
| 0·64 | 31·9 |
| 0·63 | 28·4 |
| 0·62 | 24·35 |
| 0·61 | 19·45 |
| 0·60 | 12·7 |
| 0·5926 | 0 |

$\vartheta = 0{\cdot}20$

| $M_{cl}$ | $\varphi$ (deg) |
|---|---|
| 0·86 | 69·95 |
| 0·85 | 68·3 |
| 0·84 | 66·65 |
| 0·83 | 64·9 |
| 0·82 | 63·2 |
| 0·81 | 61·4 |
| 0·80 | 59·6 |
| 0·79 | 57·7 |
| 0·78 | 55·8 |
| 0·77 | 53·8 |
| 0·76 | 51·7 |
| 0·75 | 49·6 |
| 0·74 | 47·4 |
| 0·73 | 45·1 |
| 0·72 | 42·2 |
| 0·71 | 40·0 |
| 0·70 | 37·3 |
| 0·69 | 34·3 |
| 0·68 | 31·1 |
| 0·67 | 27·4 |
| 0·66 | 23·2 |
| 0·65 | 18·1 |
| 0·64 | 10·6 |
| 0·6348 | 0 |



(57974) E

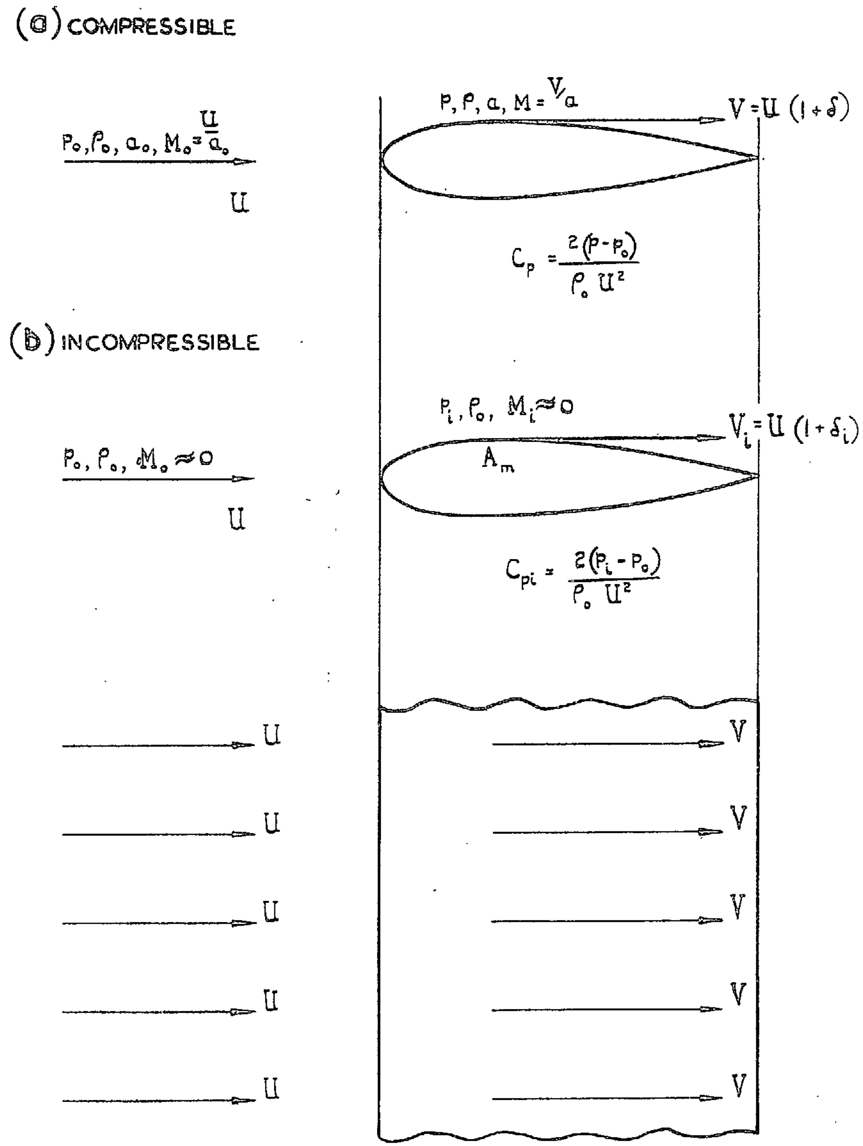


FIGS. 1a and 1b. Two-dimensional flow past a straight infinite wing. Compressible and incompressible.

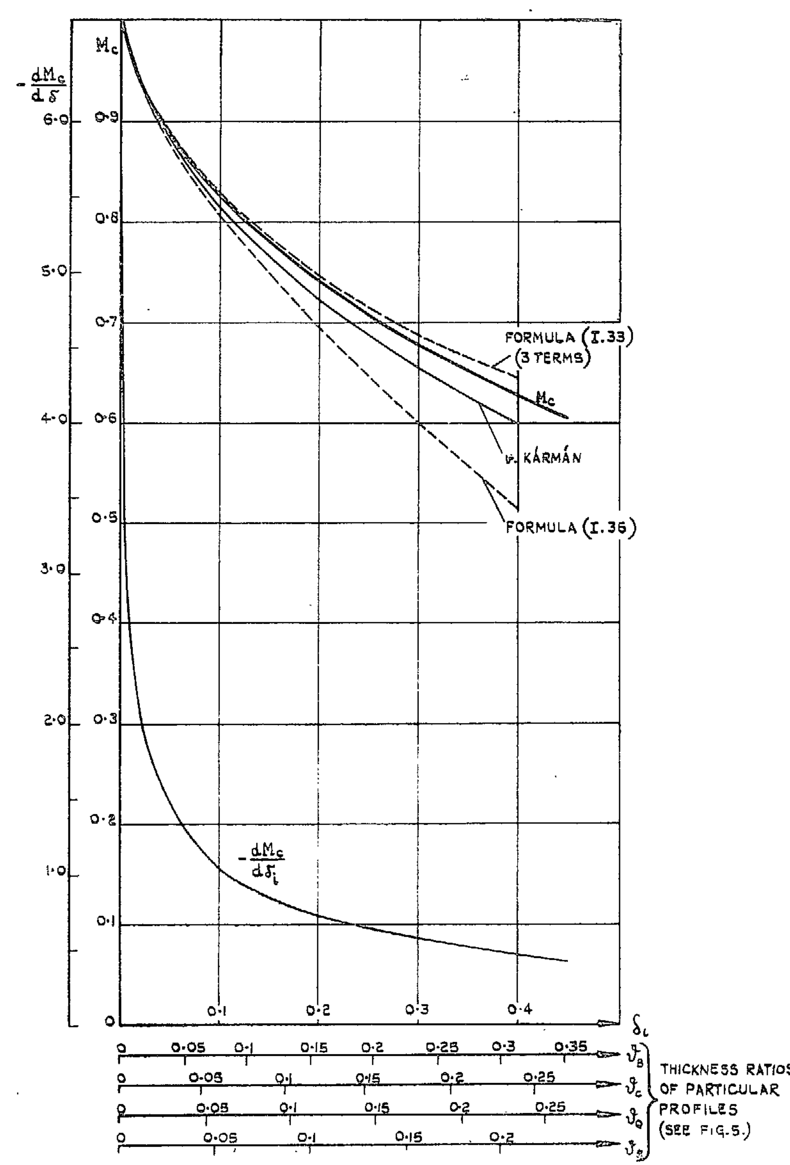


FIG. 2. Critical Mach numbers for a straight infinite wing (two-dimensional flow) against maximum supervelocity ratio $\delta_i$ and against thickness ratio $\vartheta$ for several profiles.

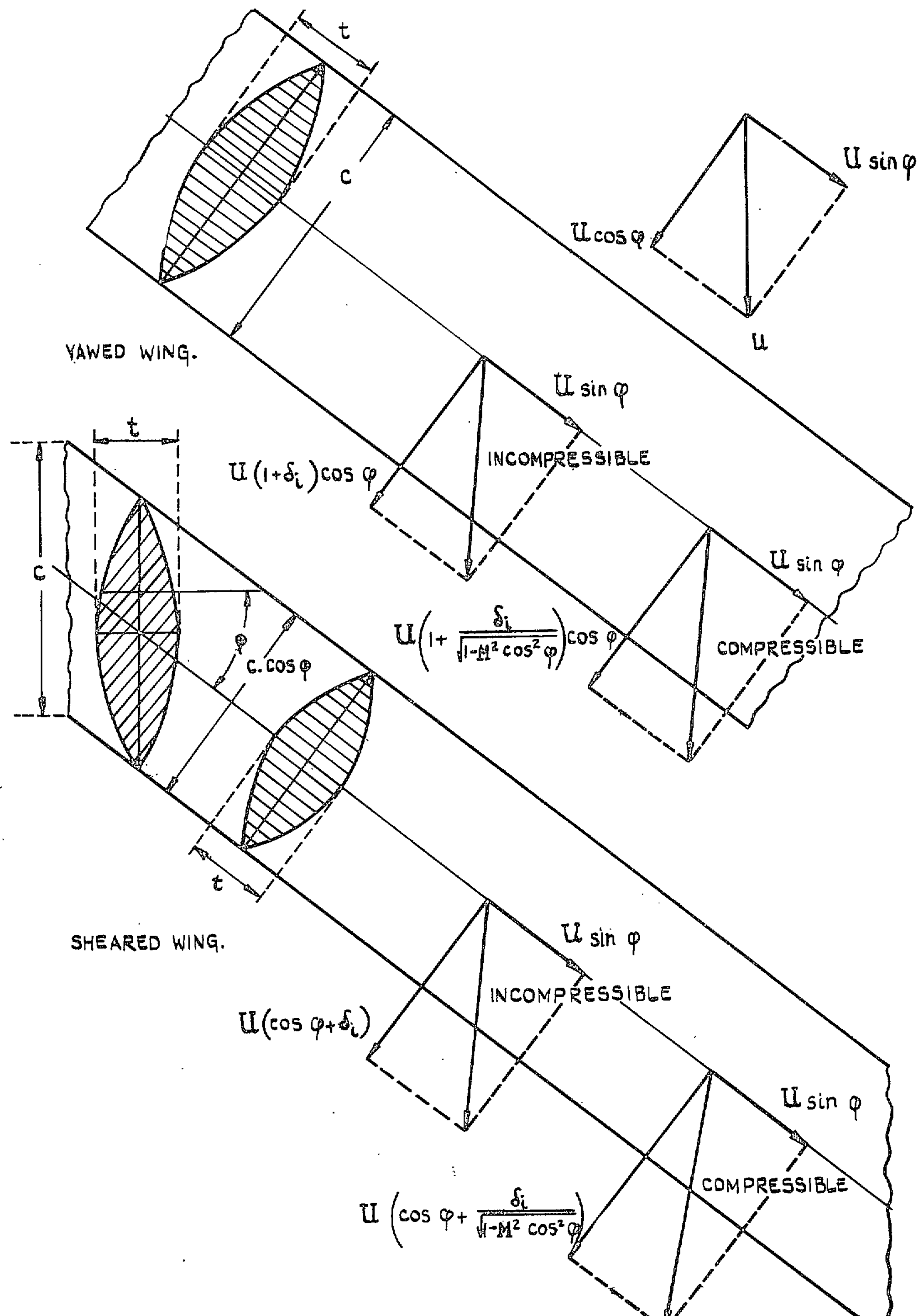


FIG. 3. Velocity components on infinite sheared or yawed wing, relevant for determining critical Mach number.

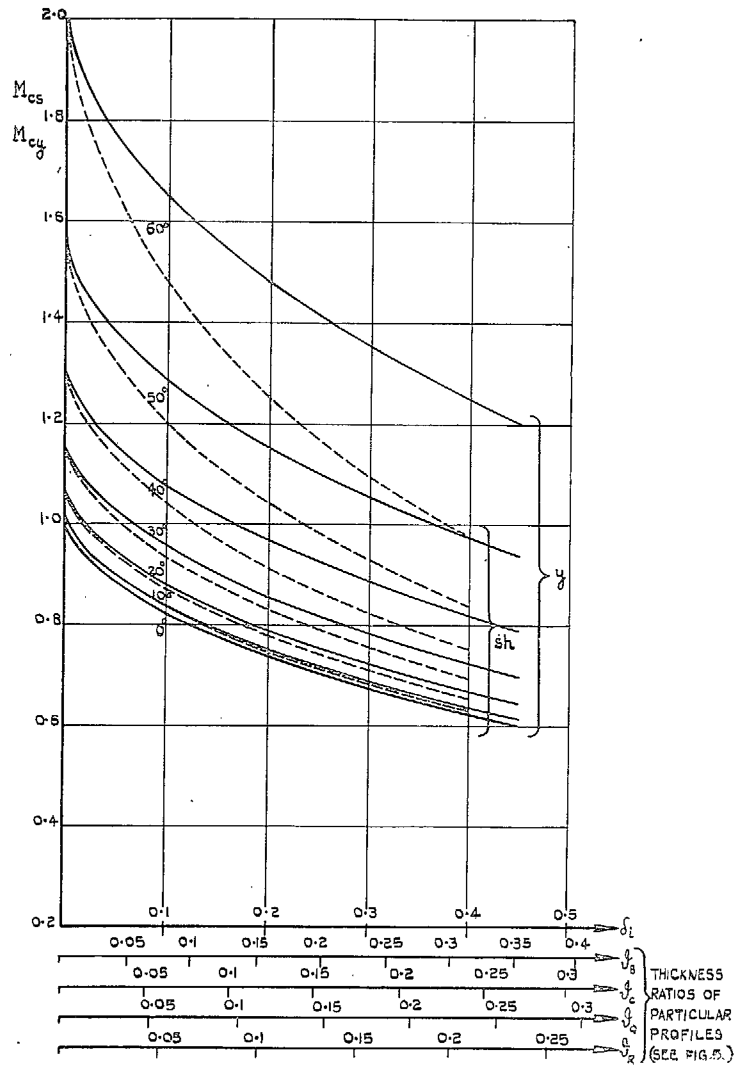


FIG. 4. Critical Mach numbers for infinite sheared and yawed wings of varying angle $\varphi$, against maximum supervelocity ratio $\delta_i$ and against thickness ratio $\vartheta$ for several profiles.

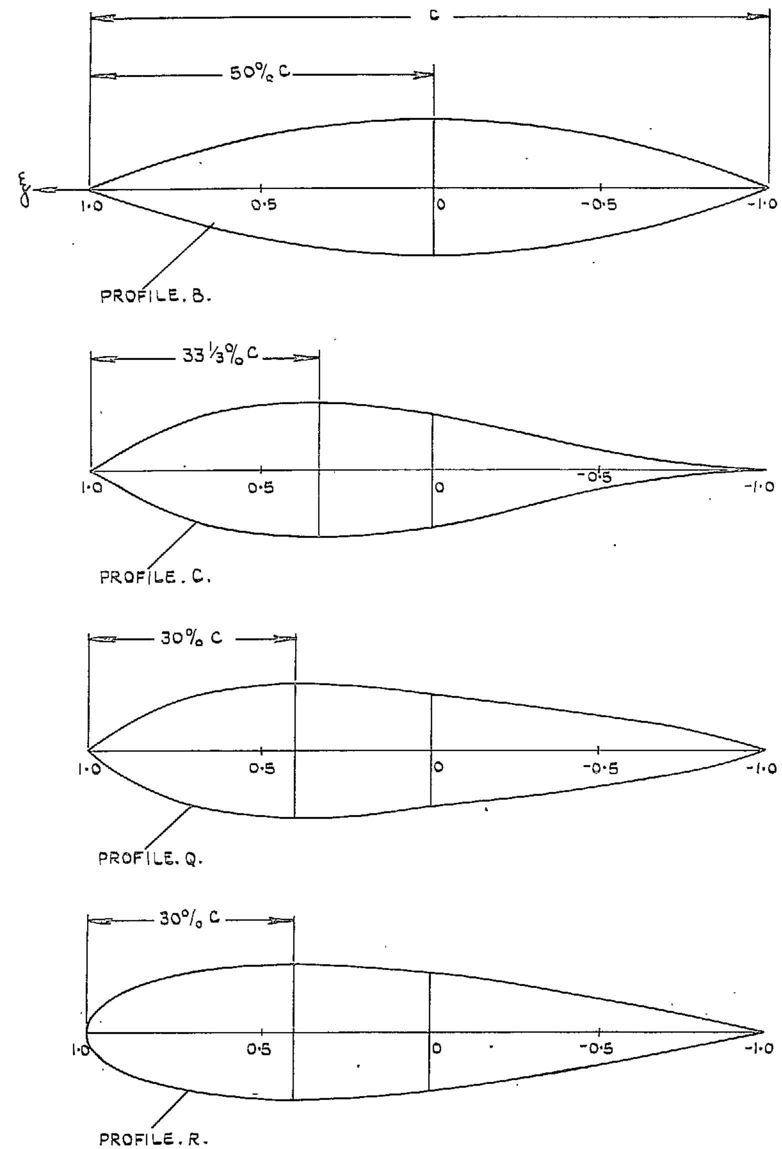


FIG. 5. Four wing profiles.

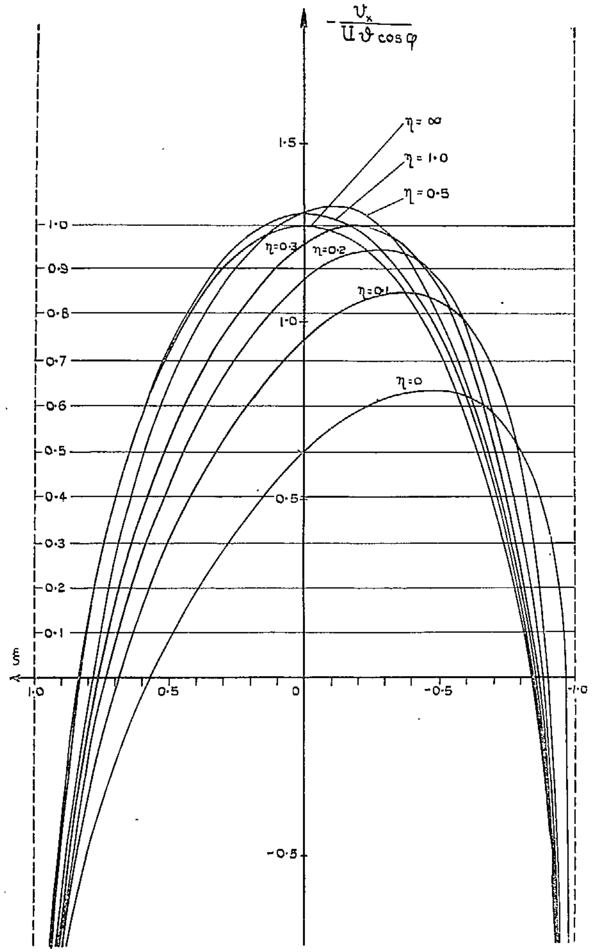


FIG. 6. Supervelocity distribution. Tip area. Profile B. $\varphi = 53° 8'$.

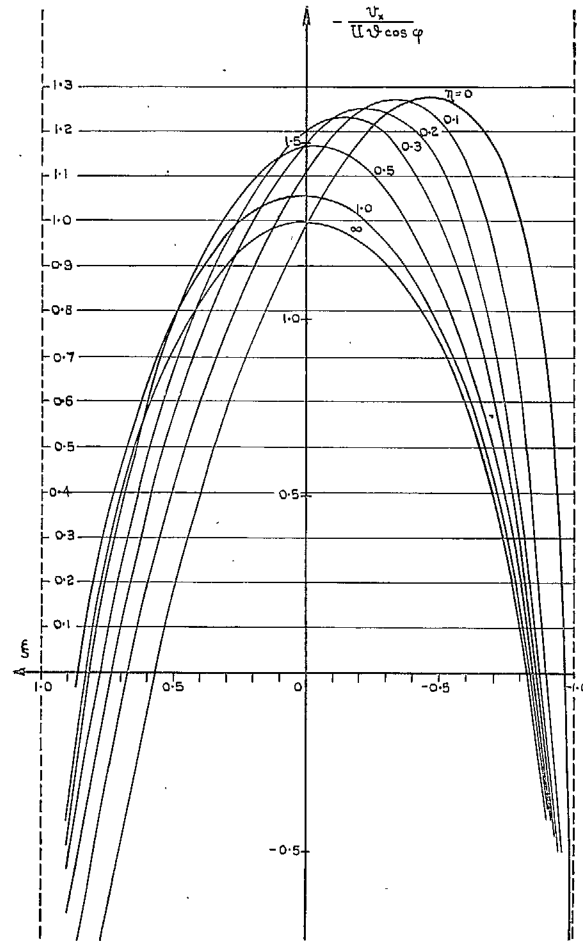


FIG. 7. Supervelocity distribution. Kink area. Profile B. $\varphi = 53° 8'$.

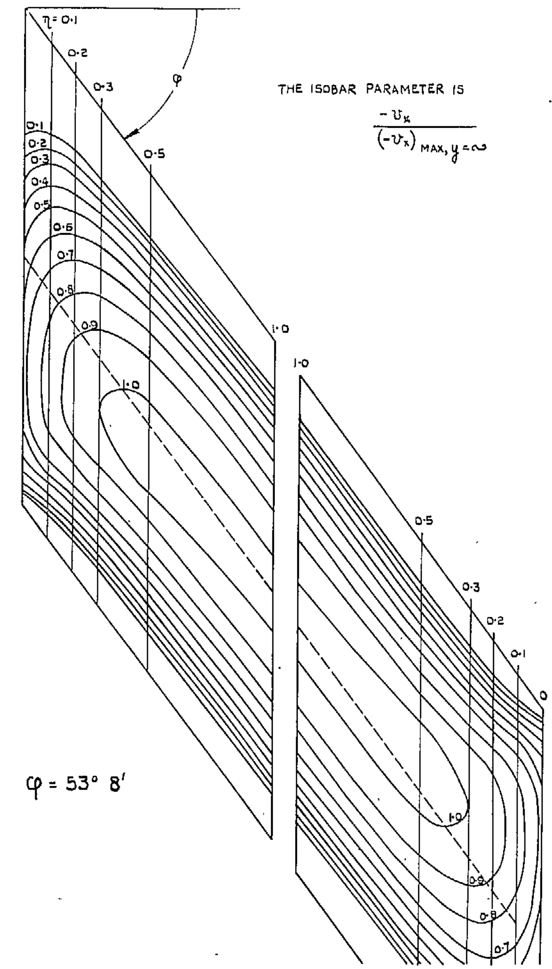


FIG. 8. Isobars on a sheared wing. Profile B.

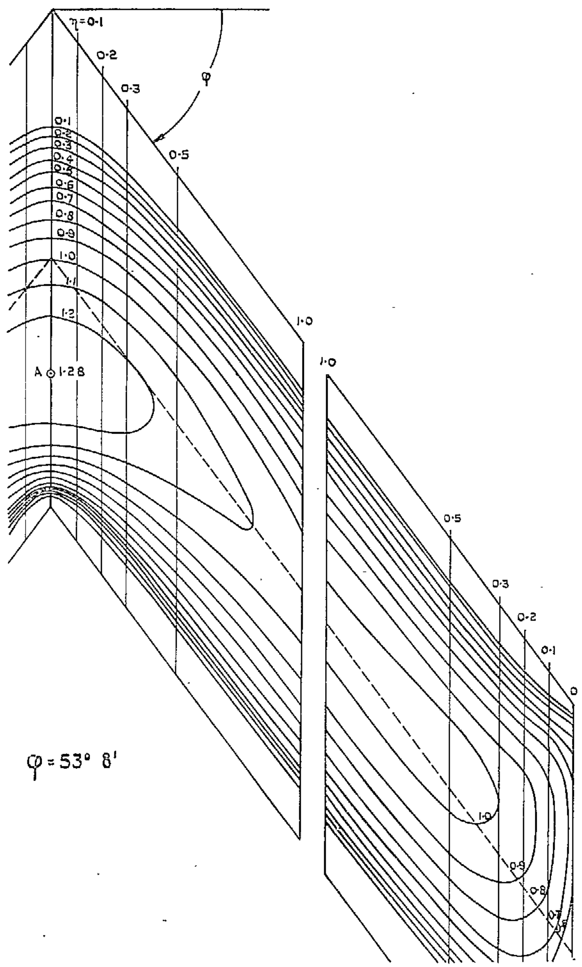


FIG. 9. Isobars on a swept-back wing. Profile B.

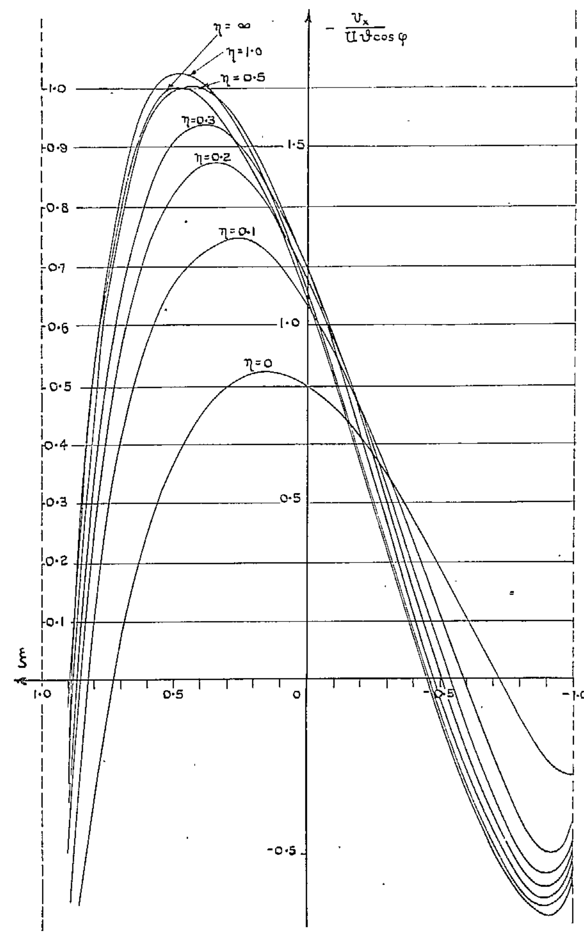


FIG. 10. Supervelocity distribution. Upstream tip area. Profile C. $\varphi = 53°\ 8'$.

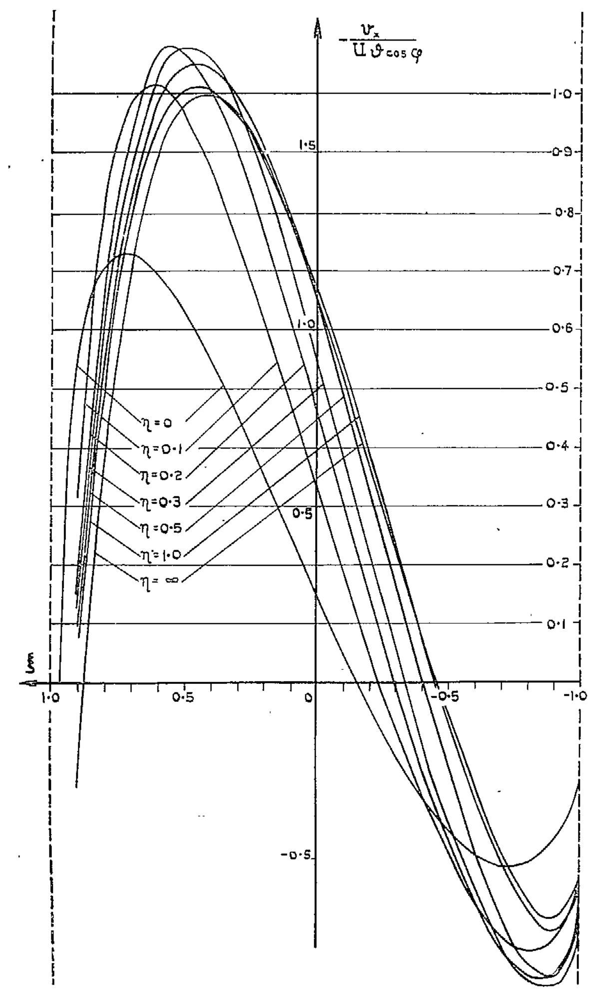


FIG. 11. Supervelocity distribution. Downstream tip area. Profile C. $\varphi = 53°\ 8'$.

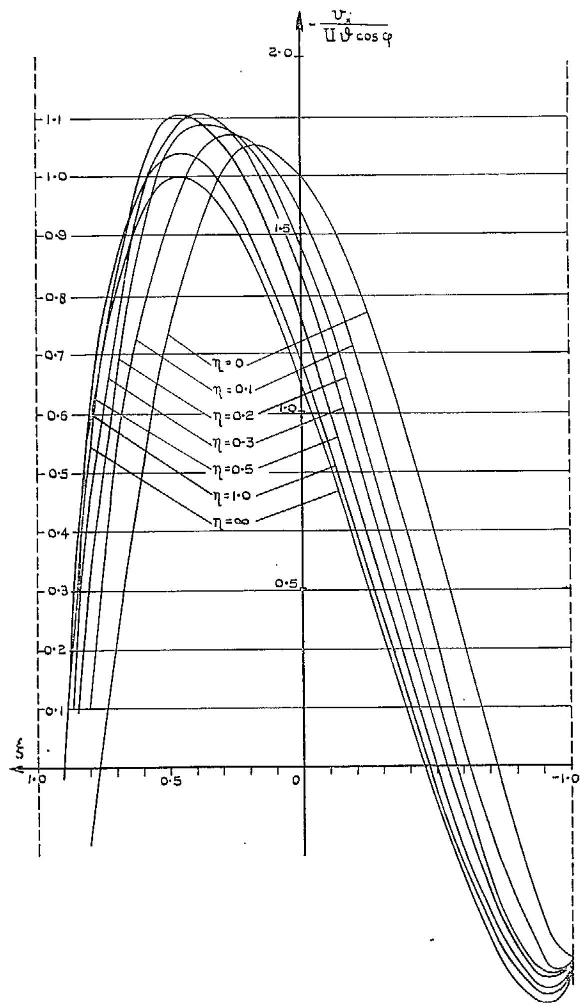


FIG. 12. Supervelocity distribution. Kink area. Profile C. $\varphi = 53° 8'$.

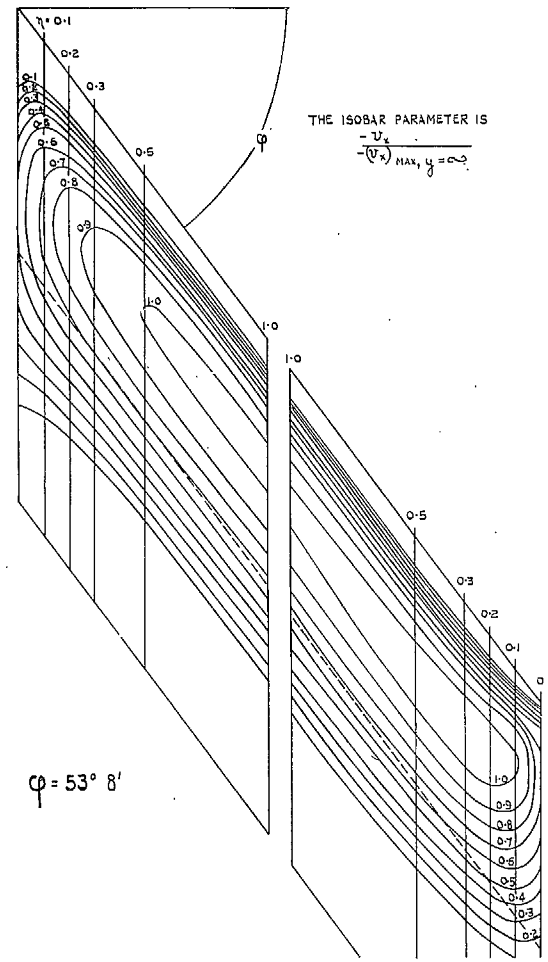


FIG. 13. Isobars on a sheared wing. Profile C.

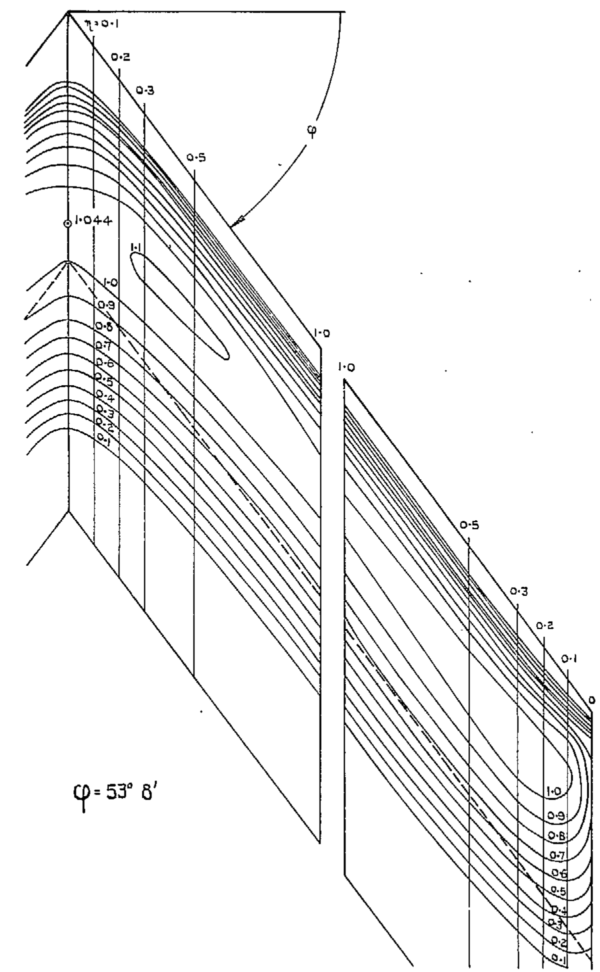


FIG. 14. Isobars on a swept-back wing. Profile C.

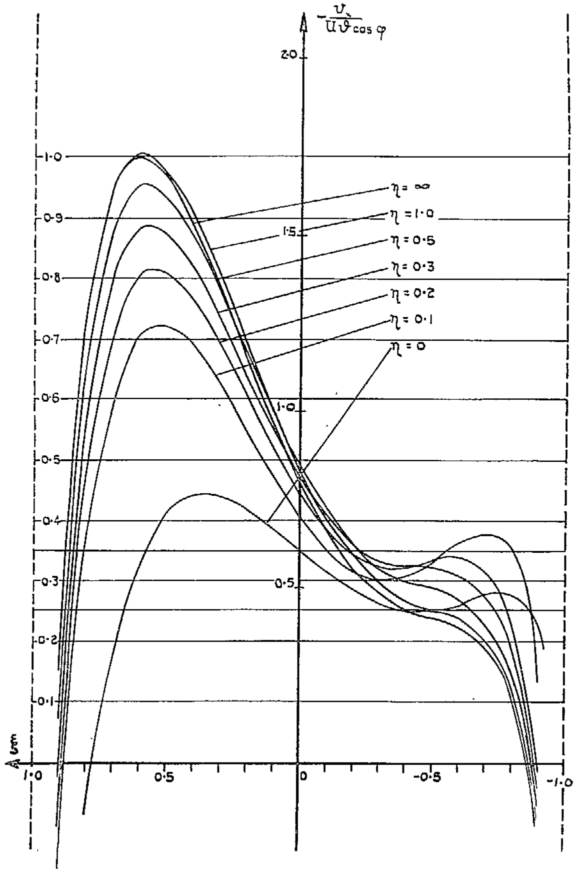


FIG. 15. Supervelocity distribution. Upstream tip area. Profile Q. $\varphi = 53° 8'$.

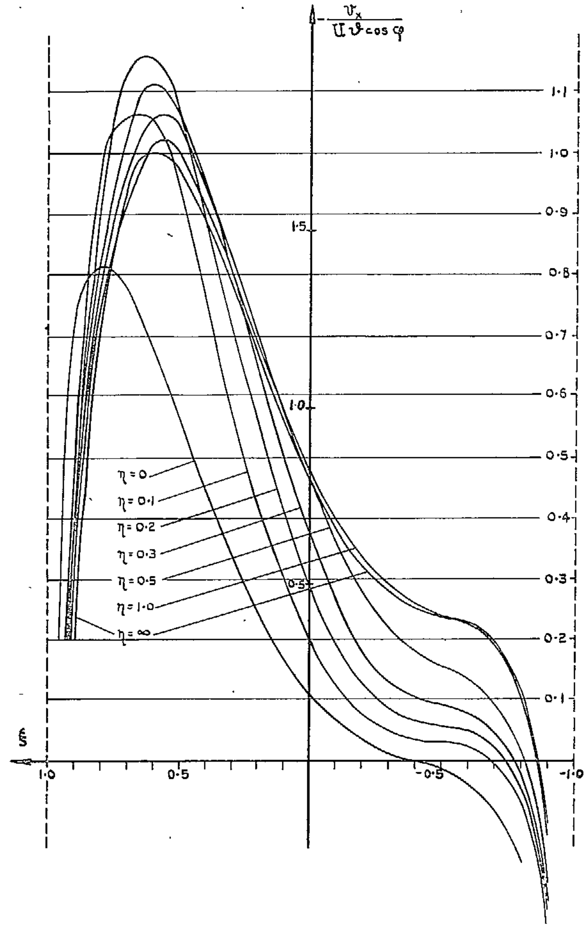


FIG. 16. Supervelocity distribution. Downstream tip area. Profile Q. $\varphi = 53° 8'$.

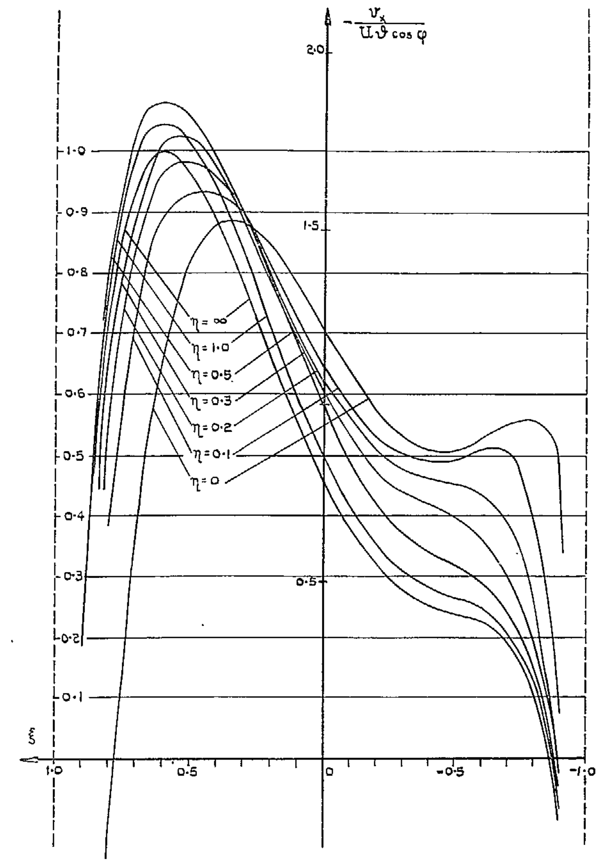


FIG. 17. Supervelocity distribution. Kink area. Profile Q. $\varphi = 53° 8'$.

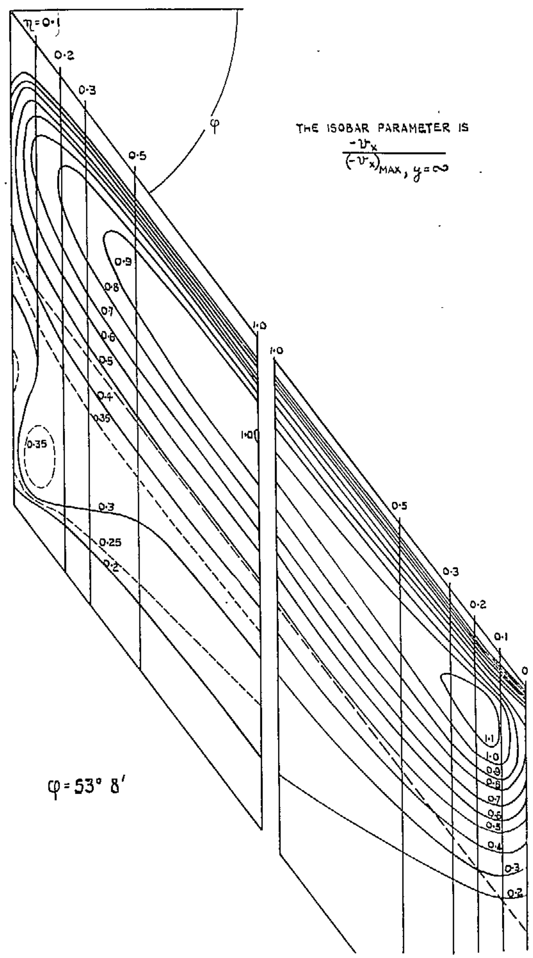


FIG. 18. Isobars on a sheared wing. Profile Q.

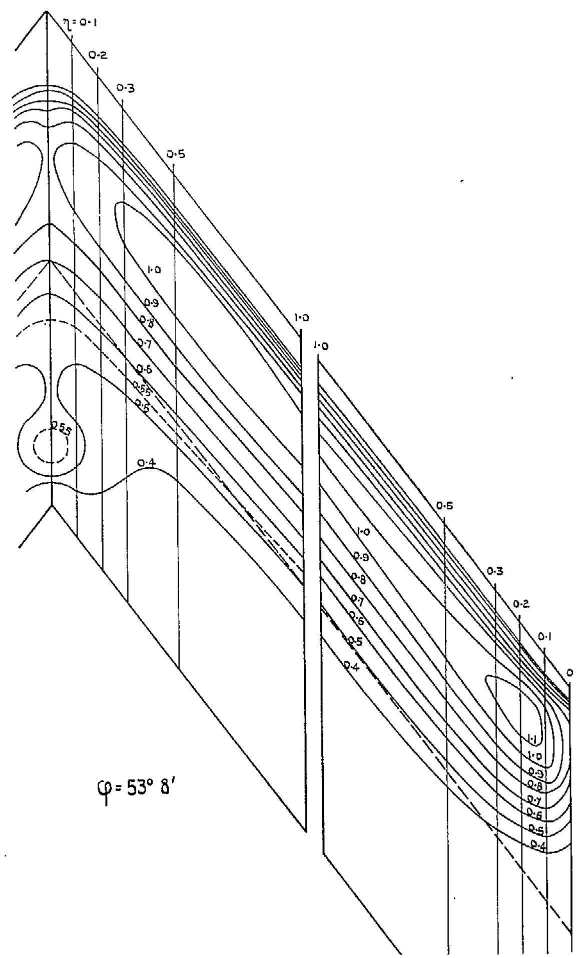


FIG. 19. Isobars on a swept-back wing. Profile Q.

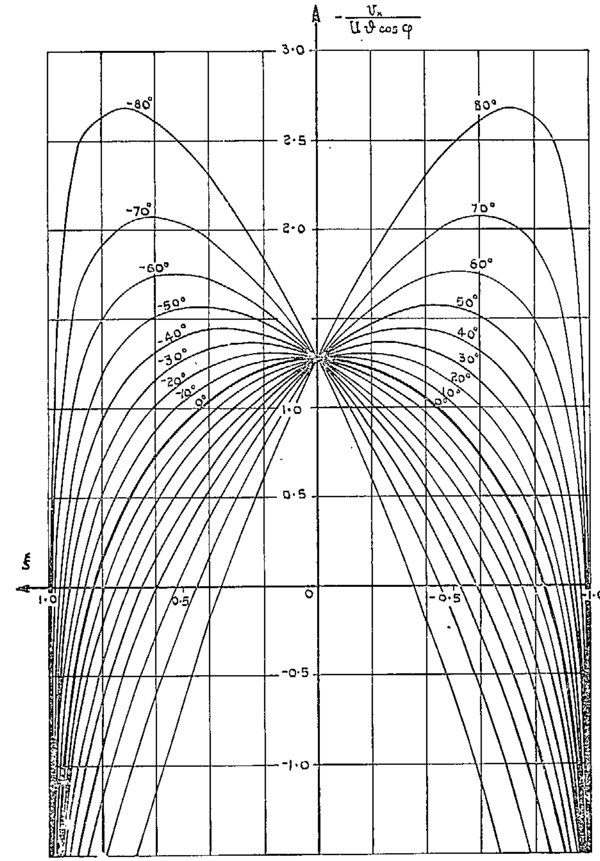


FIG. 20. Supervelocity distributions in the kink section, compared to that at infinity, for different angles of sweep. Profile B.

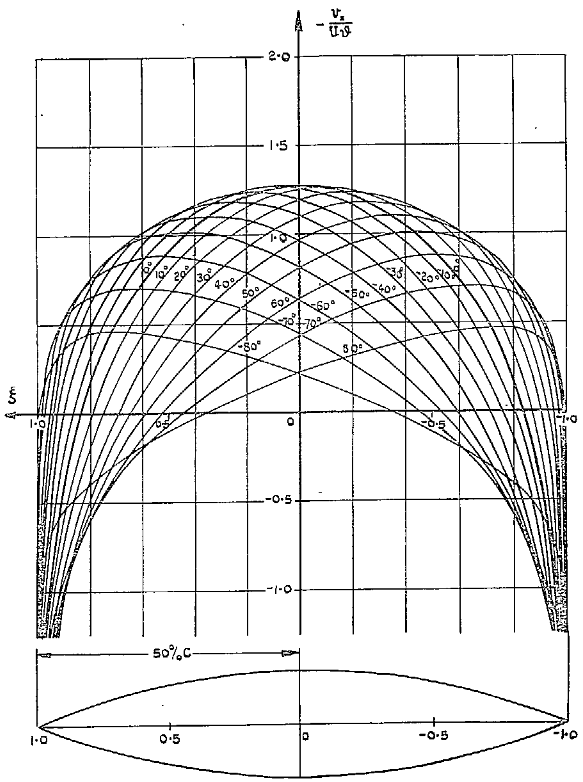


FIG. 21. Supervelocity distributions in the kink section, compared to that on an upswept wing, for different angles of sweep. Profile B.

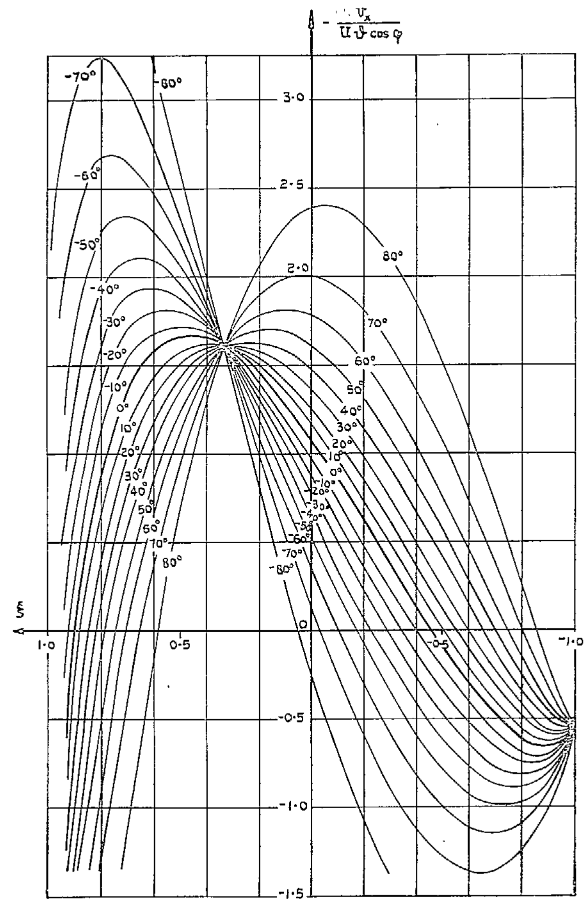


FIG. 22. Supervelocity distributions in the kink section, compared to that at infinity, for different angles of sweep. Profile C.

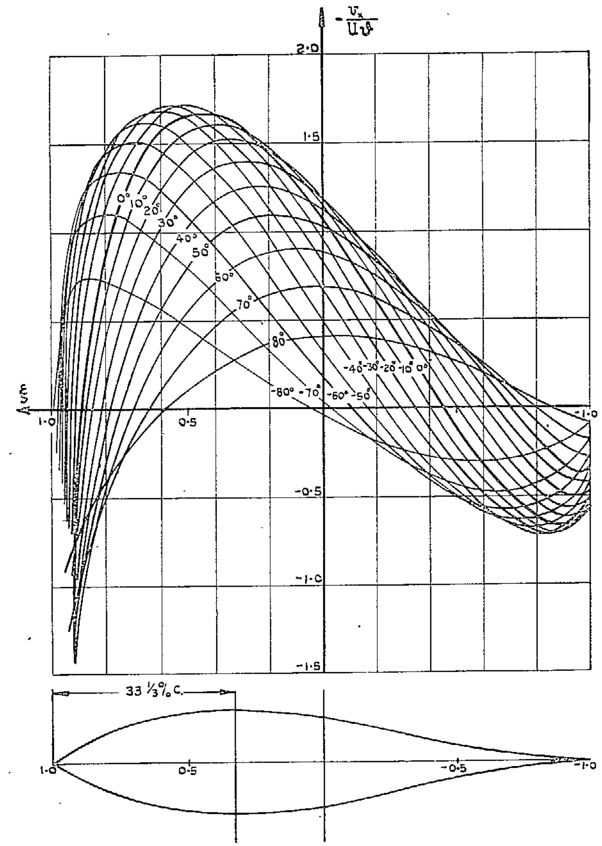


FIG. 23. Supervelocity distributions in the kink section, compared to that on an unswept wing, for different angles of sweep. Profile C.

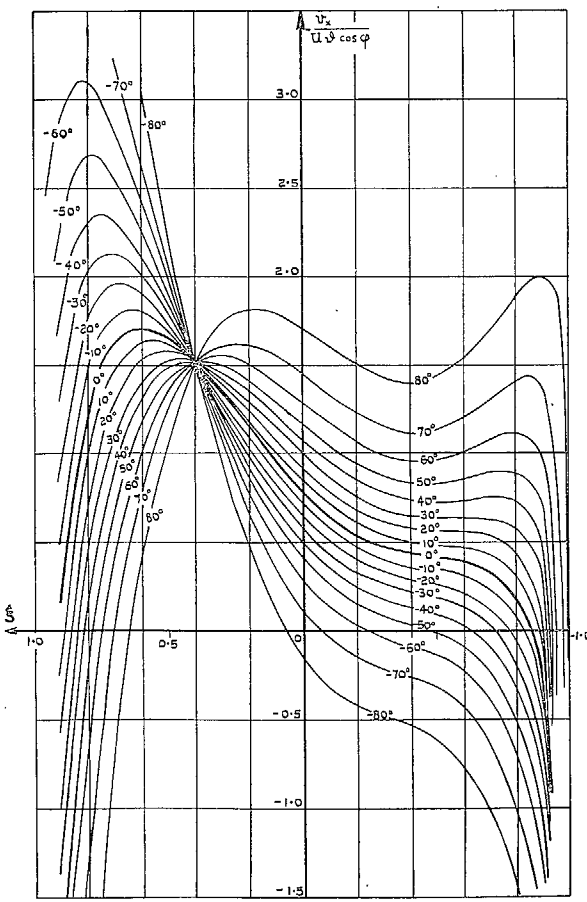


FIG. 24. Supervelocity distributions in the kink section, compared to that at infinity, for different angles of sweep. Profile Q.

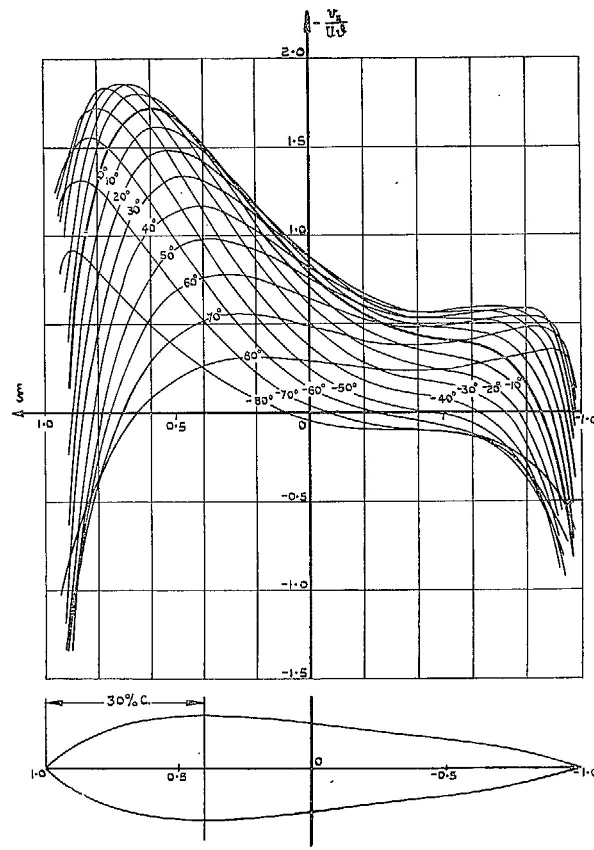


FIG. 25. Supervelocity distributions in the kink section, compared to that on an unswept wing, for different angles of sweep. Profile Q.

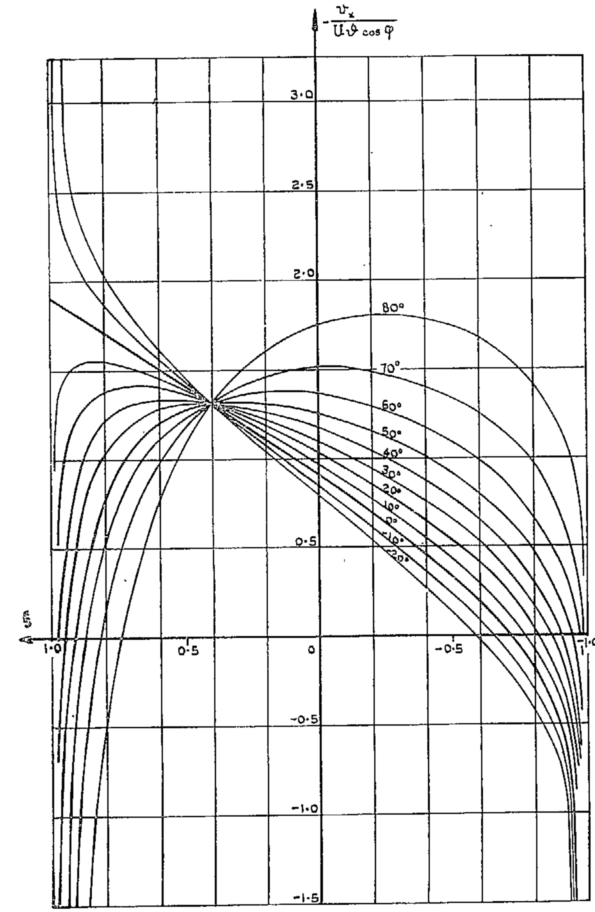


FIG. 26. Supervelocity distributions in the kink section, compared to that at infinity, for different angles of sweepback. Profile R.

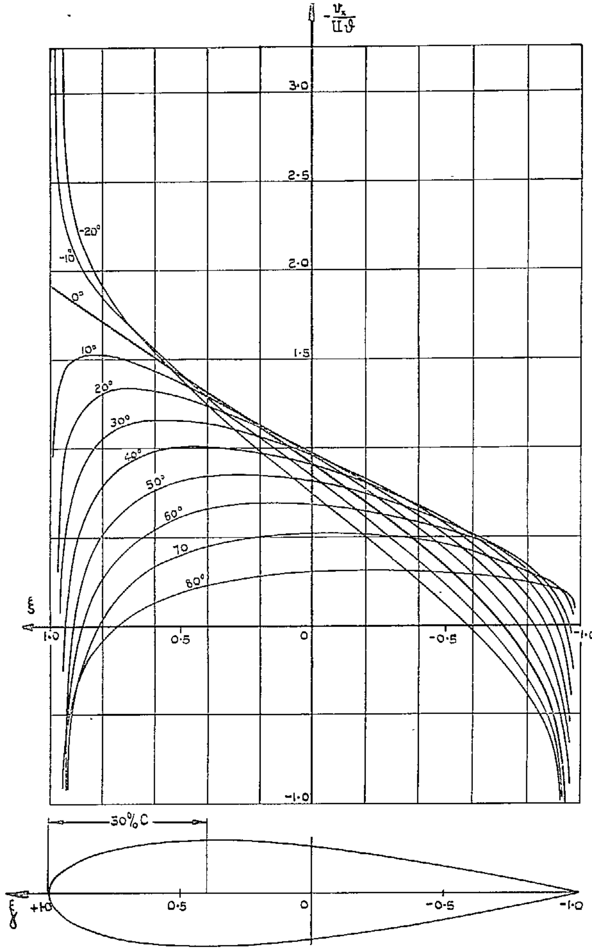


FIG. 27. Supervelocity distribution in the kink section, compared to that on an unswept wing, for different angles of sweep-back. Profile R.

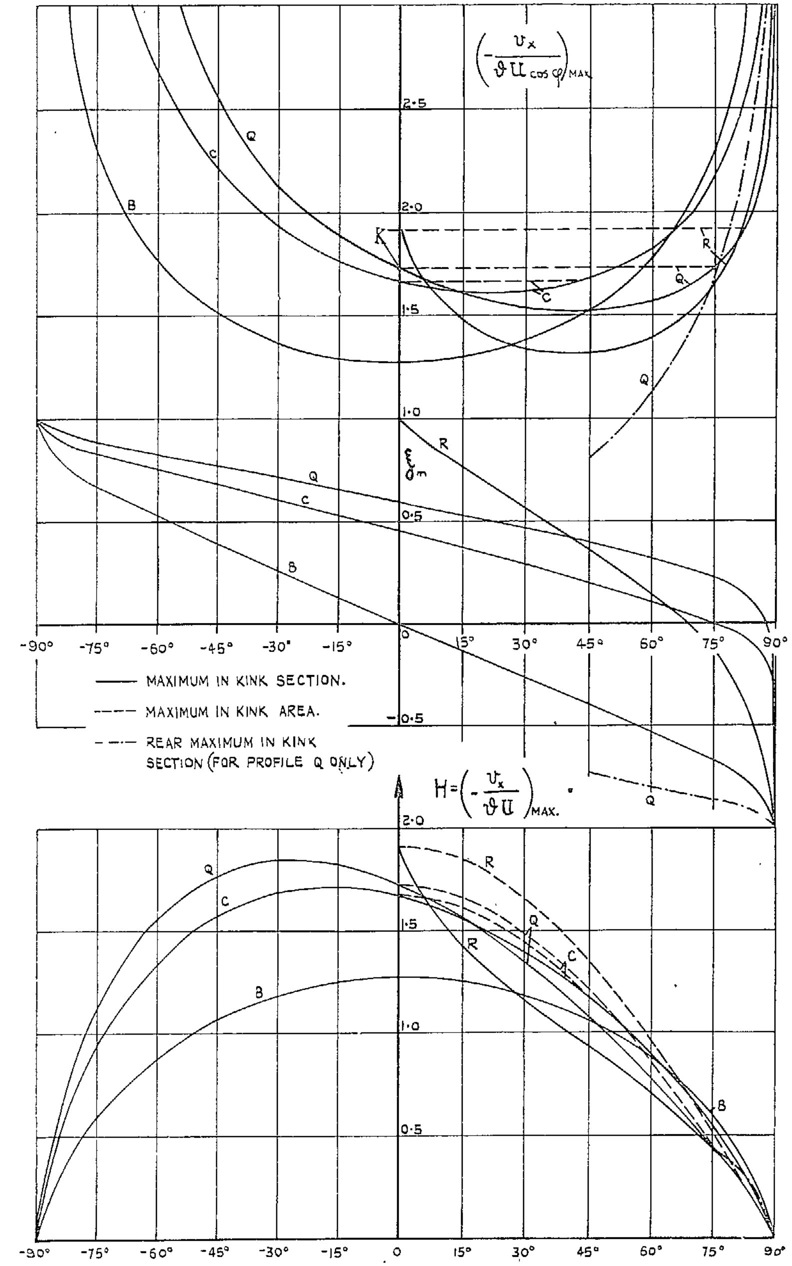


FIG. 28. Maximum supervelocity ratios for wings with varying angle of sweep. Profiles B, C, Q and R.

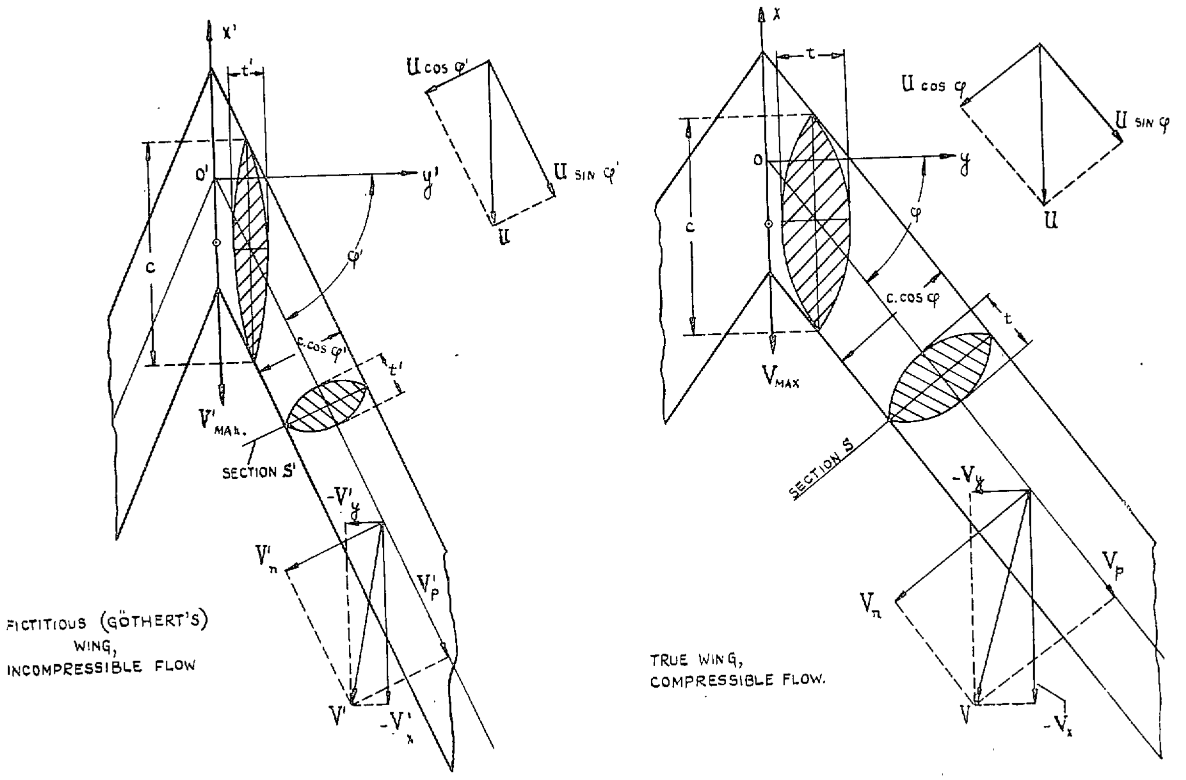


FIG. 29. Velocity components on untapered swept-back wing relevant for determining critical Mach numbers.

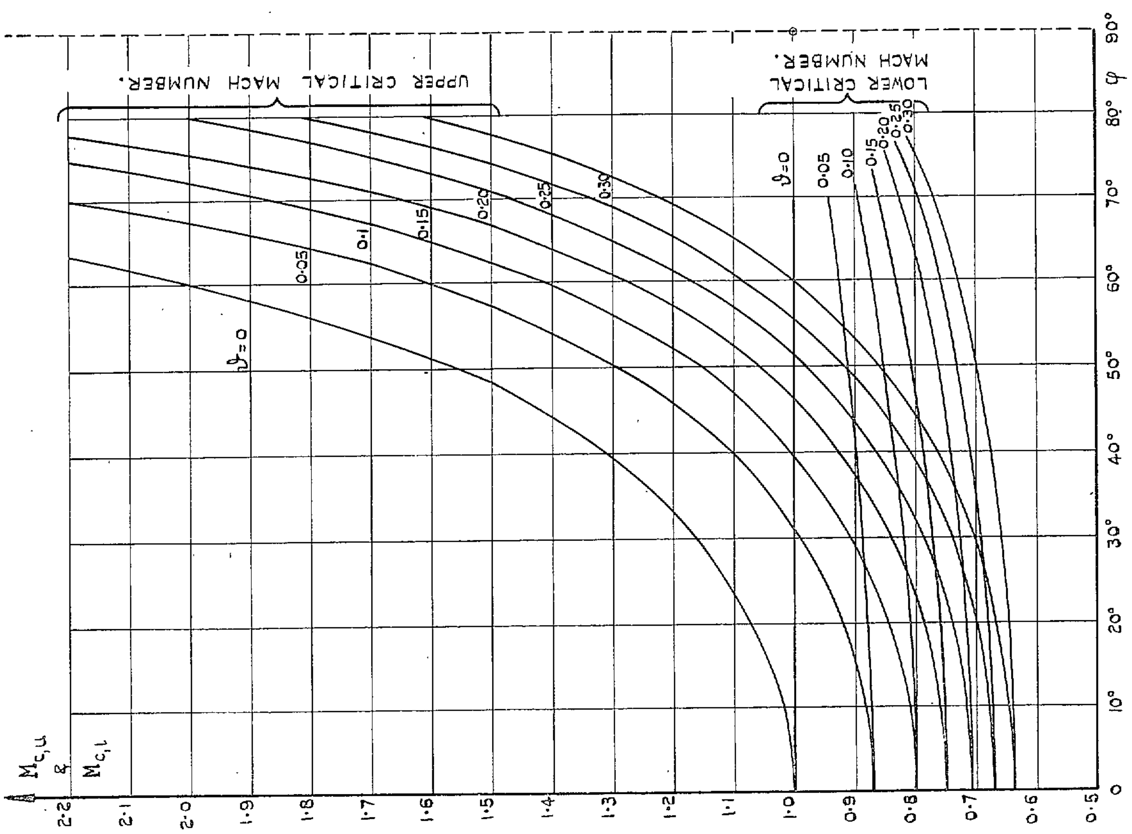


FIG. 30. Upper and lower critical Mach numbers for swept wings. Profile B.

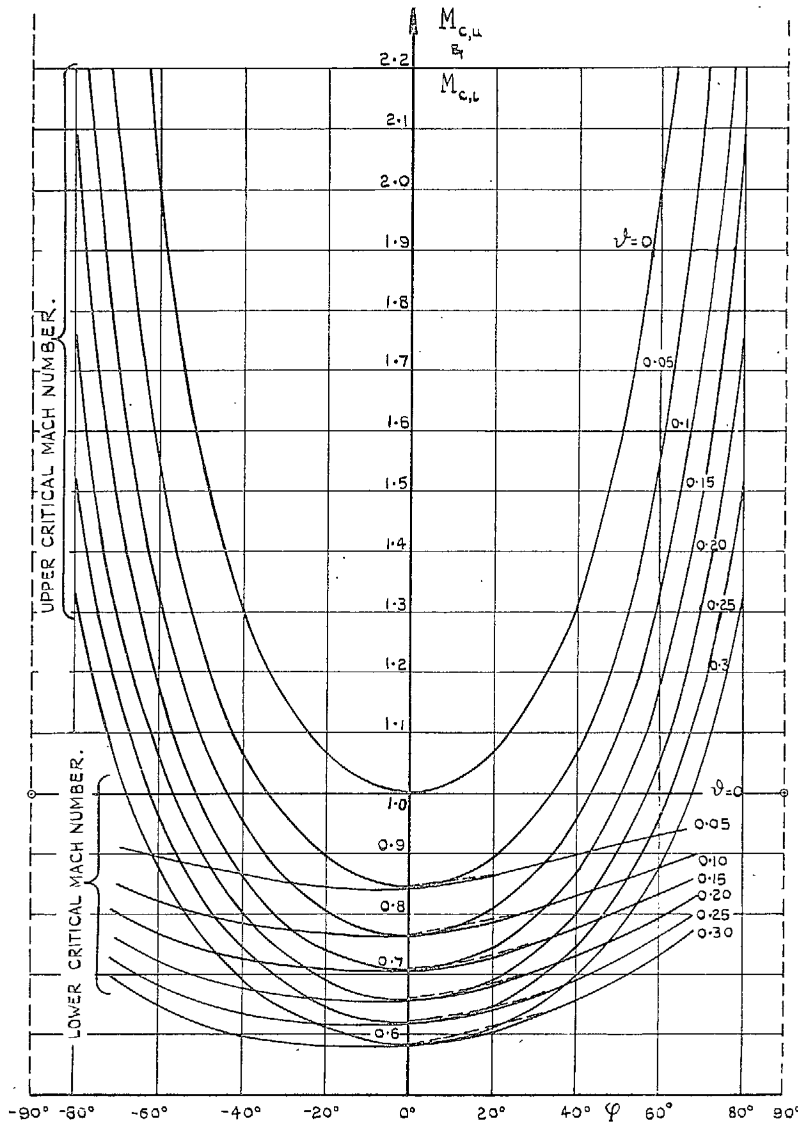


FIG. 31. Upper and lower critical Mach numbers for swept wings. Profile C.

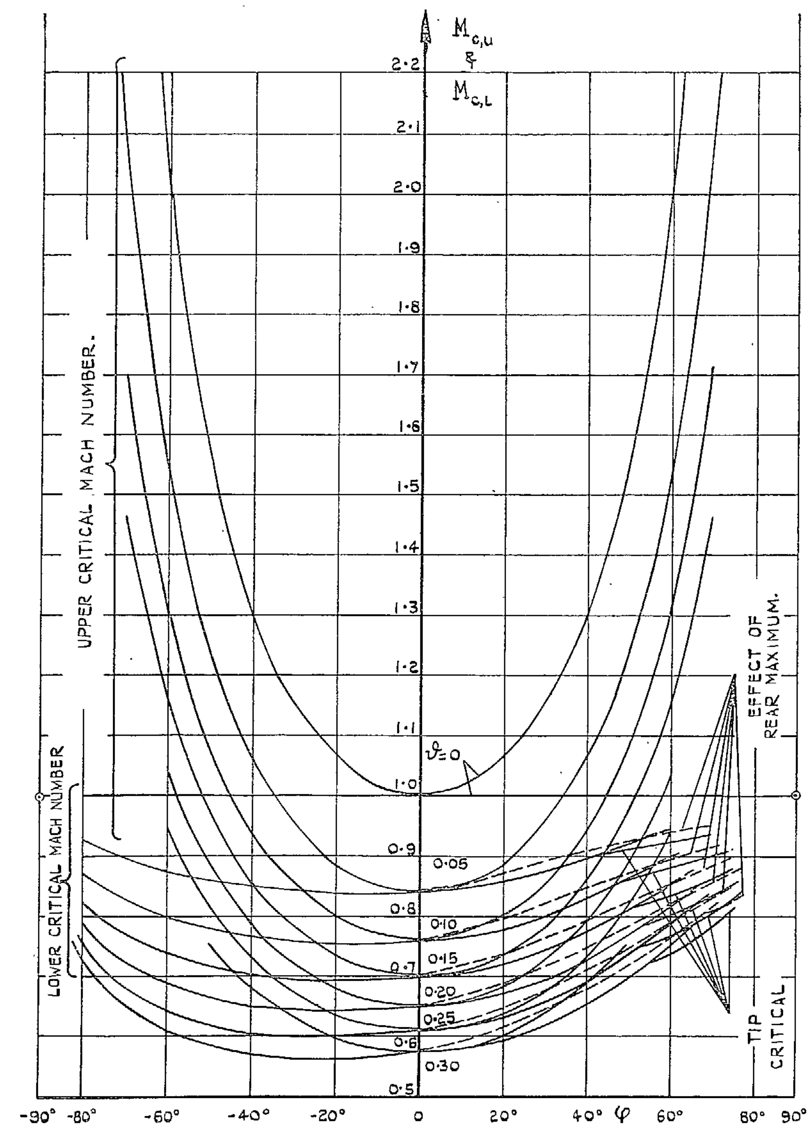


FIG. 32. Upper and lower critical Mach numbers for swept wings. Profile Q.

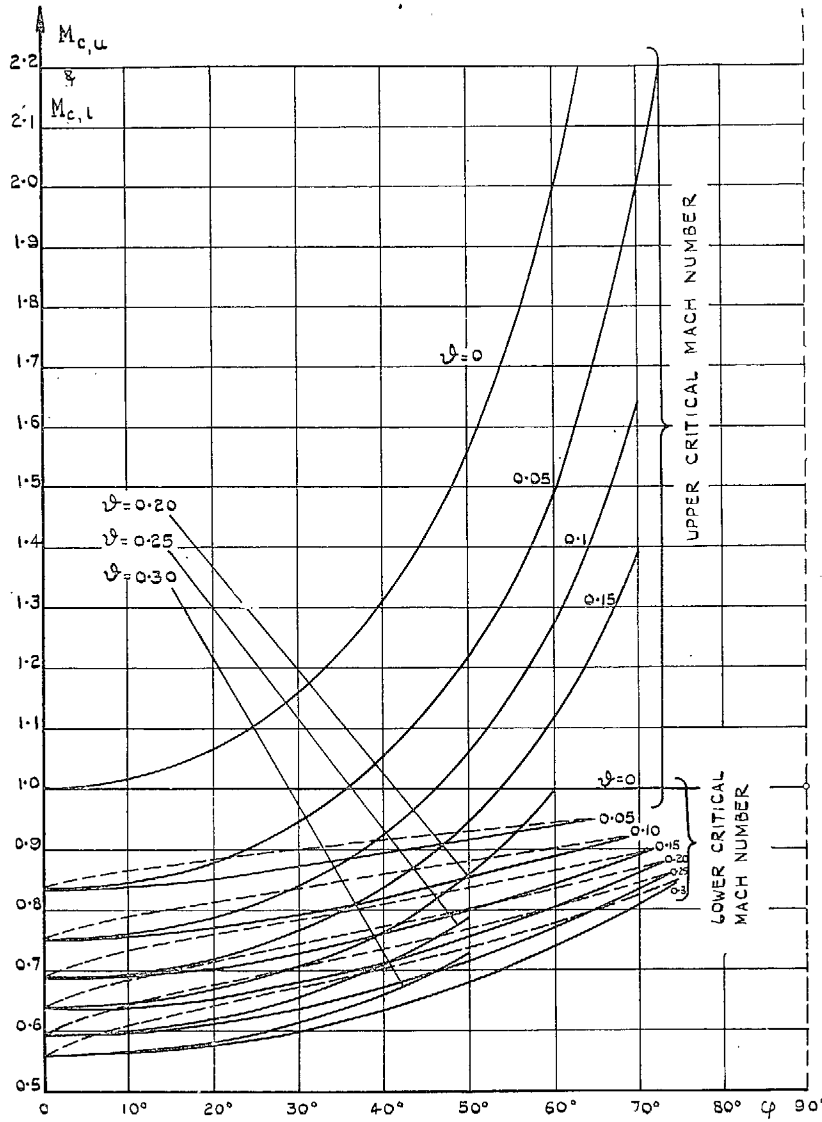


FIG. 33. Upper and lower critical Mach numbers for swept-back wings. Profile R.

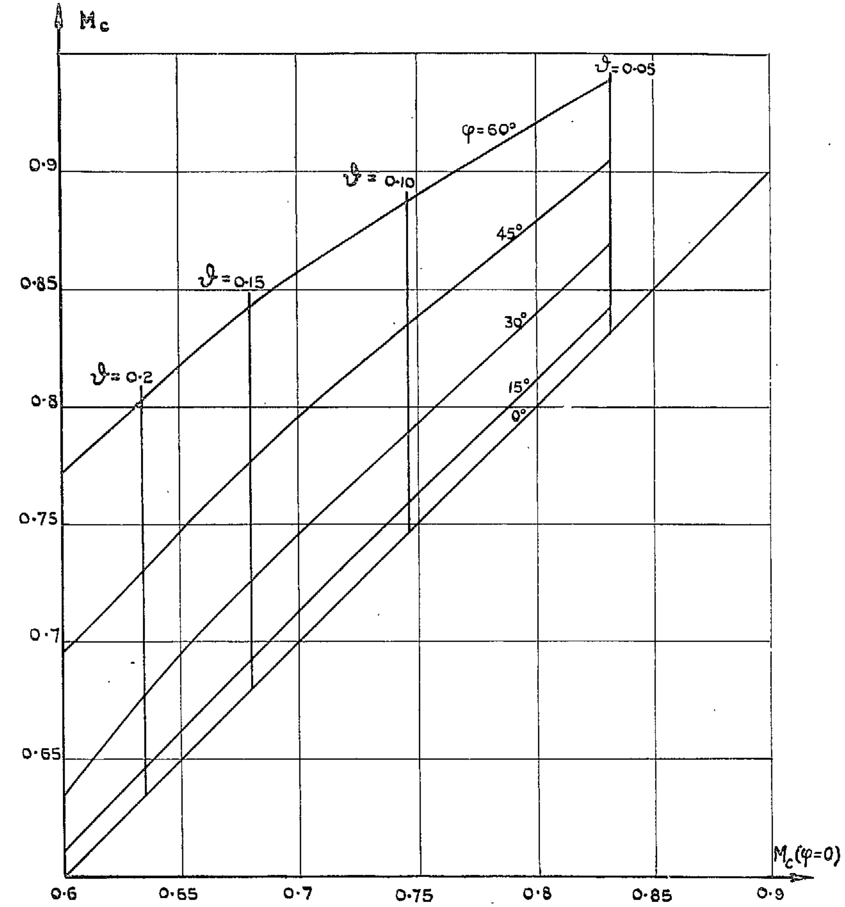


FIG. 34. Improvement of the lower critical Mach number with increasing angle of sweep. Profile B.

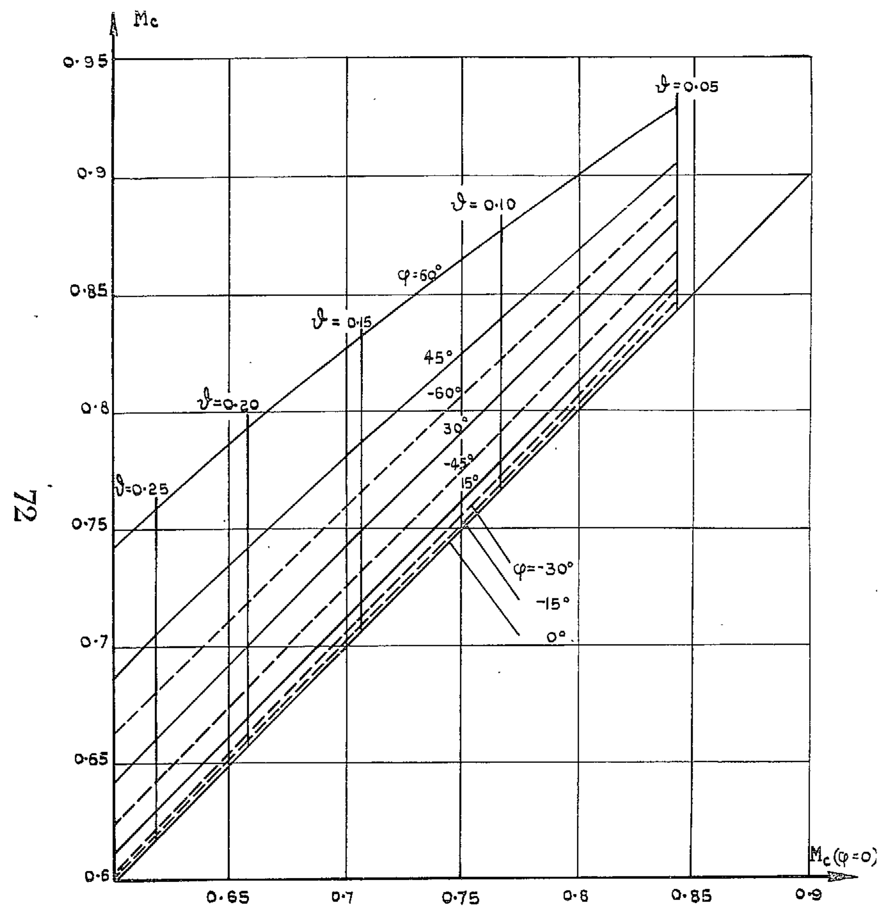

FIG. 35. Improvement of the lower critical Mach number with increasing angle of sweepback or sweep forward. Profile C.

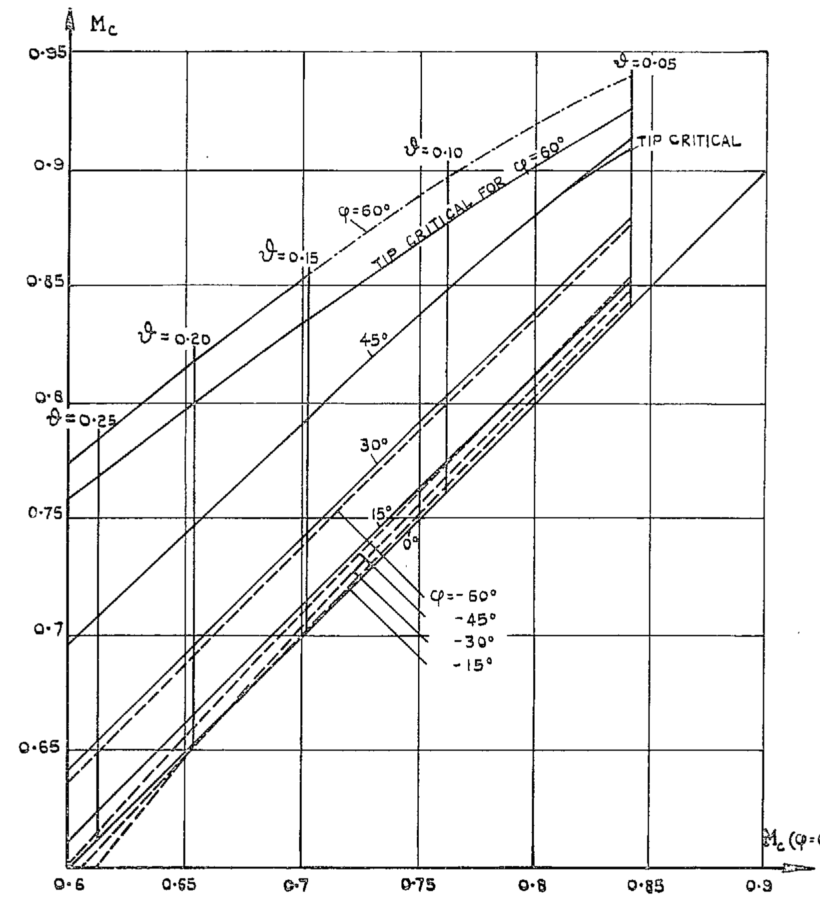

FIG. 36. Improvement of the lower critical Mach number with increasing angle of sweepback or sweep forward. Profile Q.

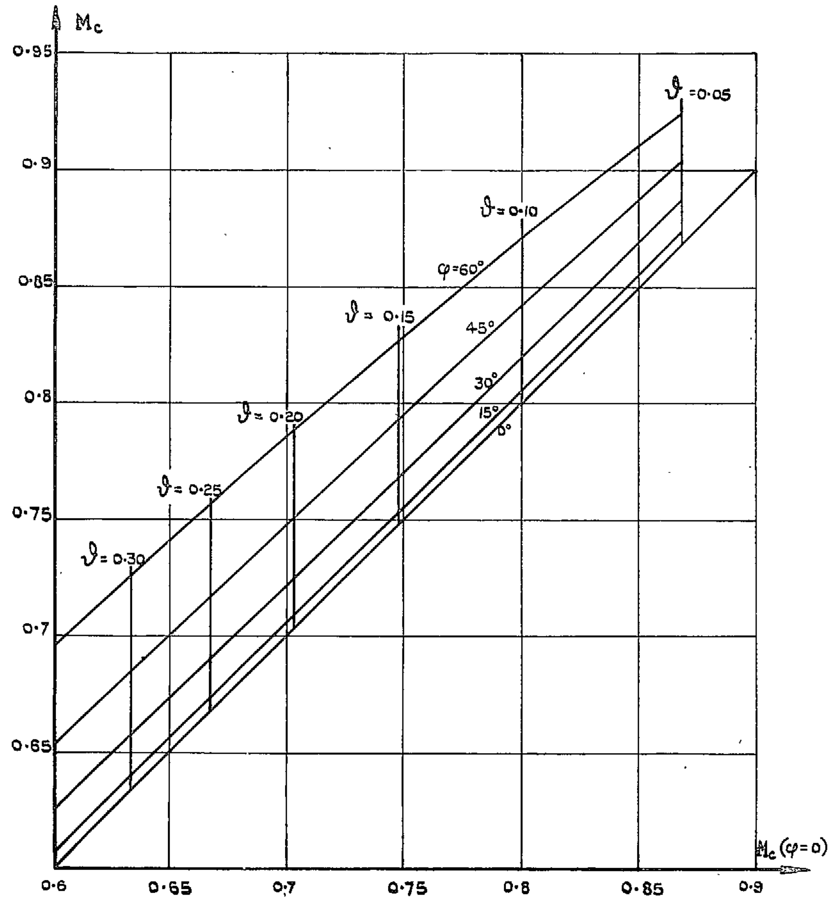


FIG. 37. Improvement of the lower critical Mach number with increasing angle of sweepback. Profile R.

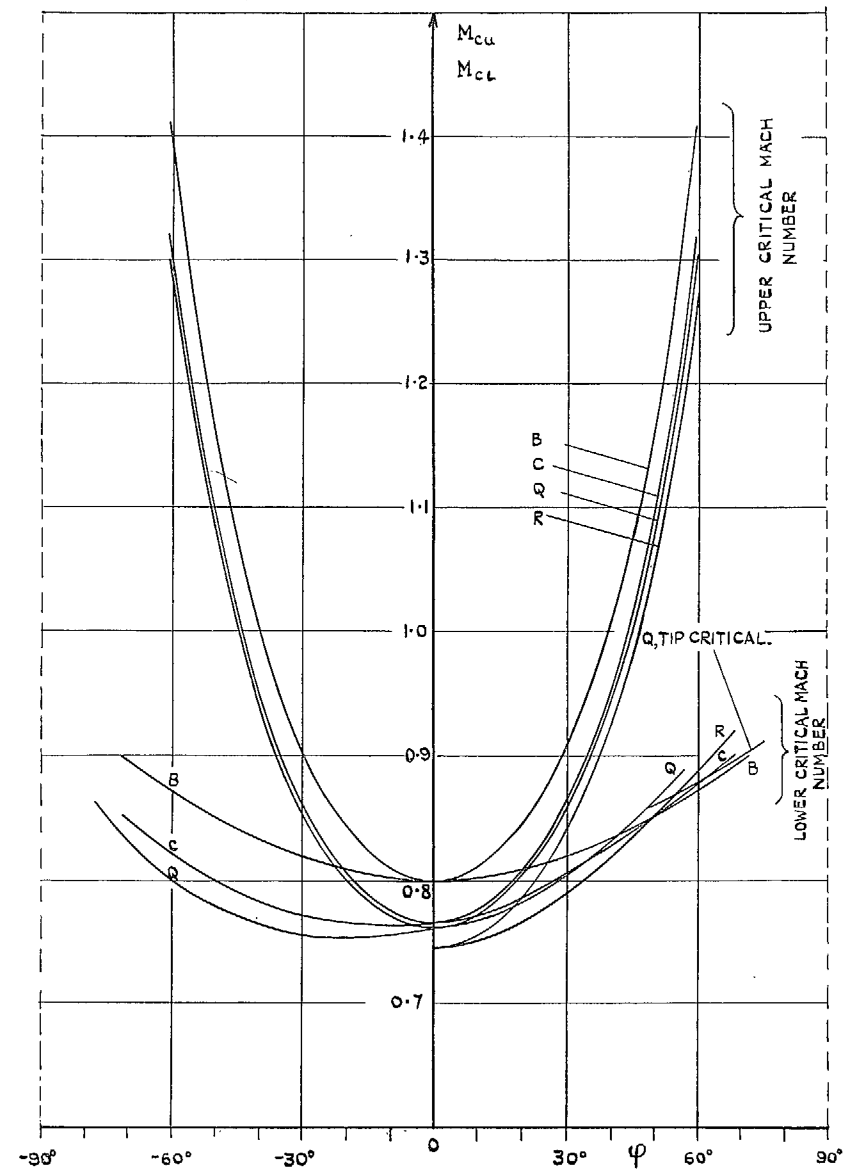


FIG. 38. Upper and lower critical Mach numbers at varying angle of sweep, for 4 different profiles. Thickness ratio 10 per cent.

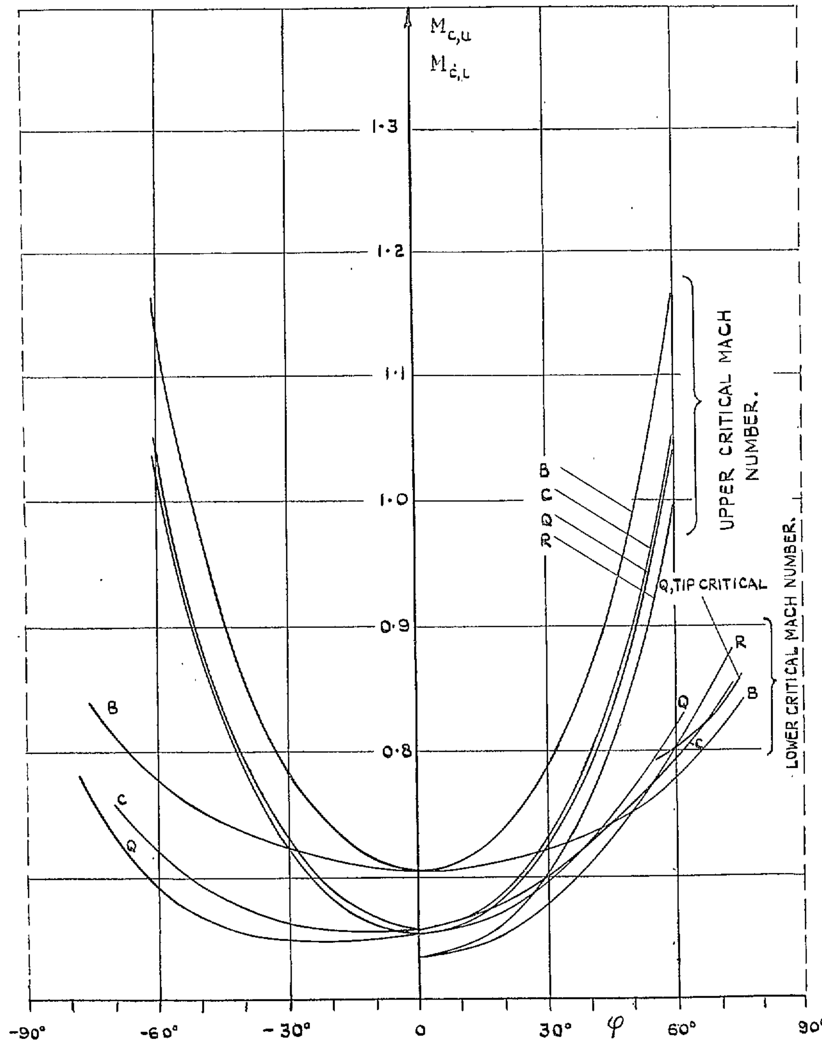


FIG. 39. Upper and lower critical Mach numbers at varying angle of sweep, for four different profiles. Thickness ratio 20 per cent.



(57974) Wt. 17/680 K.9 1/54 Hw. PRINTED IN GREAT BRITAIN

# Publications of the Aeronautical Research Council

## ANNUAL TECHNICAL REPORTS OF THE AERONAUTICAL RESEARCH COUNCIL (BOUND VOLUMES)

1936 Vol. I. Aerodynamics General, Performance, Airscrews, Flutter and Spinning. 40s. (40s. 9d.)
Vol. II. Stability and Control, Structures, Seaplanes, Engines, etc. 50s. (50s. 10d.)

1937 Vol. I. Aerodynamics General, Performance, Airscrews, Flutter and Spinning. 40s. (40s. 10d.)
Vol. II. Stability and Control, Structures, Seaplanes, Engines, etc. 60s. (61s.)

1938 Vol. I. Aerodynamics General, Performance, Airscrews. 50s. (51s.)
Vol. II. Stability and Control, Flutter, Structures, Seaplanes, Wind Tunnels, Materials. 30s. (30s. 9d.)

1939 Vol. I. Aerodynamics General, Performance, Airscrews, Engines. 50s. (50s. 11d.)
Vol. II. Stability and Control, Flutter and Vibration, Instruments, Structures, Seaplanes, etc. 63s. (64s. 2d.)

1940 Aero and Hydrodynamics, Aerofoils, Airscrews, Engines, Flutter, Icing, Stability and Control, Structures, and a miscellaneous section. 50s. (51s.)

1941 Aero and Hydrodynamics, Aerofoils, Airscrews, Engines, Flutter, Stability and Control, Structures. 63s. (64s. 2d.)

1942 Vol. I. Aero and Hydrodynamics, Aerofoils, Airscrews, Engines. 75s. (76s. 3d.)
Vol. II. Noise, Parachutes, Stability and Control, Structures, Vibration, Wind Tunnels. 47s. 6d. (48s. 5d.)

1943 Vol. I. (*In the press.*)
Vol. II. (*In the press.*)

## ANNUAL REPORTS OF THE AERONAUTICAL RESEARCH COUNCIL—

| | | | |
|---|---|---|---|
| 1933–34 | 1s. 6d. (1s. 8d.) | 1937 | 2s. (2s. 2d.) |
| 1934–35 | 1s. 6d. (1s. 8d.) | 1938 | 1s. 6d. (1s. 8d.) |
| April 1, 1935 to Dec. 31, 1936. | 4s. (4s. 4d.) | 1939–48 | 3s. (3s. 2d.) |

## INDEX TO ALL REPORTS AND MEMORANDA PUBLISHED IN THE ANNUAL TECHNICAL REPORTS, AND SEPARATELY—

April, 1950 - - - - R. & M. No. 2600. 2s. 6d. (2s. 7½d.)

## AUTHOR INDEX TO ALL REPORTS AND MEMORANDA OF THE AERONAUTICAL RESEARCH COUNCIL—

1909–1949. R. & M. No. 2570. 15s. (15s. 3d.)

## INDEXES TO THE TECHNICAL REPORTS OF THE AERONAUTICAL RESEARCH COUNCIL—

| | | |
|---|---|---|
| December 1, 1936 — June 30, 1939. | R. & M. No. 1850. | 1s. 3d. (1s. 4½d.) |
| July 1, 1939 — June 30, 1945. | R. & M. No. 1950. | 1s. (1s. 1½d.) |
| July 1, 1945 — June 30, 1946. | R. & M. No. 2050. | 1s. (1s. 1½d.) |
| July 1, 1946 — December 31, 1946. | R. & M. No. 2150. | 1s. 3d. (1s. 4½d.) |
| January 1, 1947 — June 30, 1947. | R. & M. No. 2250. | 1s. 3d (1s. 4½d.) |
| July, 1951. | R. & M. No. 2350. | 1s. 9d. (1s. 10½d.) |

*Prices in brackets include postage.*

Obtainable from

HER MAJESTY'S STATIONERY OFFICE

York House, Kingsway, London, W.C.2; 423 Oxford Street, London, W.1 (Post Orders: P.O. Box 569, London, S.E.1); 13a Castle Street, Edinburgh 2; 39, King Street, Manchester, 2; 2 Edmund Street, Birmingham 3; 1 St. Andrew's Crescent, Cardiff; Tower Lane, Bristol 1; 80 Chichester Street, Belfast, or through any bookseller

S.O. Code No. 23-2821

R. & M. No. 28